The role of *Osr1* in postnatal muscle development and muscle regeneration

Dissertation

Submitted in Partial Fulfilment of the Requirements for the Degree of
Doctor rerum naturalium

to the Department of Biology, Chemistry and Pharmacy
of the Freie Universität Berlin

by
Jürgen Stumm

Berlin, May 2016

This thesis was carried out during the period of September 2011 and June 2016 at the Max-Planck-Institute for Molecular Genetics under the supervision of Prof Simone Spuler.

Supervisor:	Prof Simone Spuler
Second examiner:	Prof Sigmar Stricker

Date of the viva voce/defense: 11.07.2016

I declare that this thesis entitled "The role of *Osr1* in postnatal muscle development and muscle regeneration" has been composed solely by myself and that it has not been submitted, in whole or in part, in any previous application for a degree. Except where states otherwise by reference or acknowledgment, the work presented is entirely my own.

Berlin, May 16th 2016

. . . . . .

Jürgen Stumm

Table of Contents

1 Introduction

Movement of vertebrates such as birds and mammals is enabled by the skeletal musculature. Voluntary contractions of muscles provide force transmitted via tendons to bones, which allows for performing of directed actions.

After birth, during a juvenile phase of adolescence, basic musculature further develops. Muscles increase in mass and thereby in strength. This muscle growth during the early postnatal stage requires coordinated interactions of various tissue cell types. By reaching adult age this developmental process is completed.

In the adult, muscle functionality is sustained by a constant maintenance of homeostasis. In case of muscle damage repair mechanisms are deployed to regenerate affected muscle tissue, aiming for a re-establishment of muscle homeostasis. Active maintenance and repair of a functional skeletal muscle system is constantly required during the entire life span of animals. Daily routines, physical stress exposure and lesions caused by sports or accidents lead to injuries of different severeness. Whether small scale micro-injury or serious trauma, the regenerative process is realized by a dynamic and complex interplay of various cell types, including resident muscle stem cells, non-myogenic stem cells and cells of the immune system.

The precise intra- and intercellular mechanisms underlying postnatal muscle growth and muscle regeneration is not fully understood, yet, and subject of extensive research.

1.1 Developmental origin of the musculoskeletal system

In vertebrates the musculature is divided into three major types, smooth muscle, cardiac muscle and skeletal muscle. Smooth muscle forms vessel walls of large blood vessels and is found in the walls of the intestine tract including gut and colon. Cardiac muscle constitutes the heart muscle. Both types comprise involuntary muscle as they are not under conscious control. In contrast, skeletal muscle is a voluntary muscle type, and represents the largest single organ [Lieber, 2010].

The musculoskeletal system is of mesodermal origin, and requires an orchestrated interplay of muscle, tendon, bone and connective tissue formation. These tissue types originate from developmental mesodermal compartments. Muscle and parts of the axial skeleton such as ribs and vertebrae, are derived from the paraxial mesoderm. Connective tissue, tendons and bones in the limb descend from the lateral plate mesoderm [Gilbert, 2013].

During early embryogenesis segmental structures are formed from the paraxial mesoderm in craniocaudal direction to either side of the neural tube and notochord. These segments are called somites. The ventral part of the somites forms the sclerotome,

which will give rise to the axial skeleton. The remaining portion of the somites,the dermomyotome, is divided into three regions. The central part is referred to as dermatome and will mainly give rise to the back dermis. Two lateral regions provide the myotomes that produce muscle precursor cells. Muscle precursors closest to the neural tube will give rise to primaxial intercostal musculature and the deep muscles of the back. The myogenic precursors farthest from the neural tube will form abaxial muscles, including muscles of the body wall, limb muscles from somites on limb level, and tongue from cranial somites. During progression of embryonic muscle development limb muscle precursors delaminate from the abaxial myotome lip and migrate to the site of limb muscle formation. Once a basic muscle prepatterning is established, most muscle precursors further undergo myogenic differentiation [Gilbert, 2013, Christ and Ordahl, 1995] (fig.1). Early committed myogenic precursors express *Paired box 3* (*Pax3*), during progressive differentiation *Paired box 7* (*Pax7*) [Seale et al., 2000], and differentiated into myoblasts they express myogenic regulatory factors such as *Myf5* or *MyoD* [Rudnicki et al., 1993, Braun et al., 1992]. However, some muscle precursors remain undifferentiated surrounding the mature muscles as muscle stem cells, also referred to as satellite cells [Mauro, 1961, Gilbert, 2013].

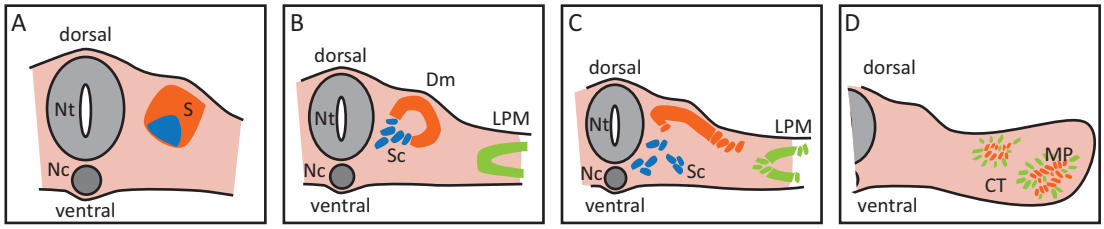

Figure 1: Developmental muscle formation requires coordinated patterning by myogenic precursors and connective tissue.
A Somites (S) are segmentally formed lateral at either side of the neural tube (Nt) and notochord (Nc). **B** The dorsal part of the somite forms the dermomyotome (Dm), the ventral part provides the sclerotome (Sc). The lateral plate mesoderm (LPM) is located at the lateral end. **C** Myogenic precursors delaminate from the dermomyotome to migrate to muscle differentiation sites such as trunk or limb. **D** In the limb, connective tissue precursors provide a muscle prepattern. Morphogenetically coordinated connective tissue (CT) and myogenic precursors (MP) form muscle pattern for terminal myogenic differentiation.

Undergoing terminal differentiation myoblasts fuse to myotubes that will form multinucleated myofibers [Wright et al., 1989]. After fusion of myoblasts to myofibers motor protein myosin II is formed. Myosin II is a compound of two myosin heavy chains (MyHC) and four light chains, and provides contractile functionality [Weiss and Leinwand, 1996]. An embryonic isoform of MyHC (embMyHC) is expressed during embryonic and fetal stages in the mouse, then gradually declines as fibers maturate. Myofibers can be divided into slow and fast twitch muscle fibers [Cho et al., 1994, Hughes et al., 1993]. Both fiber types expose distinct contractile and metabolic properties determining the function of the muscle. While slow twitch fibers mainly rely

on oxidative phosphorylation to produce energy, fast twitch fibers metabolize anaerobically. But in the course of fiber formation not all muscle precursor cells contribute to muscle fibers. By asymmetrical cell division a fraction of myogenic precursors is generated that will remain in the tissue as such, maintaining the stem cell pool. These Pax7+ muscle precursors remain quiescent [Schultz et al., 1978, Lepper et al., 2009] residing under the basal lamina, a layer of extracellular matrix that surrounds the formed myofibers. Based on their location peripherally resided and attached to the muscle fiber plasma membrane these cells are called satellite cells [Mauro, 1961]. They are first observed at fetal stage E16.5 in the mouse, after the formation of the basal lamina.

Temporally and spatially linked to migration of myogenic precursors and muscle morphogenesis, connective tissue from the lateral plate mesoderm was proposed to organize the muscle patterning. Limb muscle is developed from muscle precursors from somites on limb level migrating into the forming limb bud. However, muscle patterning is not intrinsically determined in these precursors, as demonstrated in the avian system. After transplantation of somites at the cranial end to forelimb level sites, precursors from these engrafted somites formed a patterning for normal wing musculature [Chevallier et al., 1976, Chevallier et al., 1977]. Hence, muscle precursors in all somites contain identical organogenetic potential. Provision of information for spatial region-specific organization of muscle formation was attributed to local connective tissue [Armand et al., 1983].

A prepatterning by connective tissue fibroblasts was suggested to support muscle formation by determining sites of myogenic differentiation [Kardon et al., 2003] (fig.1). This conceptual role of muscle connective tissue fibroblasts was demonstrated using the transcription factor TCF4 as a marker for this cell type [Mathew et al., 2011]. Moreover, TCF4+ connective tissue fibroblasts promote differentiation of nearby myogenic precursors into slow twitch muscle fibers by extrinsic regulation. Ablating 50% of TCF4+ fibroblasts leads to a significant reduction in slow twitch fibers in some muscle types such as the *soleus* muscle.

The T-box transcription factors *Tbx5* and *Tbx4* are expressed in the lateral plate mesoderm prior and during limb bud formation of fore- and hindlimbs, respectively [Hasson et al., 2010]. Although they are not expressed in the myogenic cell lineage but in mesenchymal progenitors and connective tissue, deletions of these genes result in disrupted muscle patterning. This muscle mispatterning is attributed to connective tissue deformities which highlights a required interplay of muscle precursors and connective tissue for proper muscle development.

Expression *MyoD* expression is crucial for myogenic precursors to differentiate to myoblasts during muscle formation. It was demonstrated that *Hox* genes exhibit

functional intrinsic roles in the control of *MyoD* expression in premyoblasts [Hashimoto et al., 1999, Yamamoto and Kuroiwa, 2003]. However, expression of these *Hox* genes, *Hoxa-11* and *Hoxa-13* in myogenic precursors is induced by sonic hedgehog (SSH) and its downstream factor bone morphogenetic factor-2 (BMP2) via mesenchymal cells.

In summary, muscle and muscle connective tissue are of distinct developmental origin. A coordinated development and morphogenesis of both is required for proper myogenesis. Muscle connective tissue constitutes an important component of the niche in which muscle and its progenitors reside. Its prepatterning is essential for the muscle patterning and a functional musculature.

1.2 Juvenile muscle growth

While prenatal myogenic development results in an organized basic musculature at the time of birth, muscle development proceeds after birth in terms of muscle growth and increase in muscle mass. This developmentally active phase takes place during a juvenile phase, that is the first three weeks after birth in the mouse.

1.2.1 Satellite cells and their environment are developmentally active during early postnatal phase

During the juvenile stage of the mouse, the first three weeks after birth, an intense increase in muscle mass is observed. This can be explained by either an increase in the number of myofibers, hyperplasia, or an increase in the size of fibers, hypertrophy. In the mouse hypertrophy is the main reason for muscle growth [Ontell et al., 1984]. It was reported that during the early postnatal growth phase the *extensor digitorum longus* (EDL) hindlimb muscle in the mouse increases in size of individual myofibers exclusively, an increase in the number of fiber was not observed [White et al., 2010]. In rats the cause of this increase could be tracked back to muscle stem cells, the satellite cells [Moss and Leblond, 1971, Moss and Leblond, 1970, Shafiq et al., 1968].

Many of these muscle stem cells are in a highly proliferative state (~80%) in both growing mouse and rat during the first three weeks after birth [Schultz, 1996, Shinin et al., 2006]. Satellite cells expand and further differentiate to myoblasts. Fusion of myoblasts to already formed myofibers provides new myonuclei, hence increases individual fiber mass. Myoblast fusion and with it hypertrophy are stimulated by the expression of nitric oxide synthase by stromal fibroblasts [Dahlman et al., 2010]. Furthermore, expression of embMyHC in myofibers, which marks immature fibers, is repressed by muscle connective tissue fibroblasts at the time of birth. This repression is mediated non-cell-autonomously by TCF4 regulated gene expression in fibroblasts.

At the age of three weeks embMyHC expression in myofibers is not detectable anymore [Mathew et al., 2011]. This demonstrates a crucial role for connective tissue fibroblasts in the promotion of myogenic maturation.

The proportion and absolute number of satellite cells gradually decreases throughout the growth phase. While at the age of 14 days a portion of 11% of all cells is represented by satellite, at the age of 17 weeks, in fully grown up adults, this portion has decreased to 3%, as described for the EDL muscle [Allbrook et al., 1971, Schultz, 1974]. At the same time the number in myonuclei increases 5-fold [White et al., 2010]. Once the muscle has matured satellite cells turn mitotically quiescent and reside in their niche [Schultz et al., 1978].

However, the complete picture of cell types, intra- and intercelluar mechanisms involved, is still poorly understood.

1.3 Adult homeostatic muscle

A mature skeletal muscle constitutes a contractile compound unit that connects bones via tendon linkages. Each muscle is ensheathed by a rigid connective tissue layer, the epimysium, which is assumed to play an important role in transmitting contractile force [Sanes, 1994]. The muscle bulk comprises of numerous of fascicles. These fascicles are bundles of muscle fibers enveloped in a connective tissue layer, the perimysium. Muscle fibers, or myofibers, pose the basic functional components of skeletal musculature. Resulting from the fusion of myoblasts, myofibers are large elongated, post-mitotic multinucleated cells, also referred to as syncitia. Nuclei are positioned peripheral inside the fiber body. Fibers are surrounded by the endomysium, an extracellular matrix (ECM) provided by collagenous proteins such as the major components collagen type VI and fibronectin that form a discrete network of beaded microfilaments [Zou et al., 2008].

A single myofiber is surrounded by an outer ECM layer, the basal lamina, which contains collagen type IV fibrils [Noonan et al., 1991], and specific proteins such as laminin [Engvall et al., 1990]. The basal lamina is linked to the surrounding ECM via an anchorage between collagen type IV and type VI [Kuo et al., 1997]. The fiber itself is delimited from the basal lamina by the plasma membrane called sarcolemma, under which the myonuclei are localized. Within the cytoplasma of fibers myofibrils are located, units that execute actual contractile force (fig.2).

Quiescent satellite cells in healthy homeostatic muscle reside in between the sarcolemma and the basal lamina, which represents their niche. In this niche satellite cells have contact to myofibers through the apical surface, and to ECM by the basal lamina [Mauro, 1961]. Myogenic commitment of satellite cells is under the control of intrinsic key transcription factors, such as Pax7 [Lepper et al., 2009] or MyoD [Sam-

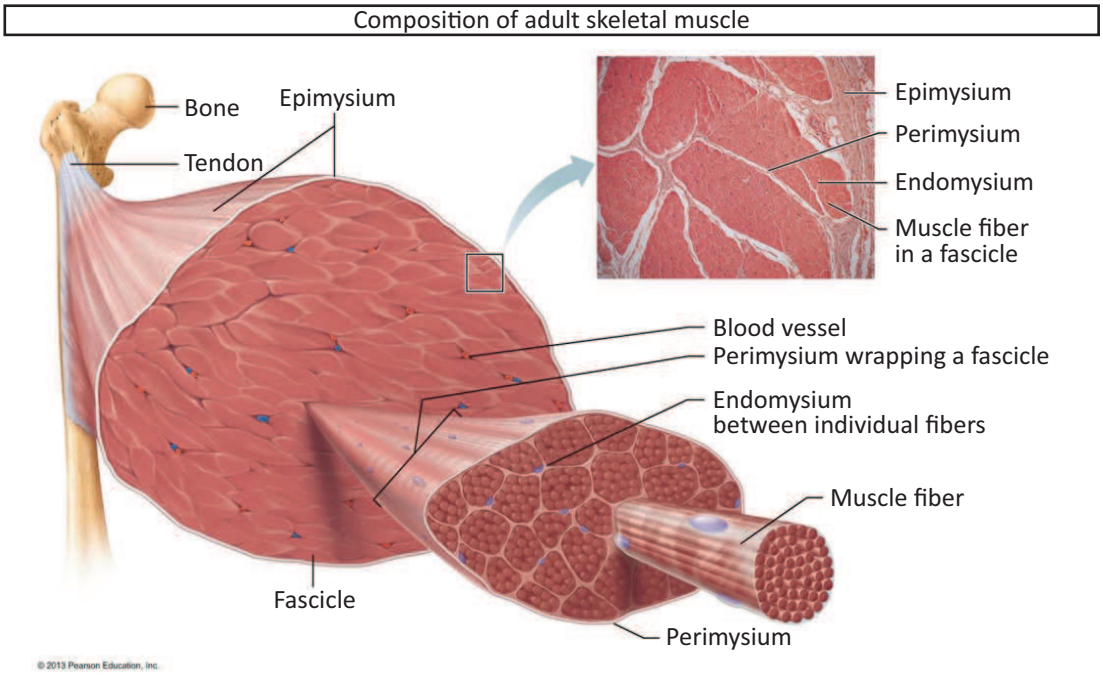

Figure 2: Composition of skeletal muscle.
Adult skeletal muscle transmits contractile forces to bone via tendons. A muscle strand is composed of numerous fascicles that are enveloped by a rigid connective tissue layer, the epimysium. In between the fascicles blood vessels are located for oxygen and nutrient supply. Each single fascicle consists of myofibers, bundled by the perimysium, a connective tissue layer delineating the fascicle. The space in between myofibers, large multinucleated cells, is filled with extracellular matrix, the endomysium. Endomysium and perimysium comprise the muscle interstitium, which houses various interstitial cell types and blood vessels. Source: Pearson Education, 2013.

basivan et al., 2011, Lepper et al., 2011, Yablonka-Reuveni et al., 2008], but also extrinsically regulated by the ECM. The composition of the matrix regarding elasticity and stiffness directs stem cell lineage specification and regulates expression of myogenic marker genes *Pax7* or *MyoD*, thus influences differentiation of satellite cells in the niche [Boonen et al., 2009, Gilbert et al., 2010].

By experimental engineering of ECM compositions it was demonstrated that modulating substrate matrix elasticity can alter proliferation [Gilbert et al., 2010], migration [Raab et al., 2012, Vincent et al., 2013] and differentiation of stem cells [Saha et al., 2008, Engler et al., 2006]. Collagen IV, one of the major components of the basal lamina, and collagen type VI, a main constituent of the ECM, are considered to be predominantly contributed by tissue resident interstitial fibroblasts [Sanderson et al., 1986, Zou et al., 2008]. Freshly isolated murine satellite cells cultured in presence of native collagen type VI expose a higher percentage of *Pax7* expression, a transcriptional marker for satellite cell quiescence in adult muscle, than without supplement [Urciuolo et al., 2013]. This implies a regulation of satellite cell quiescence by the secretion of collagen type VI of resident interstitial fibroblasts.

Furthermore, neighboring tissue and resident cell types provide signaling to support

the regulation of satellite cell state [Beauchamp et al., 2000]. Paracrine soluble cytokines, chemokines, and other molecules are released from neighboring tissue, such as myofibers or microvasculature, and adjacent resident cells including resident interstitial cell types and immune cells. Also systemic factors maintain the quiescent state of satellite cells or promote their proliferation and differentiation [Brack et al., 2007, Ten Broek et al., 2010].

In healthy homeostatic muscle satellite cells are essentially mitotically quiescent in their niche. While during early postnatal growth muscle stem cells proliferate and terminally fuse to fibers, in adult homeostatic muscle less than 1% of satellite cells incorporate into fibers in 6-8 weeks old mice [Ontell et al., 1984, Grounds and McGeachie, 1989, Keefe et al., 2015].

1.3.1 Cell types resident to the muscle interstitium

The muscle interstitium includes the space in between the single fibers, the endomysium, and the perimysium, and is populated by a variety of tissue resident cell types. These cell types play important roles in orchestrating maintenance of muscle homeostasis and repair (fig.3).

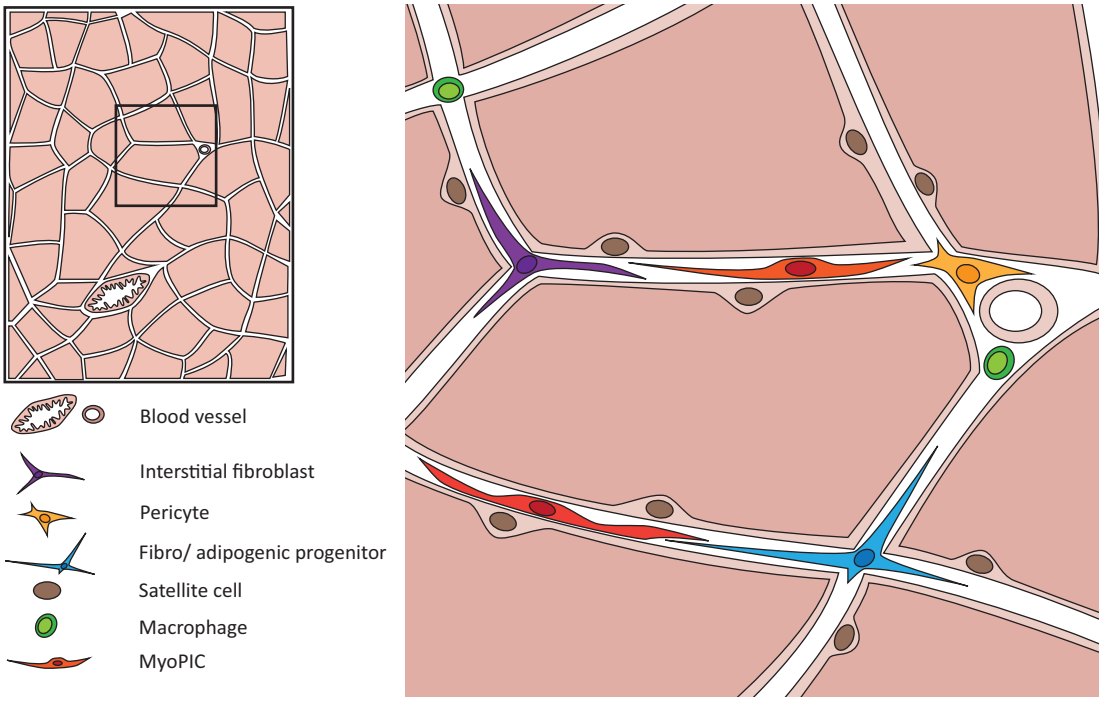

Figure 3: The muscle interstitium accommodates various cell types.
The space in between muscle fibers, the muscle interstitium, is comprised of the perimysium and the endomysium. It consists of extracellular matrix mainly composed of collagenous proteins, and enables communication and interaction of diverse resident cell types. These interstitial populations include fibroblasts, pericytes, fibro/ adipogenic progenitors, PICs and resident macrophages. Also structural elements are contained in the interstitium, such as blood vessels and capillaries. Illustration based on Kyryachenko *et al.*, 2016 [Kyryachenko et al., 2016].

1.3.1.1 Satellite cells

Satellite cells, are muscle stem cells and hold the major myogenic activity in adult muscle [Collins et al., 2005, Sherwood et al., 2004, Kuang et al., 2007]. They remain quiescent and localized beneath the basal lamina of muscle fibers in healthy muscle [Mauro, 1961], as elaborated in detail above, expressing *Pax7*. Inactive satellite cells highly express cell surface proteins such as integrin-α7 and β1, or dystroglycan. These proteins function as receptors to mediate signals transported via the laminin-rich ECM, suggested to communicate quiescence [Mayer et al., 1997, Cohn et al., 2002]. Active Notch signaling is crucial for the maintenance of quiescence. Satellite cell specific deletion of RBP-Jκ, a nuclear factor required for Notch signaling, resulted in the depletion of the satellite cell pool due to spontaneous activation and premature differentiation [Bjornson et al., 2012]. However, quiescence is not only supported by the environment, but also intrinsically regulated. Transcriptome analyses of quiescent satellite cells revealed an upregulation of negative regulators of the cell cycle. This quiescence signature includes *cyclin-dependent kinase inhibitors 1B* (*Cdkn1b*; *p27*), *cyclin-dependent kinase inhibitors 1C* (*Cdkn1c*; *p57*) and *sprouty 1* (*Spry1*) [Fukada et al., 2007, Liu et al., 2013].

In quiescent state they express marker genes *Pax7* [Kuang et al., 2007, Lepper et al., 2009], *integrin-α7* [Sacco et al., 2008], *SM/C-2.6* [Fukada et al., 2004] and *CD34* [Beauchamp et al., 2000].

1.3.1.2 Interstitial fibroblasts

In the limb, interstitial fibroblasts, also referred to as muscle connective tissue fibroblasts, are developmentally derived from the lateral plate mesoderm, hence are of a separate lineage than somitically derived myogenic cells [Kardon et al., 2003]. While they provided a prepatterning for muscle development during embryogenesis, they remain tissue resident in the adult. Tissue resident fibroblasts support maintaining the ECM by secretion of collagens and provide extrinsic signals required for quiescence of satellite cells, as detailedly described above. A commonly accepted molecular marker for muscle interstitial fibroblasts is TCF4 [Mathew et al., 2011].

1.3.1.3 Pericytes

Pericytes are perivascular cells, and named after their anatomical location in close proximity to small blood vessels, called capillaries, surrounding each myofiber [Poole et al., 2008]. They are wrapped by the capillary basal lamina, located on the abluminal surface of the endothelial capillary tube. While pericytes of most peripheral organs are derived from the mesoderm [Etchevers et al., 2001], the origin of peri-

cytes residing in the skeletal muscle has not been sufficiently explored. Pericytes are heterogenous, exhibiting differing marker profiles depending on the tissue they were isolated from [Bondjers et al., 2006], which poses a challenge for a clear identification of this cell type. Suggested markers for pericytes in skeletal muscle are NG2 (neural/ glial antigen 2; chondroitin sulfate proteoglycan 4) and PDGFRβ [Armulik et al., 2011]. However, these markers can also be expressed by myoblasts [Yablonka-Reuveni et al., 1990] or possess controversial fidelity regarding their specificity [Dellavalle et al., 2007, Ugarte et al., 2012]. More recently, NG2+/ PDGFRβ+ pericytes were shown to consist of two subpopulations, discriminable by expression of Nestin [Birbrair et al., 2013a]. Transplantation experiments indicated that Nestin– type-1 pericytes expressing also PDGFRα are adipogenic when engrafted into muscle. Type-2 pericytes are Nestin+ and possess myogenic differentiation potential when engrafted into skeletal muscle after injury, whereas no fatty accumulation derived from the engrafted cells was observed [Birbrair et al., 2013a].

1.3.1.4 Fibro/ adipogenic progenitors (FAPs)

Fibro/ adpipogenic progenitors (FAPs) are a subset of muscle resident interstitial cells with fibrogenic and adipogenic differentiation potential, while exhibiting no potential for myogenic differentiation. Their developmental origin is suggested to be derived from mesenchymal cells [Joe et al., 2010, Uezumi et al., 2010], but is not sufficiently elucidated. They are localized in the muscle interstitium outside the basal lamina of myofibers.

It was demonstrated that a cell population can be isolated via fluorescent-activated cell sorting (FACS) by excluding hematopoietic (CD45–/ Ter119–) and endothelial cells (CD31–), myogenic progenitors (integrin-α7–), and positive selection for both progenitor/ stem cell markers CD34 and Sca-1. These cells were reported to be uniformly positive for PDGFRα [Joe et al., 2010], a surface marker present in embryonic mesenchymal cells [Orr-Urtreger et al., 1992] which give rise to connective tissue. This CD34+/ Sca-1+ cell population represents over 85% of all PDGFRα+ muscle resident cells. Bipotency of isolated CD34+/ Sca-1+ was demonstrated by *in vitro* differentiation assays. After culturing single cells in growth medium 35% of formed colonies contained adipocytes and fibroblasts, whereas the remaining 65% were exclusively positive for fibroblasts markers ER-TR7, FSP1 and α-smooth muscle actin (αSMA). Due to this differentiation potential for fibroblasts and adipocytes these cells were referred to as FAPs [Joe et al., 2010]. This observation of bipotency is in coherence with a reported common mesenchymal progenitor of both adipocytes and fibrotic tissue in skeletal muscle [Uezumi et al., 2011]. After engraftment of labeled FAPs in healthy *tibialis anterior* muscles, donor-derived cells were not incorporated

into the recipients interstitium but gave rise to subcutaneous clusters of adipocytes. It is concluded that the fate of FAPs is controlled by the environment. This conclusion is in coherence with the observation of FAPs contributing to ectopic fibrotic and adipocytic tissue after injury [Joe et al., 2010].

In an independent approach non-hematopoietic, non-myogenic cells were sorted by FACS, selecting for PDGFRα positive and negative cells [Uezumi et al., 2010]. By *in vitro* differentiation assays adipogenic potential of exclusively the PDGFRα+ population was demonstrated. Nevertheless, this adipogenic potential was strongly inhibited by the presence of myotubes, supporting the previous report of an environment controlled differentiation of FAPs. Additionally, *in vivo* these cells only contributed to fatty formation after transplantation into a model of fatty infiltration. This model is characterized by muscle injury followed by promoted fat formation. In healthy muscle tissue FAPs did not differentiate to fat cells [Uezumi et al., 2010].

Another report demonstrates isolation of adipogenic muscle interstitial cells by FACS using surface markers CD45 and macrophage-1 antigen (Mac-1) to exclude hematopoietic cells, and Sca-1 for positive selection [Schulz et al., 2011]. By stimulation with bone morphogenetic protein 7 (BMP7) this population is highly inducible for differentiating into brown-like adipocytes *in vivo* and *in vitro*. Brown adipocytes form a type of fat morphologically and functionally distinct from white fat cells found in muscle. While other members of the BMP family are involved in the formation of white adipocytes, the role of particularly BMP7 is limited to brown adipocyte differentiation [Tseng et al., 2008], and mainly skeletal development [Karsenty et al., 1996].

Whether these cell populations overlap remains to be further clarified. Nevertheless, their common traits, such as localization in the muscle interstitium, presence of molecular surface markers Sca-1 and PDGFRα and adipogenic capacities, affirm a matching identity. By engraftment of labeled Sca-1+/ PDGFRα+ cells isolated from skeletal muscle into a mouse model for heterotopic ossification, it was demonstrated that these cells contribute to bone and cartilage formation [Wosczyna et al., 2012]. In summary, these findings emphasize a stem cell-like character of FAPs, featuring versatile potential depending on the interaction with the cellular environment they are transplanted to.

1.3.1.5 PW1-expressing interstitial cells (PICs)

A heterogeneous cell population residing in the muscle interstitium is characterized by expression of cell stress mediator *Paternally expressed gene-3* (*Peg3*), also referred to as PW1 [Mitchell et al., 2010]. PW1-expressing interstitial cells (PICs) are positive for surface markers CD34 and Sca-1, and can be separated into a myogenic and an

adipogenic subpopulation based on the expression of PDGFRα.

PDGFRα– PICs (myoPICs) are highly myogenic *in vitro*. They can contribute to muscle fibers and generate satellite cells, but they do not express satellite cell marker *Pax7*. Pax7+ satellite cells are commonly considered to be the major, if not exclusive, contributors to skeletal muscle tissue. However, it was demonstrated that myoPICs and satellite cells do not share a common progenitor. Lineage tracing experiments utilizing a $Pax3^{Cre}/ROSA^{lacZ}$ lineage tracer mouse model enabled permanent labeling of Pax3+ embryonic muscle precursor cells. While Pax3+ cells gave rise to myofibers and satellite cells, myoPICs were not derived from this myogenic lineage [Pannérec et al., 2013]. Nevertheless, myoPICs depend on a *de novo* expression of *Pax7* in the course of myogenic commitment. MyoPICs isolated from *Pax7* deficient mice did not participate in myogenesis *in vitro*. Hence, myoPICs are proposed to be a non-satellite cell progenitor population with myogenic potential.

The PDGFRα+ portion of PICs (adipoPICs) is non-myogenic but shows a strong adipogenic differentiation potential *in vitro*. This adipoPIC population is considered to overlap with the FAP population.

1.3.1.6 Macrophages

Macrophages are part of the innate immune system, and as resident macrophages they populate the muscle interstitium [Brigitte et al., 2010]. It was shown, that upon muscle injury resident macrophages become classically activated (M1) for early infiltration of the tissue to clear it from cellular debris. Alternatively activated (M2) macrophages assist with regeneration and muscle growth [Arnold et al., 2007, Deng et al., 2012]. Resident macrophages are mainly localized in the epimysium and the perimysium. Once activated, macrophages are positive for surface marker CD68 [Deng et al., 2012].

1.4 Muscle regeneration after injury

In healthy adult muscle the composition of the niche, in which satellite cells and other interstitial stem-like cells reside, is essentially static. This homeostasis is balanced and maintained by the environment imposing signals to promote quiescence.

After acute injury the composition of the niche undergoes critical changes. A rapid innate immune response is initiated. Immune cells infiltrate the tissue to clear it from cellular debris. In parallel resident interstitial cell types are activated to prepare revascularization and reorganization of the site of injury. Muscle connective tissue fibroblasts proliferate and establish a temporary tensile resistance by extensively producing ECM. This ECM production results in a so-called fibrosis that stabilizes the

tissue [Menetrey et al., 1999]. Since multinucleated myofibers are post-mitotic they are incapable of proliferation and further division to regenerate adjacent damage. Instead they depend on resident muscle progenitor cells for repair. Therefor satellite cells start to proliferate [Murphy et al., 2011], differentiate and recover the damage by fusing to new myofibers. Satellite cells represent the major population of myogenic cells in adult muscle, and their presence is indispensable for skeletal muscle regeneration [Collins et al., 2005, Sacco et al., 2008, Lepper et al., 2011, Sambasivan et al., 2011, Murphy et al., 2011]. Newly formed myofibers, resulting from fused myoblasts, are marked by centrally located nuclei, as these nuclei did not migrate peripheral, yet.

All of these events leading to muscle repair crucially depend on an orchestrated interplay and interactions of a variety of cell types at every stage of the regenerative process (fig.4).

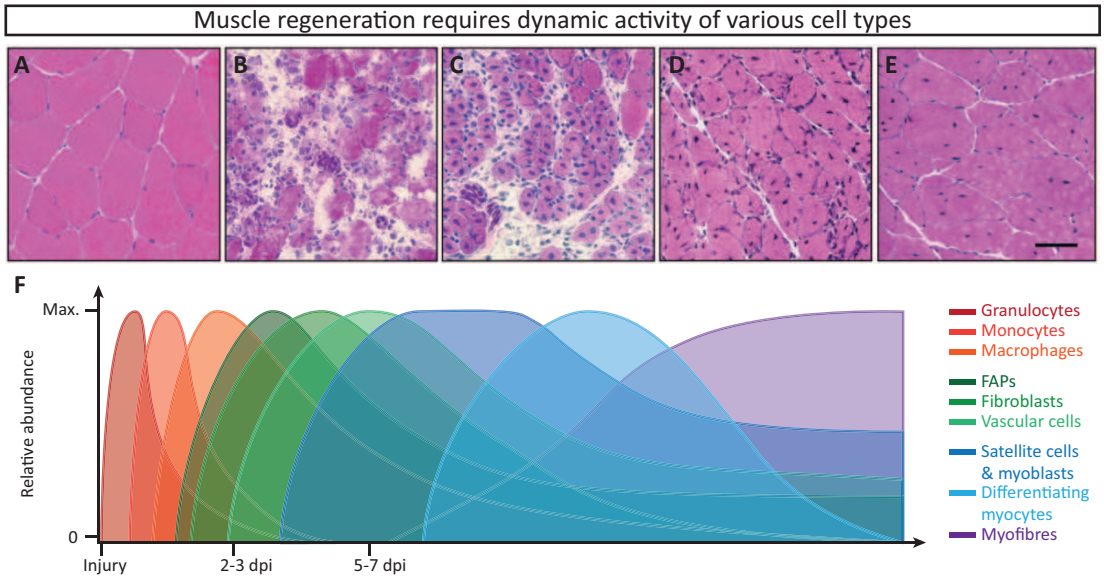

Figure 4: Muscle regeneration after injury is a concerted process of a variety of cell types involved.
A-E The niche in healthy muscle (A) undergoes drastic changes after injury. Immune cells infiltrate the tissue to remove debris (B), and a transient fibrosis is established (B-C). Pro-myogenic macrophages and other cells to promote regeneration expand (C). Fusion of muscle progenitors results in newly formed myofibers featuring centrally located nuclei (D) and regenerated muscle (E). Image adapted from Mann *et al.*, 2011 [Mann et al., 2011]. **F** Muscle injury is followed by an infiltration of immune cells (granulocytes, monocytes and macrophages) into the damaged tissue, where resident cell types (FAPs, fibroblasts, vascular cells) are activated and expand. Myogenic cells (satellite cells, myoblasts, differentiating myocytes) start to differentiate and form myofibers to repair the tissue. Displayed are the relative abundances of these cell types depending on the time after tissue damage. Illustration based on Bentzinger *et al.*, 2013 [Bentzinger et al., 2013].

1.4.1 Experimental methods for studying muscle regeneration

In order to study the regenerative process and inherent coordination of cell types, experimental methods and techniques were developed to introduce muscle damage. All models have in common an initial immune response followed by progressive reformation of new myofibers. Each technique features advantages and disadvantages and is tailored for individual purposes. Although in all models the muscle regenerates completely, the trajectories of the regenerative process vary considerably [Hardy et al., 2016].

1.4.1.1 Mechanical injury

In attempts to mimic naturally occurring muscle injuries several techniques to apply damage to muscle were developed. Some methods offer the advantage of being non-invasive. Force applied externally via abrupted impact [McBrier et al., 2009] or by crushing pressure [Dobek et al., 2013] using customized devices induces blunt traumata. Without the need for devices muscle damage can also be applied using forceps to crush the muscle, with the drawback of opening the skin [McGeachie and Grounds, 1987]. Other invasive techniques are cut lesions, where small cuts are applied to muscle strands [McGeachie and Grounds, 1987], or puncturing and piercing the muscle using syringe or acupuncture needles [Hill et al., 2003, Domingo et al., 2013].

Invasively performed application of muscle lesions can also be achieved by freezing. Applying a dry ice or liquid nitrogen cooled steel probe to the bare muscle induces damage and can result in a massive loss of 2/3 of muscle mass [Warren et al., 2007, Gayraud-Morel et al., 2007]. Freezing was also combined with crushing using dry ice cooled forceps or piercing using cooled needles [McGeachie and Grounds, 1987, Floss et al., 1997].

These techniques to mechanically damage the muscle are not selective and limited to particular tissue types, but tissue is damaged entirely.

1.4.1.2 Myotoxin mediated injury

Administration of myotoxic snake venoms is a widely-used method to study muscle regeneration. While venoms from cobra *Naja mossambica mossambica* or mamba *Dendroaspis jamesoni* are summarized as cardiotoxins (CTX), venom from tiger snake *Notechis scutatus scutatus* is referred to as notexin (NTX). However, myotoxic mechanism and application overlap for both CTX and NTX. Intramuscular injection causes a degeneration of terminally differentiated fibers and necrosis, followed by an immediate immune response and muscle repair. Selective action of these venoms does not affect mononucleated progenitors like satellite cells or structures such as blood vessels

and muscle innervation [Couteaux and Mira, 1985, Couteaux et al., 1988, Harris et al., 2003]. While morphologically final regeneration results in a similar appearance to healthy muscle, structural differences remain regarding fascicle organization [Couteaux et al., 1988].

1.4.1.3 Chemical injury

Injection of barium chloride ($BaCl_2$) can be utilized as a chemical way to cause damage to muscle for studying regeneration [Otis et al., 2014, Rogers et al., 2015]. While muscle fiber necrosis appears at the site of injection, the basal lamina and mononucleated cells remain largely intact [Caldwell et al., 1990].

1.4.1.4 Glycerol induced injury

Intramuscular injection of glycerol was characterized as an injury model specialized for studying fatty accumulation in the course of regeneration, as it occurs in certain muscle diseases [Pisani et al., 2010]. Glycerol injection induces myofiber damage by disruption of the fiber plasma membrane [Eisenberg and Eisenberg, 1968]. Regeneration is accompanied by deposition of adipocytes between muscle fibers, whereas the origin of these adipocytes and the mechanisms underlying this infiltration remains unclear [Pisani et al., 2010].

1.4.2 Immune response after muscle damage

Following muscle injury the innate immune system is activated rapidly. Within seconds to minutes tissue resident granulocytes are activated as an initial reaction of the early immune response [Brigitte et al., 2010]. These granulocytes degranulate, hence release pro-inflammatory mediators into the environment which increase permeability of capillaries to enhance infiltration of further immune cells. During the next hours more granulocytes are recruited that release factors exacerbating tissue damage [Tidball, 1995, Heredia et al., 2013]. Attracted by this burst of collateral damage, monocytes infiltrate the tissue, from eight hours on post injury [Brigitte et al., 2010]. Within the next 24 to 48 hours thereafter monocytes give rise to macrophages that become the major cell subset at the site of damaged tissue for the next days. Activated by pro-inflammatory interleukins (IL) and cytokines, their function lies in clearing the tissue by phagocytosis, but also in rescuing myoblasts and myotubes from apoptosis [Sonnet et al., 2006]. During the progression of the regenerative process M2 macrophages activated by anti-inflammatory type 2 cytokine signals including IL-4 and IL13 predominantly populate the site of injury [Arnold et al., 2007]. M2 macrophages were proposed to assist in myogenic repair and growth [Robertson et al., 1993]. Inhibition

of the alternative M2 macrophage activation by reduction of relevant signaling resulted in smaller regenerated myofibers. This observation indicates a direct influence of macrophages on the myogenic repair mechanisms [Ruffell et al., 2009]. Macrophage abundance fades in the course of terminal regeneration [Brigitte et al., 2010].

1.4.3 Facilitation of regenerative myogenesis by interstitial progenitors

Effective muscle regeneration not solely depends on myogenic cells. Tissue resident cell types were shown to play crucial roles in the promotion of muscle repair.

1.4.3.1 Fibro/ adipogenic progenitors are activated after injury to facilitate regeneration

During ongoing immune response after muscle injury, early in regeneration the number of fibro/ adipogenic progenitors (FAPs) dramatically increases [Joe et al., 2010]. These muscle resident cells are quiescent in healthy muscle, but are rapidly induced to proliferate after NTX induced injury [Joe et al., 2010].

The cause of this FAP activation was attributed to immune cells during early innate immune response [Heredia et al., 2013]. Type 2 signaling, particularly via IL-4/ IL-13 secretion of granulocytes, not only mediates programming of anti-inflammatory pro-myogenic M2 macrophages, but also a regenerative potential in FAPs [Heredia et al., 2013]. In wildtype mice eight days post CTX injury fibers with centrally located nuclei were observed, indicative of proceeding regeneration. In IL-4/ IL-13 knock-out mutants and in granulocyte deficient mice these were largely absent. Further analyses revealed coinciding peaking expression of IL-4 in granulocytes and IL-4Rα in FAPs during an early time frame two days after CTX induced injury. As a result of this IL-4 mediated communication between both cell types, FAPs start to proliferate 48h after injury and reach a dramatically increased number 24h later [Heredia et al., 2013, Joe et al., 2010].

Functionally, FAPs facilitate regeneration by efficient phagocytosis of debris *in vitro* [Heredia et al., 2013]. A PDGFRα conditional knock-out of IL-4Rα resulted in persistence of debris, larger areas of injury, and decreased formation of regenerated muscle fibers.

In addition, FAPs promote regeneration by further expression of several factors known to favour myogenic differentiation. After expansion of FAPs in the damaged tissue after NTX injury, they show elevated expression levels of IL-6 and insulin-growth factor 1 (IGF-1) by ten-fold increase. Both are secreted factors reportedly promoting satellite cell mediated hypertrophy [Serrano et al., 2008, Bodine et al., 2001]. Muscle hypertrophy is defined by differentiation of satellite cells to myoblasts

in order to fuse to myofibers resulting in increased muscle mass. This direct and tissue context independent regulatory function was demonstrated by co-culturing FAPs and satellite cells. After seven days of cultivation, expression of satellite cell markers was significantly reduced in the presence of FAPs, while expression of myoblast markers was coherently increased [Joe et al., 2010].

1.4.3.2 Pericytes contribute to myofibers and revascularization

Pericytes remain resident in the muscle interstitium, mainly closely associated to blood vessels, and are activated after injury exposing regenerative capacities [Armulik et al., 2011]. The underlying mechanisms of this activation, and whether these cells expand in the damaged tissue remain unknown [Boppart et al., 2013]. Myogenic type 2 pericytes, defined by PDGFRβ+/ NG2+/ Nestin– trait, can enter the satellite cell compartment, start expressing satellite cell marker Pax7 [Birbrair et al., 2013b, Dellavalle et al., 2011] and contribute to muscle regeneration by fusing to fibers [Birbrair et al., 2013b]. This myogenic contribution was also observed after injection of FACS purified PDGFRβ+/ NG2+ pericytes into CTX injured muscle [Crisan et al., 2008], whereas contribution was even higher after chemically induced injury after $BaCl_2$ [Dellavalle et al., 2011].

As a cell type characterized by its localization, pericytes are also involved in revascularization. They are the first cells invading newly vascularized tissue [Nehls et al., 1992], to guide and determine where newly formed blood vessels spread [Nehls et al., 1992, Ozerdem et al., 2001, Ozerdem and Stallcup, 2003, Birbrair et al., 2014]. Moreover, myogenic type 2 pericytes expose angiogenic potential *in vitro*, and *in vivo* in a model of ischemia, for this pericyte subset forms CD31+ blood vessels [Birbrair et al., 2014].

1.4.3.3 Muscle connective tissue fibroblasts regulate satellite cell activation

During the process of muscle regeneration a transient ECM is formed to support myogenic repair mechanisms such as migration of myogenic progenitors or myoblast fusion [Mann et al., 2011]. Furthermore, a temporary fibrosis, scarring tissue, is established by accumulation of collagens, such as collagen type VI [Sabatelli et al., 2012], to stabilize the tissue until full regeneration [Ambrosio, 2008].

Collagen type VI was reported to be expressed at high levels and synthesized uniquely by muscle connective tissue fibroblasts [Zou et al., 2008]. These fibroblasts express *Tcf4*, particularly during muscle regeneration [Zou et al., 2008]. After $BaCl_2$ induced injury TCF4+ fibroblasts start to proliferate and rapidly expand in proximity to proliferating satellite cells, peaking at 5 days post injury [Murphy et al., 2011].

These fibroblasts are situated embedded in collagenous connective tissue which links their presence with fibrosis. Cellular ablation of TCF4+ fibroblasts after injury not only reduces muscle connective tissue, it also results in an impairment of myogenic regeneration. Loss of these fibroblasts leads to a premature activation and differentiation of satellite cells, hence a depletion of the muscle stem cell pool and reduced number of regenerated myofibers [Murphy et al., 2011].

1.5 Intramuscular fatty accumulation

In older adults [Visser et al., 2005, Goodpaster et al., 2004] or in various muscular dystrophy diseases a failure in muscle regeneration can lead to ectopic fibrosis [Shi-wen et al., 2007] and fatty accumulation [Wren et al., 2008]. One of the most severe cases of dystrophy, Duchenne muscular dystrophy (DMD), is caused by an X-linked deletion of the dystrophin gene [Morales et al., 2013]. The dystrophin protein is an essential component of the myofiber plasma membrane, its loss impairs the sarcolemma stability and desintegrates muscle tissue context. Upon acute muscle injury, inflammatory immune reaction persists leading to progressive muscle atrophy. The transient fibrotic scar is further excessively infiltrated with fibroblasts and adipocytes [Natarajan et al., 2010]. In DMD this fatty degeneration of muscle can result in fat replacing almost the entire muscle [Banker and Engel, 2004].

Precise molecular mechanisms underlying the misregulation of the entire regenerative process is still unclear. As cellular origin for fibroblasts and adipocytes in this malicious context myogenic progenitors, pericytes and FAPs were proposed. Satellite cells can spontaneously enter an alternative mesenchymal lineage commitment, and differentiate to adipocytes *in vitro* [Shefer et al., 2004]. However, muscle stem cells as the main source of ectopic fat was not sufficiently supported by *in vivo* studies yet.

Transplantation studies have revealed fibrogenic capacities of Nestin– pericytes [Birbrair et al., 2013b]. In older mice these pericytes produce collagens and contribute to fibrous tissue deposition. In addition, culturing of isolated cells leads to lipid containing adipocytes, indicating adipogenic potential *in vitro*. And after engraftment into a model of fatty accumulation after glycerol induced muscle injury these pericytes contribute to ectopic fat, which confirms adipogenic potential *in vivo* [Birbrair et al., 2013a]. This adipogenic subset of pericytes is characterized by expression of PDGFRα, a surface marker also attributed to fibro/ adipogenic progenitors FAPs. While the function of PDGFRα and its ligands involves pathways regulating cell growth, proliferation, differentiation, survival, and migration [Guida et al., 2007, Besançon et al., 1998, Erovic et al., 2012, Andrae et al., 2008], their role in skeletal muscle adipogenesis remains unclear.

Ectopic fat cell deposition caused by FAPs was demonstrated by transplantation

of FACS isolated FAPs into glycerol induced mice [Uezumi et al., 2010]. In contrast, these cells did not give rise to adipocytes after CTX injury, indicating an environment controlled lineage commitment. In *mdx* mice, a commonly used dystrophin deficient mouse model for DMD, FAPs promote the regeneration potential of satellite cells during disease progression [Mozzetta et al., 2013]. However, FAPs isolated from mdx mice subjected to adipogenic cultivation exposed increased differentiation to adipocytes compared to wildtype FAPs.

1.6 *Osr1* expression during skeletal muscle development

Odd skipped (*Odd*) in Drosophila and *Odd skipped related* (*Osr*) in other vertebrates are genes of the pair-rule class, and encode for zinc-finger transcription factors.

Odd-skipped was originally identified by its involvement in zygotic segmentation in Drosophila embryos. Mutants for *Odd* expose a phenotypic loss of odd-numbered segments [Coulter and Wieschaus, 1988, Nüsslein-Volhard and Wieschaus, 1980]. Odd is a zinc-finger transcription factor and a gene of the pair-rule class. It is expressed in stripes during segmentation (fig.5A). During further Drosophila embryogenesis it acquires a dynamic expression. Functionally, *Odd* can act as a transcriptional repressor [Goldstein et al., 2005] and activator [Saulier-Le Dréan et al., 1998].

In vertebrates, two genes homologous to Drosophila *Odd* could be identified, *Odd-skipped related 1* (*Osr1*) and *Odd-skipped related 2* (*Osr2*). In the mouse *Osr1* is located on chromosome 12:9,574,442-9,581,499 oriented on the forward strand. It consists of three exons, of which exon 2 contains the start codon ATG. OSR1 is assembled of 266 amino acids and and has a mass of 29.6kDa. Three zinc-finger domains are located in the C-terminal half of the protein. *Osr2* is located on chromosome 15: 35,296,098-35,303,304 on the forward strand and consists of four exons. The *Osr2* open reading frame spans exon 2 to exon 4. OSR2 consists of 276 amino acids and has a molecular weight of 30.5kDa. Both *Osr* genes are highly conserved among vertebrates including human [Stricker et al., 2006, Lan et al., 2001, Debeer et al., 2002, Katoh, 2002, So and Danielian, 1999]. While *Osr1* and *Osr2* show distinct temporal and spatial expression, their proteins were proposed to be functionally equivalent [Gao et al., 2009].

Osr1 and *Osr2* expression patterns were characterized in chicken, where in early development *Osr1* is expressed in the intermediate mesoderm and lateral plate mesoderm, and *Osr2* in the endoderm (fig.5B). Both genes are expressed mainly in distinct regions with partial overlaps [Stricker et al., 2006]. During progressing development of the chick *Osr1* is strongly expressed in limbs, but also in the heart and other mesenchyme derived tissues. In mouse embryos, *Osr1* is expressed in the limb mesenchyme, associated to early pre-muscle masses at developmental stages E11.5 and

E12.5. While *Osr2* expression overlaps to a small portion it is expressed almost exclusively more distal (fig.5C). *Osr1* expression was proposed as one of the earliest marker for irregular connective tissue [Stricker et al., 2012].

Functional studies were performed *in vitro* using primary embryonic chicken cells. While *Osr1* expression confers connective tissue properties it represses chondrogenesis and osteogenesis. In mouse, gene targeting approaches were conducted. *Osr1* deficient mutant mice are lethal at early fetal stage due to severe heart and intermediate mesenchyme development defects [Wang et al., 2005]. The intermediate mesenchyme gives rise to the urogenital system. The functional role of *Osr1* expression in the intermediate mesenchyme was excessively studied, which revealed crucial involvement in kidney development [James et al., 2006, Mugford et al., 2008, Xu et al., 2014].

The function of *Osr1* during mouse development was attributed to connective tissue-mediated control of muscle formation (in review; PhD thesis) [Vallecillo García, 2016]. Cells expressing *Osr1* are located in between muscle fibers (fig.5D), partially co-expressing *Tcf4 in vivo* and other markers for connective tissue such as *Pdgfr*α *in vitro*. In mutants a muscle patterning phenotype (fig.6A, B), a reduced number of myogenic cells, impaired myogenic differentiation and terminal fusion of myoblasts to myofibers were observed. This phenotype was explained by *Osr1* regulated expression of various genes comprising the ECM including collagen type VI, and reduction of

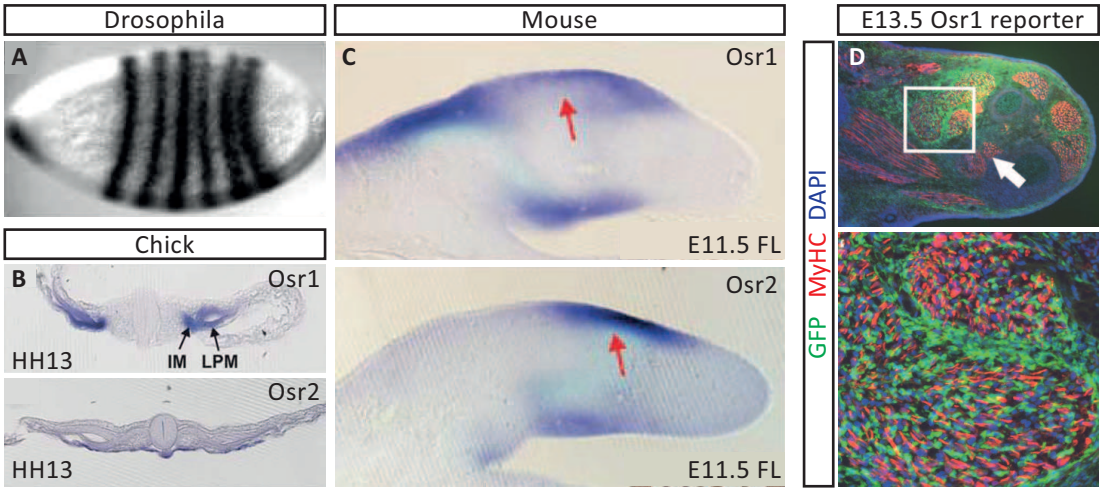

Figure 5: Osr expression pattern during embryonic development in Drosophila, chick and mouse.
A *Osr1* RNA in situ hybridization shows a stripe pattern during Drosophila segmentation [Saulier-Le Dréan et al., 1998]. **B** At developmental stage Hamburger Hamilton (HH) 13 of the chick *OSR* RNA *in situ* hybridization reveals expression pattern of *OSR1* in the intermediate (IM) and lateral plate mesoderm (LPM), *OSR2* in the endoderm [Stricker et al., 2006]. **C** *Osr* RNA *in situ* hybridization shows expression of *Osr1* and *Osr2* in mouse forelimbs (FL) of developmental stage E11.5. *Osr2* is expressed in distinct regions to *Osr1* (red arrows) [Stricker et al., 2006]. **D** Using an *Osr1*-GFP reporter mouse model *Osr1* expression on E13.5 hindlimbs is located in cells in between muscle fibers (MyHC) [Vallecillo García, 2016]. Box and arrow indicate magnified region below.

ECM component fibronectin on protein level. Thus, *Osr1* mutants show an impaired organization of the ECM. In consequence, the basal lamina delineating myofibers showed a disrupted morphology, as indicated by collagen IV staining. Furthermore, *Osr1* deficiency resulted in a decreased expression of cytokine *Cxcl12*. Signaling of CXCL12 and its receptor CXCR4, which is expressed in myogenic progenitors, were reported to be involved in muscle progenitor migration and maintenance [Rehimi et al., 2010, Vasyutina et al., 2005].

To study the fate of cells expressing *Osr1* at embryonic stage, lineage tracing experiments were performed. For these experiments so-called lineage tracer mouse models were utilized. These models enable permanent genetic labeling of specifically Osr1+ cells and identification of these cells at a later stage regardless gene expression at that time or occurred cell differentiation in the meantime. It was demonstrated that Osr1+ cells at E11.5 are non-myogenic (fig.6C) and contribute to interstitial cells at late fetal stage E18.5 (fig.6D).

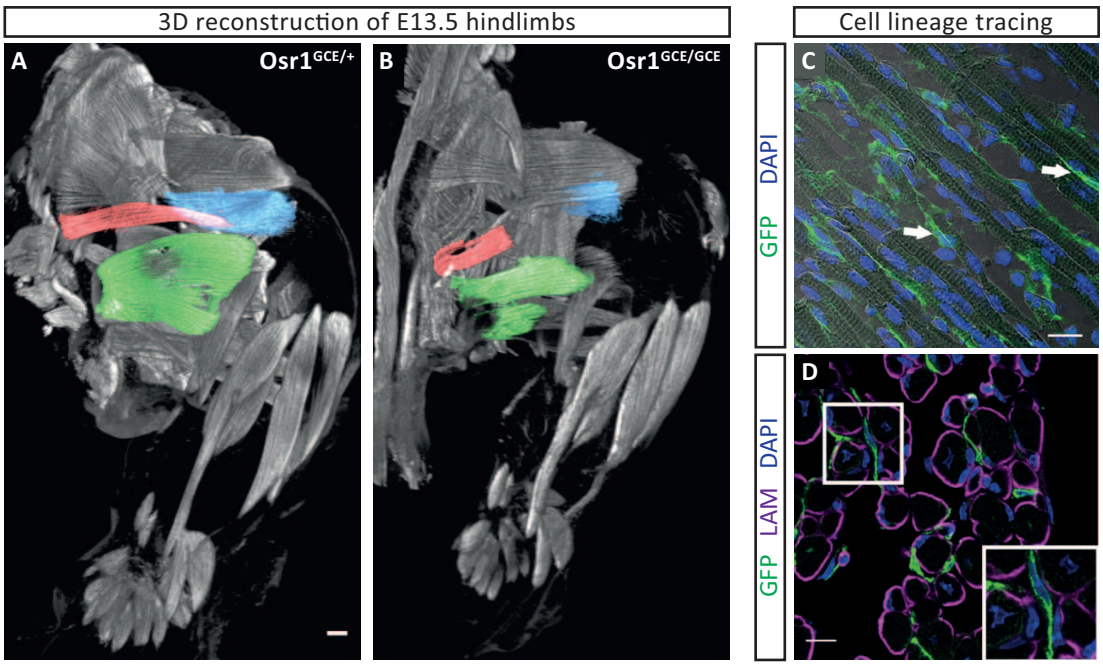

Figure 6: *Osr1* is expressed in non-myogenic cells and is required for muscle patterning. **A** Cell lineage tracing studies demonstrate non-myogenic potential of early embryonic Osr1+ cells. Cells were labeled (GFP) at E11.5 using a lineage tracer mouse model, and tissue analyzed at E18.5. Brightfield imaging indicates muscle fiber structures. **B** E11.5 Osr1+ cells give rise to muscle interstitial cells at E18.5. Myofiber basal laminae are stained for laminin. **C, D** 3D reconstruction of E13.5 hindlimbs of heterozygous (C) and homozygous (D) knock-outs of *Osr1*. Three highlighted muscles (blue, red, green) show patterning phenotype in homozygotes compared to heterozygotes. Images by Pedro Vallecillo García, 2016 [Vallecillo García, 2016].

1.6.1 Transient interstitial progenitor cell population

Muscle development is not completed at the time of birth. During the first 3 weeks after birth of the mouse this development proceeds in form of postnatal muscle growth. Early postnatal muscle represents a highly dynamic and developmentally active environment. As such it is subject of intensive research. While *Osr1* is expressed in muscle tissue throughout prenatal myogenesis, potential expression during this juvenile phase is not clear.

Recently, presence of a muscle resident cell population during the phase of juvenile muscle growth was reported [Mitchell et al., 2010, Pannérec et al., 2013]. This population is non-hematopoietic (CD45–/ Ter119–), positive for progenitor cell marker CD34 (CD34+) and shows medium expression of stem cells antigen-1 (Sca-1_{med}). During the first three weeks of age, this cell population progressively declines and is not detectable anymore in older specimen (fig.7) [Pannérec et al., 2013].

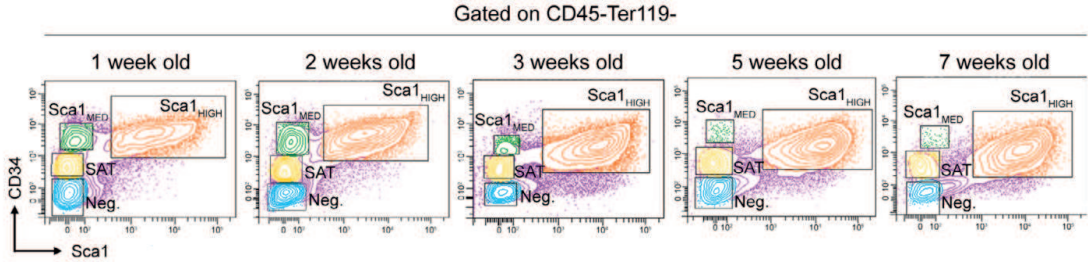

Figure 7: A transient, non-myogenic muscle interstitial cell population is present only during adolescence.
FACS sorting discriminates a non-hematopoietic (CD45–/ Ter119–) population CD34+/ Sca-1_{med} (green) distinct from myogenic progenitors (yellow) that decreases in number during the first 3 weeks of age and is not detectable anymore at older age [Pannérec et al., 2013].

PW1-expressing interstitial cells (PICs) are a muscle resident cell population characterized by expression of cell stress mediator PW1 [Mitchell et al., 2010]. During postnatal growth PICs are detectable in the transient cell population CD34+/ Sca-1_{med}, accounting for over 90% of this population in 1 week old mice [Mitchell et al., 2010]. By *in vitro* cultivation myogenic capacities were attributed to these juvenile PICs as they became positive for myogenic regulatory factor MyoD, although initially Pax7–. Engraftment of juvenile PICs into the *tibialis anterior* muscle indicated contribution to myofibers, but also to interstitial cells. Additionally, *in vitro* differentiation assays demonstrated smooth muscle fate and adipogenic differentiation potential [Pannérec et al., 2013], which is not the case for satellite cells. These observations indicate multiple potentials of the juvenile PW1+/ Pax7– PIC population. During the early postnatal muscle growth phase PICs express many genes essential for angiogenesis, including neural/ glial antigen 2 (NG2) [Dellavalle et al., 2007].

1.7 Aims of the study

The adult skeletal musculature is a complex system comprising various types of tissue. Its functionality requires muscle fiber contractions to provide forces. These forces are mediated by rigid connective tissue and transmitted to bones via tendons, resulting in directed movement. However, musculature is rather a homeostatic than a static system and requires constant maintenance.

This homeostatic balance is challenged by day-to-day wear or compromised by tissue damage in case of injury. After muscle injury, clearance of the affected tissue from debris is performed mainly by the immune system. However, interstitial fibro/ adipogenic progenitors were reported to possess phagocytic potential as well. Tissue resident cells prepare a pro-myogenic environment in which activated satellite cells can rebuild muscle mass. Angiogenic cells revascularize the regenerating tissue. These events are not implemented autonomously and independent of each other but require a carefully orchestrated coordination in the course of muscle regeneration.

During prenatal muscle development of the mouse, *Osr1* is expressed in muscle connective tissue. Connective tissue was proposed to regulate the muscle patterning and provide cues for an organized muscle formation. Functional studies demonstrated a crucial requirement of *Osr1* in this context. Lineage tracing experiments had indicated that embryonic Osr1+ cells give rise to muscle resident interstitial cells at the time of birth. Muscle development is not completed at birth but proceeds during the juvenile phase comprising the first 3 weeks after birth in terms of muscle growth. *Osr1* expression during this juvenile phase of muscle development as well as during muscle regeneration was not clarified.

The aim of this study was to investigate the expression of *Osr1* in postnatal situations of muscle development, such as the juvenile phase and muscle regeneration after injury, in mouse models.

Transient presence of interstitial cells was reported for the juvenile growth phase which might imply remaining activity of prenatal cell types. The observation that embryonic non-myogenic multipotent Osr1+ cells are functionally involved in muscle patterning and neonatally maintained as interstitial cells suggested a derived progenitor population in postnatal mice. Moreover, early fetal *Osr1* mutants show impaired fusion of myoblasts to myofibers. The process of myoblasts fusing to muscle fibers is particularly specific to the juvenile phase. Thus, involvement of *Osr1* expression during this developmentally active stage was presumed. By investigating potential postnatal Osr1+ cells further characterization of resident cells and elucidation of mechanisms underlying cellular interplay required for postnatal muscle growth was aspired.

Besides the focus on juvenile muscle growth, studies of *Osr1* expression after muscle injury in adult specimen were planned. Crucial requirement of muscle connective tissue was reported for effective muscle regeneration. Regeneration is considered a process of muscle development, which depends upon satellite cell activation, differentiation and fusion to muscle fibers. Furthermore, deposition of transient extracellular matrix is implemented. During prenatal myogenesis *Osr1* is expressed in muscle connective tissue where it is functionally involved in muscle precursor fusion to myofibers and extracellular matrix production. These observations lead to the assumption of an involvement of *Osr1* in the developmental phase of myogenic repair. Furthermore, identification and characterization of Osr1+ cells was planned, as well as the determination of their differentiation potential.

To investigate the functional role of *Osr1* in the tissue repair process, studies of muscle regeneration in *Osr1* deficient mice were planned. The aim was to further clarify and decypher the function of interstitial cells during muscle regeneration and provide a better understanding of the complex regenerative system.

2 Material

2.1 Instruments

Instruments used and their manufacturers are listed in table 1, separated in according categories.

Table 1: Instruments

Name	Supplier
Centrifuges	
Microtiterplate centrifuge 5416	Eppendorf
Microcentrifuge 5415 D	Eppendorf
Chilling centrifuge 5417 R	Eppendorf
Thermocyclers	
GeneAmp PCR System 2700	Applied Biosystems
GeneAmp PCR System 2720	Applied Biosystems
GeneAmp PCR System 9700	Applied Biosystems
ABIPrism HT 7900 Realtime Cycler	Applied Biosystems
Microscopy	
Microscope DMR	Leica
Camera AxioCam HRc	Zeiss
Microscope Axiovert 200M	Zeiss
Camera AxioCam MRm	Zeiss
Stereo microscope MZ6	Leica
Stereo microscope MZ7-5	Leica
Light source KL1500 LCD	Leica
LSM700	Zeiss
Histology	
Microtome Cool Cut HM355S	Microm
Cryotome H560	Microm
Embedding station EC 350-1&2	Microm
Dehydration stationTP 1020	Leica
Other instruments	
PIPETMAN Classic® P2	Gilson
PIPETMAN Classic® P20	Gilson
PIPETMAN Classic® P200	Gilson
PIPETMAN Classic® P1000	Gilson
Nanodrop	Thermo Scientific
TissueLyser	Qiagen
IKAMAG RET Magnetrührer #4236	IKA
Thermomixer comfort	Eppendorf
Thermomixer comfort	Eppendorf

2.2 Reagent Kits

Table 2 lists kits used and their main purpose.

Table 2: Reagent kits

Name	Manufacturer	Used for
QuickExtract™	Cambio	DNA extraction
RNeasy Mini Kit	Qiagen	RNA purification
PCR DIG Probe Labeling Kit	Roche	Southern Blot
NucleoSpin® Gel and PCR Clean-up	Macherey-Nagel	DNA purification
Wizard® Genomic DNA Purification Kit	Promega	DNA purification
SYBR® Green PCR Master Mix	Applied Biosystems™	qPCR
TaqMan® Reverse Transcription Reagents	Applied Biosystems™	cDNA synthesis

2.3 Enzymes

Restriction enzymes, ligases, polymerases and other DNA modifying enzymes were purchased from MBI Fermentas.

2.4 Chemicals

Unless denoted otherwise (tab.3), all chemicals were supplied by Merck (Darmstadt), Sigma-Aldrich (Deisenhofen) and Roth (Karlsruhe).

Table 3: Other chemicals

Name	Manufacturer	Used for
Ketamin	Gräub AG	Anesthetic
Xylazine (Rompun® 2%)	Bayer AG	Anesthetic
Dako Pen	Dako	Immunohistochemistry

2.5 Mouse strains

Mouse strains used and their references are listed in table 4. Animals at the age of 2-6 months were considered as adult.

Table 4: Mouse strains

Strain	Origin
Osr1-GCE	AP McMahon, University of California, USA [Mugford et al., 2008]
Osr1-MFA	Targeting vector by Aris Economides, Regeneron Inc., USA
ROSA26-lacZ	P Soriano, Dpt of Dev. and Regen. Biology, USA [Soriano, 1999]
ROSA-mTmG	L Luo, Stanford University, USA [Muzumdar et al., 2007]
Flpe deleter	Provided by Dr Heiner Schrewe, MPI-MG, Germany

2.5.1 Reporter/ Cre-deleter Osr1-GCE

The Osr1-GCE mouse line was provided by Andrew P. McMahon, University of California, USA. This mouse model contains a knock-in at exon 2 of the Osr1 gene. The start codon ATG at the beginning of exon 2 is replaced by a cassette carrying the gene for enhanced GFP (eGFP) and for the fusion protein CreERT2 (fig.8). Fusion of Estrogen Receptor Type 2 (ERT2) to Cre recombinase modifies the enzyme to be translocatable into the nucleus by estrogen derivates such as tamoxifen. While CreERT2 is located in the cytoplasma, induction by tamoxifen translocates it into the nucleus to perform genomic recombination. Replacement of the start codon on exon 2 by this cassette renders the Osr1 gene non-functional, thus causes an Osr1 knock-out. However, no phenotype due to haploinsufficiency was reported, indicating developmentally sufficient expression from only one allele [Mugford et al., 2008, Vallecillo García, 2016].

Figure 8: The Osr1-GCE allele.
In this mouse model the start codon ATG at the beginning of exon 2 is replaced by a CreERT2 gene cassette (green, blue), the remaining part of exon 2 is non-functional. Both genes, eGFP and Cre, are linked by an IRES site (orange) to provide identical expression of both genes.

2.5.2 Multifunctional mouse line Osr1-MFA

The generation of an Osr1-MultiFunctionalAllele (Osr1-MFA) mouse line, as described below, was based on a construct provided by Aris Economides of Regeneron Inc., USA. This construct was designed for homologous recombination of the Osr1 locus in murine embryonic stem cells (mESCs). While the 5' homology arm is located in the

first intron, and the 3' homology arm downstream of the third exon, these arms flank the last 2 of in total 3 exons. A successfully recombined locus features a knocked in lacZ/ neomycin gene cassette, and an inverted exon 2 (fig.9). Hence, transgenic mice carrying this allele are Osr1 knock-out lacZ reporter mice. Furthermore, included FRT and FRT3 sites enable the generation of conditional Osr1 knock-out mice by crossings with mouse lines that ubiquitously express flippase (Flpe deleters). Two FRT sites span the lacZ/ neomycin cassette and the inverted exon, both FRT3 sites only flank exon 2, whereas the downstream FRT3 site is located outside the FRT marked region. Both pairs FRT and FRT3 are each oriented in an opposing way. This enables flipping of exon 2 into sense direction and excision of the lacZ/ neomycin cassette at the same time. Resulting, exon 2 and an inverted non-functional eGFP gene is flanked by *lox2372* sites, similar to FRT sites in the previous step. *LoxP* sites only span eGFP. Again both element pairs *lox2372* and *loxP* are oriented conversely. Here, Cre recombinase can flip the region according to the *lox2372* sites and subsequently excise between both *loxP* sites. Thus, exon 2 is eliminated rendering the Osr1 gene non-functional, and eGFP flipped in sense direction, essentially resulting in a knock-out eGFP reporter.

Figure 9: The Osr1-MFA allele.
This transgenic allele replaces the last 2 of 3 exons of the Osr1 gene. While it functions as an Osr1 knock-out lacZ reporter, it contains FRT (blue triangles) and FRT3 (orange triangles) elements to enable flipase to recombine the locus into a conditional knock-out. After recombination the allele provides a functional Osr1 gene, featuring *lox2372* (red arrow) and *loxP* (purple arrow) sites for Cre recombination into a Osr1 knock-out eGFP reporter.

2.5.3 Lineage tracer mouse lines ROSA26-lacZ and ROSA26-mTmG

ROSA26-lacZ and ROSA26-mTmG mouse lines feature reporter genes incorporated into the ROSA26 locus, which provides constitutive, ubiquitous gene expression. ROSA26-lacZ mice contain a lacZ reporter gene with a preceding *loxP* flanked stop codon that renders the reporter gene inactive. Cre-mediated recombination of this locus excises the stop codon and lacZ will be permanently expressed in this and descendant cells. Comparably, ROSA26-mTmG mice contain a cassette consisting of a membranous Tomato (mT; mTOM) fluorescent dye and a consecutive stop codon, both flanked by *loxP* sites. Following these 2 elements a gene for membranous GFP (mG; mGFP) fluorescent dye resides. Cre-mediated recombination excises mT and removes the stop codon for mG will be permanently expressed. This genetic labeling is inherited to descendant cells.

Osr1$^{GCE/+}$ were crossed with ROSA26$^{lacZ/lacZ}$ or ROSA26$^{mTmG/mTmG}$, respectively, to obtain mice heterozygous for both the Osr1-GCE allele and the ROSA26 reporter allele. This results in lineage tracer mouse lines Osr1-ROSA26lacZ and Osr1-ROSA26mTmG. After inducing the Cre from the Osr1-GCE allele by intraperitoneal tamoxifen injection ROSA26 reporter alleles are recombined in case of current Osr1 expression. This leads to a genomic labeling of these cells by permanent expression of either mG or lacZ (see fig.11 and 10). By cell division this labeling is inherited to descendant cells.

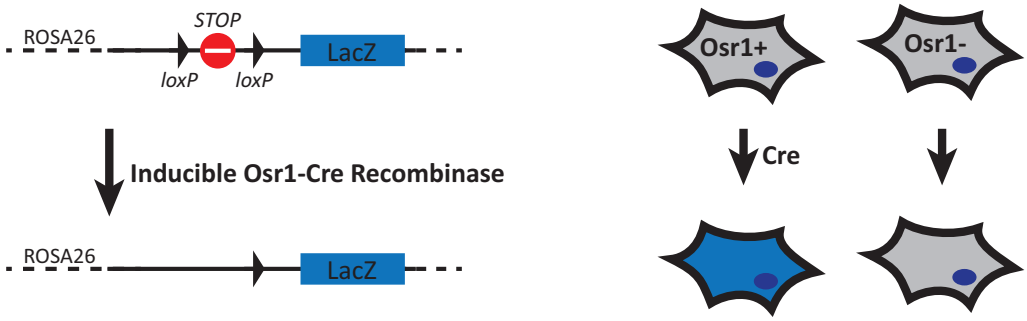

Figure 10: Osr1-ROSA26lacZ lineage tracer mouse line.
Osr1-ROSA26lacZ lineage tracer mice carry a lacZ gene inactivated by a preceding floxed stop codon. Upon induction of the inducible Osr1 promotor driven Cre by tamoxifen this stop codon is floxed out. All cells expressing Osr1 at the time of induction, and their descendants, will be permanently labeled by lacZ expression.

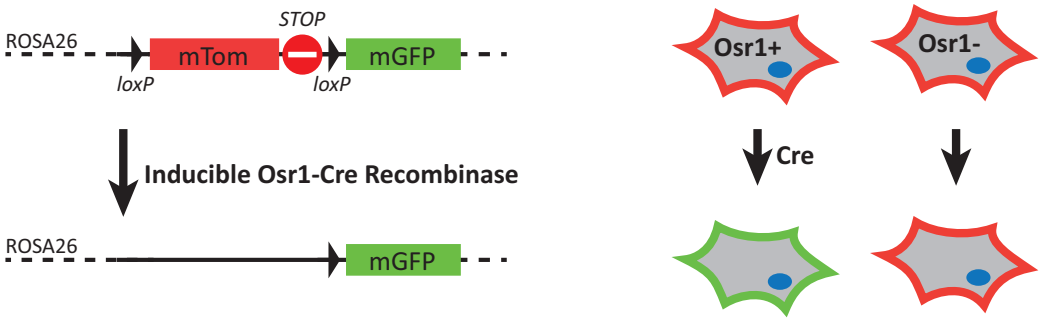

Figure 11: Osr1-ROSA26mTmG lineage tracer mouse line.
The Osr1-ROSA26mTmG lineage tracer mouse line features an inducible Osr1-driven Cre and an mTmG gene cassette. This cassette ubiquitously expresses mT. Upon induction of Cre by tamoxifen administration the mTmG cassette is recombined and the mT gene including its terminating stop codon deleted from the genome exclusively in cells expressing Osr1 at the time of induction. These cells will permanently express mG instead, regardless genes expressed or progressive cell differentiation.

2.6 Buffers

Buffers used and their components are listed in table 5. They were prepared in bidistilled H_2O if not particularly noted. If not mentioned otherwise, all other solutions were prepared according to Sambrook, et al. 2001.

Table 5: Buffers

Name	Components	Used for
Acetylation Buffer	10% FCS 1.3% triethiloamine 0.15% fuming HCl	RNA in situ hybridization
Prehybridization Buffer	25% formamide 5x SSC 5x Denhardt's solution in DEPC-H_2O	RNA in situ hybridization
TNB (Blocking Buffer)	0.1M TRIS-HCl, pH 7.5 0.15M NaCl 0.5% Blocking reagent in DEPC-H_2O	RNA in situ hybridization
TNT (Washing buffer)	0.1M TRIS-HCl, pH 7.5 0.15M NaCl 0.05% Tween 20 in DEPC-H_2O	RNA in situ hybridization
Denaturation Solution	0.5M NaOH 1.5M NaCl	Southern blotting
Neutralization Solution	0.5M Tris-HCl pH 7.5 1.5M NaCl	Southern blotting
1M NaPi	1M Na_2HPO_4 H_3PO_4 to pH7.2	Southern blotting
10xDIG1	1M Maleic acid 1.5M NaCl NaOH to pH7.5	Southern blotting
Church Washing Buffer	40mM NaPi 1%SDS	Southern blotting
Church Hybridization Buffer	0.5mM NaPi 7% SDS 1mM EDTA pH8.0	Southern blotting
DIG3	100mM Tris pH9.5 100mM NaCl	Southern blotting

2.7 Antibodies

Primary and secondary antibodies used and their specifics are listed in table 6.

Table 6: Antibodies

Name	Host	Supplier
Primary antibodies		
anti-GFP (ab13970)	chicken	Abcam, Cambridge, UK
anti-β-gal (40-1a)	mouse	DSHB, Iowa, USA
anti-Laminin (L9393)	rabbit	Sigma-Aldrich, Taufkirchen, Germany
anti-Col4 (AB769)	goat	Merck Millipore, Darmstadt, Germany
anti-PDGFRα (ab61219)	rabbit	Abcam, Cambridge, UK
anti-PDGFRβ [Y92](ab32570)	rabbit	Abcam, Cambridge, UK
anti-NG2 (AB5320)	rabbit	Merck Millipore, Darmstadt, Germany
anti-TCF4 [C48H11](2569S)	rabbit	Cell Signaling, Danvers, USA
anti-αSMA (ab5694)	rabbit	Abcam, Cambridge, UK
anti-Perilipin A/B (P1873)	rabbit	Sigma-Aldrich, Taufkirchen, Germany
anti-CD31 (2H8)	hamster	DSHB, Iowa, USA
Secondary antibodies		
Alexa Fluor 488 anti chicken (A-11039)	goat	Molecular Probes
Alexa Fluor 488 anti mouse (A-21202)	donkey	Molecular Probes
Alexa Fluor 568 anti rabbit (A-11011)	goat	Molecular Probes
Streptavidine-Alexa Fluor 488	-	Molecular Probes
FACS antibodies		
anti-Ter119(APC)(557909)	rat	BD Biosciences, New Jersey, USA
anti-CD45(APC)(559864)	rat	BD Biosciences, New Jersey, USA
anti-Sca-1(AlexaFluor®700)(56-5981-82)	mouse	eBioscience, San Diego, USA
anti-CD34(eFluor®450)(48-0341-82)	mouse	eBioscience, San Diego, USA
anti-PDGFRα(PE)(12-1401-81)	mouse	eBioscience, San Diego, USA

2.8 Primers

A list of all primers and according sequences are listed in table 7-8. PCR primers were designed using BiSearch (http://bisearch.enzim.hu/).

Table 7: Common primers

Name	Sequence 5' -> 3'	Used for
mTmG-wt-F	CTCTGCTGCCTCCTGGCTTCT	Genotpying mTmG
mTmG-wt-R	CGAGGCGGATCACAAGCAATA	Genotpying mTmG
mTmG-mut-R	TCAATGGGCGGGGGTCGTT	Genotpying mTmG
GCE-com-F	CCCTCTTCCTGTCTTTGCAG	Genotpying Osr1-GCE
GCE-mut-R	GTAGGTCAGGGTGGTCACGA	Genotpying Osr1-GCE
GCE-wt-R	CTGGCTTAGGGTGAATGACG	Genotpying Osr1-GCE
TU1-F	TCCTGCATTTCGTACAGGGTT	Osr1-MFA CNV qPCR
TU1-R	ACGCTGTCCTACAACAATATCAGA	Osr1-MFA CNV qPCR
TU2-F	GCATGCCATGTTTGCATCGTT	Osr1-MFA CNV qPCR
TU2-R	GGCAGAGACATACATGTTGACA	Osr1-MFA CNV qPCR
Albumin-qPCR-F	CTGCAATCCTGAACCGTGT	qPCR CNV control
Albumin-qPCR-R	TTCCACCAGGGATCCACTAC	qPCR CNV control
MFA-F	ATGGTGAGCAAGGGCGAGGAG	Genotpying Osr1-MFA
MFA-R	CGGTGGTGCAGATGAACTTCAGGG	Genotpying Osr1-MFA
FLOX-F	GCTTAGAATTCAGGAACTGGG	Genotpying Osr1-FLOX
FLOX-R	CTGGCAGAGACATACATGTTG	Genotpying Osr1-FLOX
FLOX-wt-F	GCTTAGAATTCAGGAACTGGG	Excision-PCR Osr1-KO
FLOX-ex-R	CTGTTTCTGGGGTTGTGAGT	Excision-PCR Osr1-KO
Osr1-qPCR-F	TGTAGCGTCTTGTGAACAGC	qPCR Osr1
Osr1-qPCR-R	GCACACTGATGAGCGACCT	qPCR Osr1
GAPDH-qPCR-F	CTGCACCACCAACTGCTTAG	qPCR Housekeeping
GAPDH-qPCR-R	GGATGCAGGGATGATGTTCT	qPCR Housekeeping

Table 8: Oligonucleotides for Southern blot probe generation

Name	Sequence 5' -> 3'	Used for
Neo-probe-F	CCACAGTCGATGAATCCAGAAAAG	Neomycin SB probe
Neo-probe-R	TTTTGTCAAGACCGACCTGTCCG	Neomycin SB probe
MFA-probe-F	GATCTCCGTGAAAGTGAGAGCAGTT	5'Osr1-MFA SB probe
MFA-probe-R	CCCAAGCAGAGTCCAATTGTGAGGT	5'Osr1-MFA SB probe

2.9 Software and web tools

Microsoft Office 2010	Microsoft
NCBI	http://www.ncbi.nlm.nih.gov/
UCSC Genome Browser	https://genome.ucsc.edu/
Ensembl	http://www.ensembl.org/index.html
Vector NTI®	Thermo Fisher Scientific
SeqMan	DNASTAR
FlowJo	FlowJo Enterprise
BLAST	http://blast.ncbi.nlm.nih.gov/Blast.cgi
SDS v2.4	Applied Biosystems
qbase+	Biogazelle
Fermentas DoubleDigest™	http://www.fermentas.com/en/tools/doubledigest
ZEN	ZEISS
AxioVision SE64 Rel.4.9	ZEISS
Reference Manager	Mendeley
Adobe CS6	Adobe Systems
CorelDraw X7	Corel Corporation
LaTeX MiKTeX 2.9	http://miktex.org/
LaTeX TeXnicCenter 2.02	http://www.texniccenter.org/

3 Methods

3.1 Animal related methods

3.1.1 Cell lineage tracing

Cells expressing a particular gene can be permanently labeled, which enables cell fate tracking across cell differentiation events. Cells will remain labeled even if they do not express the original gene anymore. This lineage tracing can be achieved *in vivo* by utilizing specific transgenic mouse lines.

Cre-mediated recombination of such lineage tracer mouse strains can be achieved by crossing with Cre expressing mouse strains. The Osr1-GCE mouse strain used contains an inducible CreERT2. This Cre enzyme is fused to the estrogen receptor type 2, by which it will remain in the cytoplasma. Tamoxifen binds to the estrogen receptor of the fusion protein and induces a translocation into the nucleus, where Cre-mediated recombination of DNA takes place.

Induction of Cre in neonatal specimen was performed by subcutaneous injection of 75µg tamoxifen (tamoxifen solution: 3µg/ µl in 90% sunflower oil/ 10% ethanol) into the neck fold using a Hamilton syringe. Adult mice were injected 3mg tamoxifen (tamoxifen solution: 20µg/ µl in 90% sunflower oil/ 10% ethanol) intraperitoneally using an 0.6mm syringe needle.

3.1.2 Freeze/ pierce injury

Mechanical injuries were applied to mice by freeze/ pierce technique. Mice were narcotized by intraperitoneal injection (0.45mm syringe) of 5µl/g bodyweight anesthetic consisting of 10% ketamine anesthetic and 2% xylazine analgetic in sterile PBS. Once sedated, mice were fixed on a heating plate warmed to 37°C using adhesive tape throughout the procedure. Calves were shaved and the skin opened above the *tibialis anterior* muscle by scalpels. Syringe needles (0.7mm) were cooled in liquid nitrogen and used to pierce the *tibialis anterior* muscle longitudinally 5 times. Finally, the wound was surgically sutured. Until recovery from anesthesia mice were kept in cages on heating plates warmed to 37°C.

3.1.3 Glycerol induced injury

Application of glycerol induced injuries was performed by intramuscular injection (0.45mm syringe) of glycerol into the *tibialis anterior* muscle. Mice were narcotized by intraperitoneal injection (0.45mm syringe) of 5µl/g bodyweight anesthetic consisting of 10% ketamine anesthetic and 2% xylazine (Rompun® 2%) analgetic in

sterile PBS. Once sedated, mice were fixed on a heating plate warmed to 37°C using adhesive tape during the procedure. The calves of the anesthesized mice were shaved, and 25µl of 50% v/v glycerol/sterile PBS injected. Until coming out from anesthesia mice were kept in cages on heating plates warmed to 37°C.

3.2 Molecularbiological methods

3.2.1 Extraction of genomic DNA

3.2.1.1 For genotyping

To determine the genotype of mouse specimen Genomic DNA was isolated from tailtips or ear biopsies, provided by the animal facility, using Cambio QuickExtract™ according the manufacturers protocol.

3.2.1.2 For sequencing

To obtain genomic DNA in order to PCR amplify particular loci for subsequent DNA sequencing Promega Wizard® Genomic DNA Purification Kit was utilized. With buffers included tissue is lysed, cell debris and protein precipitated, and remaining DNA washed and pelleted for purification. The procedure was performed according to the manufacturers recommendation.

3.2.2 Extraction of RNA

For the isolation of RNA from murine tissue, an amount of tissue recommended by the manufacturer of the Qiagen RNeasy Mini Kit was dissected and minced in 350µl RLT Buffer using scissors. The minced tissue in RLT Buffer was homogenized using a Qiagen TissueLyser and 5mm metal balls. Homogenization was performed in successive steps, each for 30s at maximum speed. Samples were cooled on ice for 3min in between each step. Final purification of RNA was performed using the Qiagen RNeasy Mini Kit according to the corresponding protocol.

3.2.3 Generation of cDNA

For expression analysis by quantitative RT-PCR (qPCR) cDNA from RNA was generated using the TaqMan Reverse Transcription Reagents (Applied Biosystems). After assessment of sample RNA concentration using a Thermo Scientific Nanodrop 1µg total RNA was transcribed in a 50µl reaction using random hexamers according to the vendors recommendations.

3.2.4 Polymerase chain reaction

3.2.4.1 Genotyping PCR

To determine the genotype of transgenic mice, previously extracted genomic DNA was subjected to polymerase chain reaction (PCR). The reagents were mixed in a ratio according to the standard PCR protocol (Tab.9) and pipetted into a chilled 0.2ml tube. Depending on the mouse strain to be genotyped, a standard PCR cycler program (Tab.10) adapted to each primers and their conditions was used (Tab.11).

Table 9: Standard PCR protocol

Amount	Reagent
20-100 ng	DNA template
2,5 µl	10x reaction buffer (provided by the institute)
1,5 µl	dNTPs (1,25 mM, Fermentas)
1 µl	5'-primer (10 µM)
1 µl	3'-primer (10 µM)
0,5 µl	DNA polymerase
add to 25µl with dd H_2O	

Table 10: Standard PCR conditions

Phase	Temperature	Time	Cycles
Initial denaturation	94°C	3min	
Denaturation	94°C	30s	
Primer annealing	depends on T_m	30s	25 - 35 cycles
Elongation	72°C	1min/ 1kb	
Final elongation	72°C	7min	
End	4°C	∞	

3.2.4.2 Relative real-time qPCR

Gene expression levels in tissue samples were assessed performing quantitative PCR (qPCR) using cDNA from previous reverse transcription of RNA.

Quantification of DNA is enabled by intercalation of green fluorescent SYBR® into double stranded DNA during the elongation step of the PCR. Fluorescence occurs only after intercalation, the exponential increase of fluorescent signal per amplification step is measured in real-time. Referencing fluorescent signal emission of a target of interest

Table 11: Primers, adapted PCR program conditions and expected product sizes

Primer name	Primer sequence	T_a	Product length
GCE-com-F GCE-mut-R GCE-wt-R	CCCTCTTCCTGTCTTTGCAG GTAGGTCAGGGTGGTCACGA CTGGCTTAGGGTGAATGACG	60°C	MUT: 300bp WT: 355bp
Osr1MFA-F Osr1MFA-R	ATGGTGAGCAAGGGCGAGGAG CGGTGGTGCAGATGAACTTCAGGG	60°C	MUT: 160bp
mTmG-wt-F mTmG-wt-R mTmG-mut-R	CTCTGCTGCCTCCTGGCTTCT CGAGGCGGATCACAAGCAATA TCAATGGGCGGGGGTCGTT	61°C	MUT: 250bp WT: 330bp
Rosa26-wt-F Rosa26-mut-F Rosa26-R	GCGAAGAGTTTGTCCTCAACC GGAGCGGGAGAAATGGATATG AAAGTCGCTCTGAGTTGTTAT	58°C	MUT: 650bp WT: 340bp
FLOX-F FLOX-R	GCTTAGAATTCAGGAACTGGG CTGGCAGAGACATACATGTTG	55°C	MUT: 295bp WT: 356bp
FLOX-wt-F FLOX-ex-R	GCTTAGAATTCAGGAACTGGG CTGTTTCTGGGGTTGTGAGT	57°C	MUT: 395bp

to a housekeeping gene expressed equally among samples studied allows for relative quantification and quantitative comparison.

Utilizing the Applied Biosystems™ SYBR® Green PCR Master Mix the reaction was carried out according to the manufacturers recommendation. Depending on the expected expression level 4-16ng cDNA as a template, 4.5pmol of forward and reverse primer and 50% 2x SYBR Green PCR Master Mix were used per reaction. Primers for qPCR were designed to span introns in order to exclude genomic DNA amplification potentially contaminating the specimen which falsifies the result. Standard curves were generated by 1:2 dilution series starting with 4-16ng cDNA decreasing to 0.25-1ng cDNA. Relative quantification was achieved by calibrating the individual cDNAs to their corresponding levels of housekeeping gene GAPDH.

The reaction was performed in 384 well plates in a volume of 12 µl on an ABIPrism HT 7900 Real-time Cycler. Final data analysis was carried out utilizing qBase+ software.

3.2.5 Agarose gel electroporation

Visualization of PCR reactions for further analyses was achieved by separation of DNA on an agarose gel, supplemented with ethidium bromide.

Agarose in TAE buffer forms a gel containing pores of size depending on the agarose concentration. Voltage applied to an agarose gel drives DNA, negatively charged by

phosphate groups, towards the anode. DNA of different sizes move with different speed, which allows for separating different products. Preparing the agarose gel with ethidium bromide enables final detection of DNA. Ethidium bromide intercalates into DNA, thus acquiring fluorescent properties by which DNA can be visualized. Evaluation of product sizes results from comparison with a DNA ladder that consists of DNA fragments of defined sizes.

Agarose gels were prepared with concentrations of agarose depending on the expected PCR product size. For products of 500bp and less 2% of agarose were used, for larger products 1.5%. 10 µl of DNA ladder was applied.

3.2.6 Sanger sequencing

Sequencing was performed by Mohsen Karbasiyan (Institute for Medical Genetics, Charité Berlin) on a ABI 3700 capillary sequencer (Applied Biosystems).The sequencing-PCR was set up using BigDye v3.1 (Applied Biosystems), according to the specifications of the manufacturer. The reaction was cleaned up with ethanol precipitation before it was transferred to the Charité for capillary electrophoresis.

3.2.7 Southern blotting

By Southern blotting technique specific genomic content can be verified. While this can be achieved by PCR methods as well, Southern blotting enables to confirm the local context of DNA elements more reliably. Genomic DNA is digested using restriction enzymes to yield a fragment of known size, and separated on an agarose gel. Separated DNA fragments on the agarose gel are blotted, that is transferred, to a nylon membrane. This is achieved by capillary action moving DNA from the gel onto the membrane placed on top of the gel. PCR generated DNA probes, complementary to the DNA sequence of the target fragment, are hybridized to the specific target fragment on the membrane. Hybridization is enabled by prior denaturation of both target DNA and probe DNA resulting in single stranded DNA. Labeling of these probes enables visualization of the hybridized fragment and analysis of the expected fragment size.

To obtain the Osr1-MFA probe complementary to a region upstream of the 5' homology arm of the transgenic construct, a PCR was performed using mouse genomic DNA as a template. The PCR product was separated on an agarose gel, the expected band corresponding to 501bp excised and purified using the NucleoSpin® Gel and PCR Clean-up kit according to the vendors manual. The already purified PCR product for the neomycin probe was provided by the laboratory. Final generation of labeled probes based on these products was performed utilizing the PCR DIG Probe Labeling

Kit following the manufacturers recommendation. The ratio of labeled to unlabeled oligonucleotides was 1:4.5.

Homologous recombination using the Osr1-MFA vector construct in murine embryonic stem cells was performed by Dr Heiner Schrewe (Department of Developmental Genetics, Max-Planck-Institute for Molecular Genetics), who also provided purified DNA of 192 expanded clones.

10µg DNA were digested with 5µl restriction enzyme BamHI in a 40µl reaction volume at 37°C overnight. This volume, together with 4µl of labeled ladder, was separated on a 1% agarose gel by 90V for 5h. The DNA inside the gel was denatured by incubation of the gel in Denaturation Solution for 30min at RT, gently agitated on a tumbler. To neutralize the denaturing salts in the gel 2 incubation steps in Neutralization Solution for 20min each on a tumbler followed.

In a tray filled with 10x SSC on top of an extension block Whatman paper was placed, overlapping the block to reach down into the SSC solution. 2 more sheets of Whatman paper matching the size of the gel were positioned on top, followed by the gel up side down. The nylon membrane was placed on the gel, again followed by 2 more sheets of Whatman paper. A batch of paper towels was sited on top to provide suction force through the gel into the membrane. Saran wrap surrounding the gel/ membrane stack prevented contact of the paper towels with surrounding Whatman paper, thus avoided a fluid stream circumventing the gel. Sealing of the entire setup using Saran wrap prevented drying-out during the blotting, which was enhanced by a weight on top of the stack. The transfer was performed overnight.

The membrane now containing the DNA was washed with 50mM NaPi for 5min gently agitated at RT. Placed in between Whatman paper for protection, the membrane was baked at 80°C for 2h to crosslink the DNA to the membrane surface. The membrane was moistened with bidistilled H_2O, and incubated in 25ml Church Hybridization Solution in a glass bottle at 65°C for 30min on a rolling device. 4µl of labeled probe was diluted in 25ml Church Hybridization Solution and heated in boiling water for 10min to denature the DNA probes. The membrane was incubated with this probe containing solution at 65°C overnight.

To remove unbound probe the membrane was washed with pre-heated Church Washing Buffer at 65°C for 10min rotating, followed by a washing step with the same buffer at RT for 10min gently agitated on a tumbler. A washing step at RT for 5min with 1x DIG1+0.3% Tween further removed unbound probe and prepared the membrane for blocking. Sealed in a plastic bag the membrane was incubated with 1x DIG1 supplemented with 10% Blocking Reagent for 30min at RT under vigorous agitation. This blocking step reduced unspecific binding of the antibody and background signal. The blocking solution was replaced with Blocking Reagent containing alkaline

phosphatase-coupled anti-DIG antibody diluted 1:20,000, and incubation for 30min at RT under vigorous agitation followed. Unbound antibody was removed by washing the membrane in 1x DIG1+0.3% Tween twice, at RT for 20min gently agitated each. A washing step in DIG3 for 5min at RT removed detergent remainder.

Signal development was performed by incubation of the membrane in CDP-*Star*® according to the manufacturers recommendations. Detection occured by exposing the membrane to a film, which was developed for analysis.

3.2.8 Fluorescence-activated cell sorting (FACS)

3.2.8.1 Preparation of single cell suspensions from murine skeletal muscle tissue

Mice were sacrificed and either *tibialis anterior* muscles or total hindlimb muscle was dissected. Tissue was minced in HBSS+ (HBSS with 1% P/S and 0.2% BSA), transferred to a 15ml Falcon tube in 10ml HBSS+ and centrifuged for 10sec at 300g. The supernatant containing fatty remains was removed and the tissue resuspended in 4ml Dissociation Solution (Tab.12) per 1g tissue. The dissociation was performed at 37°C for 90-120min, with vigorous vortexing every 10min. The final homogenous suspension was washed 3 times including successive straining through 100µm, 70µm and 40µm cell strainers.

Table 12: Dissociation Solution

Component	Concentration
Dispase II	2.4 U/ ml
Collagenase A	2µg/ ml
$CaCl_2$	0.4 mM
$MgCl_2$	5 mM
DNase I	10 ng/ ml
in HBSS	

3.2.8.2 Immunostaining of single cell suspensions for FACS

To prepare the cells for FACS antibody staining, cells of 6 adult *tibialis anterior* muscles or total hindlimb muscles of 1-2 adult mice were resuspended in 400µl HBSS++ (HBSS+ with 5ng/ ml DNase I). For blocking 1/10 vol. mouse serum was added to the suspension, followed by incubation on ice for 5min. After adding 20µl of each fluorescently labeled FACS antibody the cells were incubated for 1h on ice protected from light. The cells were washed 3 times in HBSS+ followed by centrifugation at 4°C for 5min at 300g each time, and resuspended in 300µl HBSS+. The cells were ready now for flow cytometry analysis, unless additional lacZ staining was required.

For lacZ staining of cells for FACS, the 300µl suspension was supplemented with 60µM final concentration C_{12}FDG, and incubated at 37°C for 1h protected from light. After washing 2 times in HBSS+ cells were spinned down in a centrifuge at 4°C for 5min at 300g.

3.2.8.3 Purification of single cells by FACS

To obtain a single cell suspension from adult muscle tissue in order to purify particular cell populations, a method previously described was adapted [Pannérec et al., 2013]. This method is based on FACS, which makes use of cell surface proteins as cell type specific markers. In a standardized procedure [Julius et al., 1972] cell debris and conglomerates are excluded from further analysis by light scatters. Subsequently, endothelial and hematopoietic cells and their precursors are negatively selected by distinguishing them using fluorophore coupled antibodies against specific markers CD45 and Ter119, respectively. The remaining cells were then gated on their CD34 and Sca1 expression, both markers for stem cells with different characteristics. This results in a separation of populations containing myogenic precursors (CD34+/Sca1–), osteogenic/ chondrogenic precursors (CD34–/Sca1–) and Fibro/ Adipogenic Progenitors (FAPs) (CD34+/$Sca1_{high}$). Only present during the first 3 weeks after birth a fourth population can be detected (CD34+/$Sca1_{med}$). FAPs can be further purified by gating the CD34+/$Sca1_{high}$ population on PDGFRα.
Identification of *Osr1* expressing cells was enabled by Osr1-lacZ reporter mice. The non-fluorescent substrate C_{12}FDG enters living cells, where it is metabolized by the enzyme β-galactosidase which is expressed under the control of the *Osr1* promoter. This results in the production of a fluorescent dye retained by the cell.
Tab.13 shows the antibodies used, their marker characteristics and fluorophores.

Table 13: FACS antibodies and dyes

Antigen/ substrate	Marker	Fluorophore	Excitation/ Emission (nm)
CD45	Endothelial	APC	650/660
Ter119	Hematopoietic	APC	650/660
CD34	Stem cells	E450	410/455
Sca1	Stem cells	A700	695/716
PDGFRα	Specific	PE	565/570
C_{12}FDG	β-gal substrate	-	490/514

3.3 Histological methods

3.3.1 Paraffin embedding and sectioning

Mice were sacrificed by cervical dislocation and dissected tissue immediatelly fixed in 4% PFA in PBS for 1h at RT. Subsequently, the tissue was washed 3 times in PBS, followed by dehydration for 30min in 50% ethanol in bidistilled H_2O, and further dehydrated in 70% ethanol in bidistilled H_2O over night, both at 4°C. Progressive dehydration and final paraffin impregnation was performed utilizing an automated device, set for a program described in table 14.

Table 14: Automated dehydration program for paraffin embedding

Reagent	Duration
90% ethanol	3h
95% ethanol	3h
100% ethanol	1h
100% ethanol	1h
100% ethanol	1h
UltraClear	15min
UltraClear	15min
UltraClear	30min
UltraClear/ paraffin	3h
Paraffin	3h

Paraffin impregnated tissue was embedded in paraffin in the desired orientation and sectioned using a microtome. Tissue was processed into sections of 6µm thickness, and dried over night at 37°C.

3.3.2 RNA *in situ* hybridization on paraffin sections

RNA *in situ* hybridization technique is an application to visualize specific mRNA on tissue sections, thus enables to analyze particular gene transcription in a tissue context. Labeled single stranded RNA probes are hybridized to their complementary target RNA on tissue sections. Via their labeling they can be visualized by fluorescent signal or biochemical color reaction and microscopically analyzed.

To obtain an RNA probe for *Osr1* mRNA hybridization vectors carrying the appropriate sequence [Stricker et al., 2006] were *in vitro* transcribed and labeled by incorporation of DIG coupled UTP nucleotides. This procedure was performed using the Roche DIG RNA Labeling Kit following the vendors manual.

Sectioned paraffin tissue was prepared by deparaffinization and rehydration. In subsequent steps sections were treated with 45min UltraClear, 2min 100% ethanol,

2min UltraClear, 2min 95% ethanol in bidistilled H_2O, 2min 90% ethanol in bidistilled H_2O, 2min 70% ethanol in bidistilled H_2O, and 3 washing steps in bidistilled H_2O for 5min each.

3.3.2.1 Fluorescent RNA in *situ* hybridization

For reducing hydrogen bondings sectioned tissue was acetylated in Acetylation Buffer for 10min at RT under stirring on a magnetic stirrer. 3 washing steps of 5min at RT in PBS followed. Sections were rinsed in DEPC-PBS, then potential protein interferences were reduced and enzymes degraded by tissue treatment with 1µg/ml proteinase K in DEPC-PBS for 5min at RT. Another 3 washing steps in DEPC-PBS for 5min at RT followed. To prepare the tissue for probe hybridization sections were incubated in Prehybridization Buffer under parafilm cover slips for 5h at RT in a humidified chamber. The priorly DIG labeled probe was diluted 1:200 in Prehybridization Buffer, denatured for 5min at 85°C in a thermomixer, then chilled on ice. Slides were incubated with this hybridization solution under parafilm cover slips, avoiding air bubbles, overnight at 65°C, in a chamber humidified with 50% formamide and 5x SSC.
To wash away hybridization solution, excess and unbound probe sections were washed in 2x SSC for 5min at RT, incubated in 0.2x SSC for 1h at 65°C and rinsed in 0.2x SSC at RT for 5min. For further signal detection tissues were blocked in TNB for 45min at RT under parafilm cover slips. The blocking buffer was replaced with peroxidase-coupled anti-DIG antibody (Roche #11207733910) diluted 1:100 in TNB, and sections were subjected to incubation under parafilm cover slips at RT for 30min. The slides were washed 3 times at RT in TNT, before a signal amplification step was performed. Biotinyl tyramide diluted 1:50 in amplification diluent, according to the manufacturer, was applied to the sections, and incubated for 6min at RT. Biotin is cleaved from tyramide by peroxidase and covalently bound to immediate surrounding tissue. After 3 successive washing steps with TNT at RT for 5min each, sections were incubated with AlexaFluor488®-coupled streptavidin diluted 1:100 in TNB, further supplemented with DAPI 1:2000, for 45min at RT.

After 3 final washing steps in TNT for 5min each at RT, sections were mounted in Fluoromount-G®.

3.3.2.2 BCIP/ NBT color RNA *in situ* hybridization

To reduce background signal by breaking up hydrogen bondings sections were acetylated in Acetylation Buffer for 10min at RT under stirring on a magnetic stirrer. Acetylation Buffer was washed out in 3 steps for 5min each by DEPC-PBS. Prehybridization with Prehybridization Buffer followed. Sections covered with this buffer, under parafilm cover slips, were incubated for 2h at RT. Hybridization solution, containing the probe diluted 1:100 in Prehybridization Buffer, was heated to 85°C to reduce secondary RNA structures of the probe. This hybridization solution was added to the sections immediately, that were then covered by parafilm cover slips. Incubation followed in a chamber humidified with 50% formamide and 5x SSC, over night at 65°C. After hybridization, cover slips were removed and slides washed in 2x SSC for 5min at RT. To remove unbound probe from the tissue, sections were washed in 2 successive steps in 2x SSC at 65°C for 30min each. The tissue was prepared for blocking by incubation in MABT (100mM maleic acid pH 6.0; 0.1% Tween) for 30min at RT in 2 subsequent steps. Blocking was performed by incubation in a blocking solution consisting of MABT supplemented with 5% Roche Blocking Reagent (Roche #1109617001) for 1h at RT in a chamber humidified with PBS. Detection of DIG labeled probes was initially performed by binding of alkaline phosphatase (AP) coupled anti-DIG antibody (Roche #11093274910). Antibody was diluted 1:2000 in Roche Blocking Reagent and added to the slides, that were then incubated over night at 4°C. After this incubation unbound antibody was removed by 5 washing steps in MABT for 30min at RT each. Prior to signal detection slides were washed in AP buffer NTMT twice for 10min at RT. Detection of signal was performed by development of an AP mediated color reaction. Slides were immersed into Developing Solution (5µg NBT and 2.6µg BCIP in NTMT) and incubated at 37°C protected from light until visible signal development. This reaction was stopped by washing in PBS for 5min at RT. Slides were immediately mounted using Hydro-Matrix®.

3.3.3 Cryo embedding and sectioning

After sacrificing mouse specimen by cervical dislocation tissue was dissected, immediately embedded in 6% gum tragacanth in ddH_2O, mounted on cork plates and snap frozen in liquid nitrogen cooled isopentane at -160°C. For immunohistochemistry on sections frozen tissue was sectioned at 7µm thickness using a cryostat set to -20°C chamber temperature and -22°C blade temperature.

3.3.4 Hematoxylin and eosin staining on cryosections

For hematoxylin and eosin (H&E) staining cryosections were fixed in 4%PFA in PBS for 5min at RT followed by 2 washing steps in PBS. After rinsing the sections in bidstilled H_2O the slides were incubated in Mayer´s Hematoxylin for 3min at RT, then rinsed in tab water for 10min. After again rinsing the sections in bistilled water incubation in eosin staining solution activated by 0.5% glacial acetic acid for 1min. Rinsing the slides twice in bistilled water was followed by a ethanol dehydration series. Starting with a washing step in 70% ethanol for 1min at RT, the slides were subsequently washed in 90%, 95% and 100% ethanol for 2min each. Finally, the sections were cleared in Ultraclear for 10min at RT, and mounted using Entellan®.

3.3.5 Xgal staining

Staining of lacZ reporter tissue were conducted applying Xgal staining. To stain sections on slides sections were fixed in 4% PFA in PBS for 5min at RT. Incubation in Xgal staining solution followed for 24h at 37°C protected from light (tab.15). After final washing in PBS slides were mounted using Fluoromount-G®, or if desired, subjected to H&E staining.

Table 15: Xgal staining solution

Component	Concentration
Xgal (40mg/ml in DMSO)	0.4%
$K_3Fe(CN)_6$	5mM
$K_4Fe(CN)_6$	5mM
$MgCl_2$	2mM
in PBS	

For whole mount Xgal stainings of embryos at developmental stage E12.5, specimen were first fixed in Xgal fixing solution for 1h at 4°C (tab.16), then stained in Xgal staining solution for 24h, and after washing in PBS stored in Xgal fixing solution.

Table 16: Xgal fixing solution

Component	Concentration
Formaldehdye	1%
Glutaraldehyde	0.2%
NP-40	0.02%
PBS	1% 1xPBS
in bidistilled H_2O	

3.3.6 Immunohistochemistry

Freshly prepared sections of cryotissues were fixed in 4% PFA in PBS for 10min at RT. Subsequently, 3 washing steps in PBS followed, tissues were permeabilized in 0.3% Triton-X in PBS for 10min at RT, and 3 more washing steps in PBS were applied before tissues were blocked in 5% BSA in PBS for 1h at RT.

Slides were prepared using a Dako Pen, which provided a barrier and kept the solution in place on the tissue. Antibody solution was prepared by diluting antibodies in 5% BSA in PBS. For concentrations of primary antibodies see table 17. Slides were incubated with primary antibody solution at 4°C overnight. After 2 washing steps with PBS and 2 washing steps with 0.1% BSA in PBS for 10min each, secondary antibody solution was applied to the sections. Secondary antibodies were diluted 1:500 in 5% BSA in PBS. After 1h of incubation at RT, again 2 washing steps with PBS and 0.1% BSA in PBS followed. For nuclear staining DAPI was diluted 1:1000 in PBS and applied on the tissue for 5min at RT. Afterwards, slides were washed twice in PBS for 10min and mounted using Fluoromount-G®.

Table 17: Dilutions of antibodies used for immunfluorescent stainings

Antibody	Host	Dilution
anti-GFP	chicken	1:500
anti-β-GAL	mouse	1:50
anti-LAMININ	rabbit	1:500
anti-COL4	goat	1:50
anti-PDGFRα	rabbit	1:1000
anti-PDGFRβ	rabbit	1:100
anti-NG2	rabbit	1:100
anti-TCF4	rabbit	1:100
anti-αSMA	rabbit	1:200
anti-PLINA/B	rabbit	1:250
anti-CD31	hamster	1:100
anti-COL6	rabbit	1:250
anti-CD68	rabbit	1:100

4 Results

4.1 Generation of a multi-functional transgenic mouse line Osr1-MFA

A constitutive knock-out of *Osr1* in the mouse is lethal at early fetal stage [Mugford et al., 2008]. Hence, for studying the functional role of *Osr1* in adult mice by following gene ablation strategies a mouse model that enables a conditional knock-out is required. A transgenic mouse model was generated based on a targeting construct for the generation of a so-called "multi-functional allele" [Economides et al., 2013] for *Osr1* (Osr1-MFA). This construct was provided by Aris Economides (Regeneron Inc., Tarrytown USA). In addition, it provides a functionality as an *Osr1* reporter (see fig.9).

Mice carrying this allele feature a *lacZ* reporter gene driven by the *Osr1* promotor. At the same time this allele represents a loss-of-function due to the inversion of *Osr1* exon 2. By flippase mediated recombination the second exon of *Osr1* becomes reinverted, thus regenerating a functional wild type allele, with exon 2 being flanked by *loxP* sites. This exon, of in total three, harbors the start codon ATG. Cre mediated recombination excises exon 2, thus resulting in a knock-out.

The Osr1-MFA allele was electroporated into mESCs, that were then cultivated under G418 antibiotics supplement. A neomycin resistance gene included in the construct ensured enriched survival of transgenic clones. Single clones were isolated and expanded to colonies, which were split to duplicates for further cultivation and for DNA extraction. These steps were performed by Dr Heiner Schrewe (Department of Developmental Genetics, Max-Planck-Institute for Molecular Genetics).

4.1.1 Prescreening of potentially transgenic stem cell clones for copy number variations

The extracted DNA was tested for successful recombination by applying a quantitative PCR to detect gene copy number variations (CNVs). The aim of this strategy was a quantification of the wildtype *Osr1* locus relative to a gene locus known to be a single copy gene. Such a comparison enables to evaluate heterozygous recombination of the *Osr1* locus on one allele. The albumin gene locus was used as reference as it features one copy per genome in the mouse. A quantity of the wildtype *Osr1* locus of 1.0 relative to albumin indicates alteration at the other *Osr1* allele, thus enables to preselect potentially recombined clones.

A forward primer to bind a sequence present in both the transgenic and the wildtype *Osr1* allele is combined with a reverse primer whose binding sequence is located in a Loss-Of-Allele (LOA) region. This LOA sequence included only in the wildtype

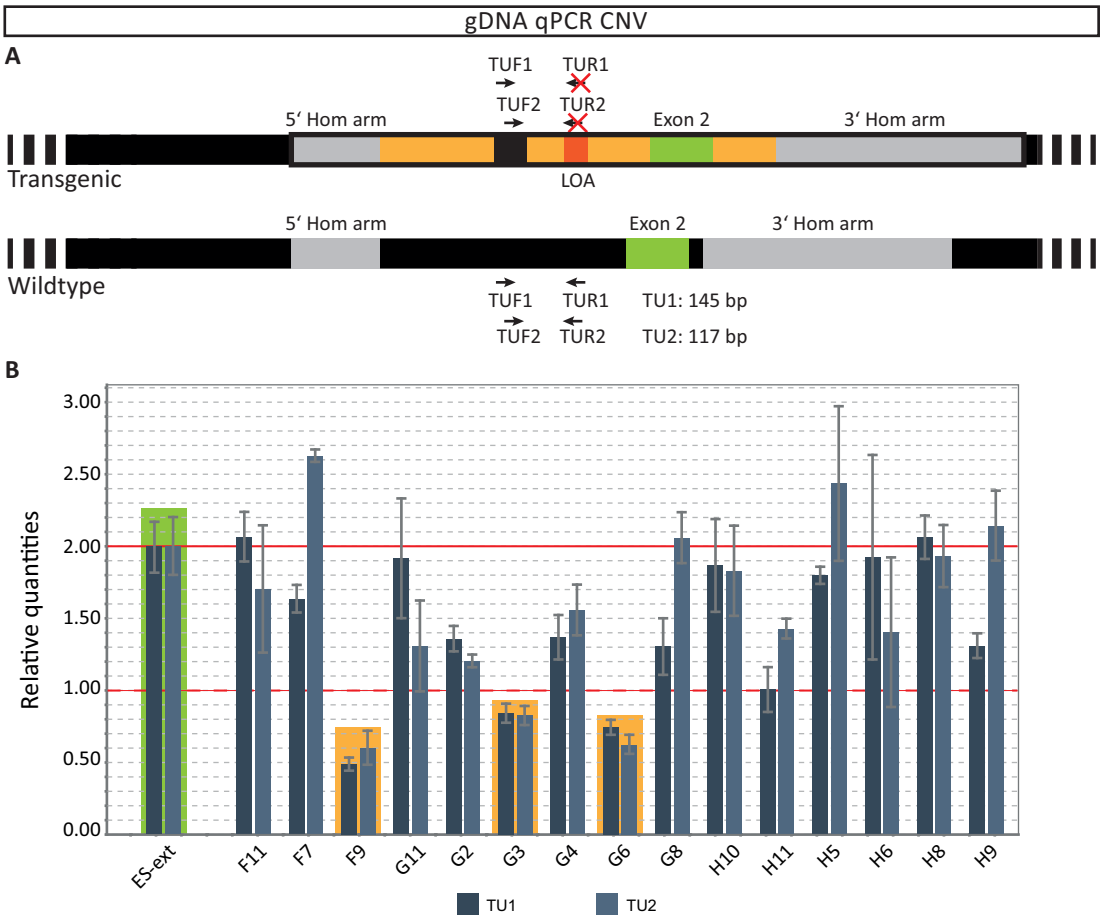

Figure 12: Quantitative qPCR to determine copy number variations in potentially recombinant mESC clones.
A Schemes of both transgenic and wildtype alleles depict the PCR strategy to determine copy number variations. A Loss-Of-Allele region (LOA) enables to differentiate between both alleles, as this LOA is deleted in the transgenic, but present in the wildtype sequence. The forward primer (TUF) binds to both alleles, the reverse primer (TUR) to the LOA region. Hence, a PCR product is generated only for the wildtype allele. Additional alternative forward and reverse primers were used to pursue the same strategy with two parallel approaches (TU1 and TU2).
B PCR results of 15 representative clones. Target locus quantification was normalized to relative albumin gene quantification. Each clone was compared to reference genomic DNA of wildtype mESC (green-shaded). This reference was set to two given the two wildtype *Osr1* loci. Clones F9, G3 and G6 (yellow-shaded) exposed a relative quantity of the wildtype allele below 50% and were therefore selected for further investigation.

allele but deleted in the transgenic construct. Hence, a PCR product only occurs for wildtype alleles, not for successfully recombined loci.

A wildtype control, consisting of murine embryonic stem cell (mESC) DNA, was set to 2.0 as it presents copies of the wildtype *Osr1* locus on both alleles. Clones F9, G3 and G6 showed an *Osr1* gene locus CNV of below 1.0 compared to the wildtype control, indicating a variation on one allele. A relative quantity of 50% suggests a heterozygous mutant carrying a wildtype as well as a transgenic locus (fig.12).

4.1.2 Verification of preselected clones by Southern blotting

Clones F9, G3 and G6 were selected for subsequent Southern blotting. This technique was applied to confirm precise insertion of the transgenic construct at the targeted site. Genomic DNA of potential clones and wildtype control were digested by restriction enzyme BamHI, separated on an agarose gel and blotted to a nylon membrane. A fragment size of 9.3kb, which spans the 5' homology arm and contains the external binding site of the 5' probe, was expected for the transgenic allele. In the wildtype genome this fragment measures 6.6kb. Specific detection of this fragment was performed by hybridization with a digoxygenin (DIG) labeled DNA probe and visualized by chemiluminescence.

A similar approach was pursued to verify the insertion of only a single copy of the

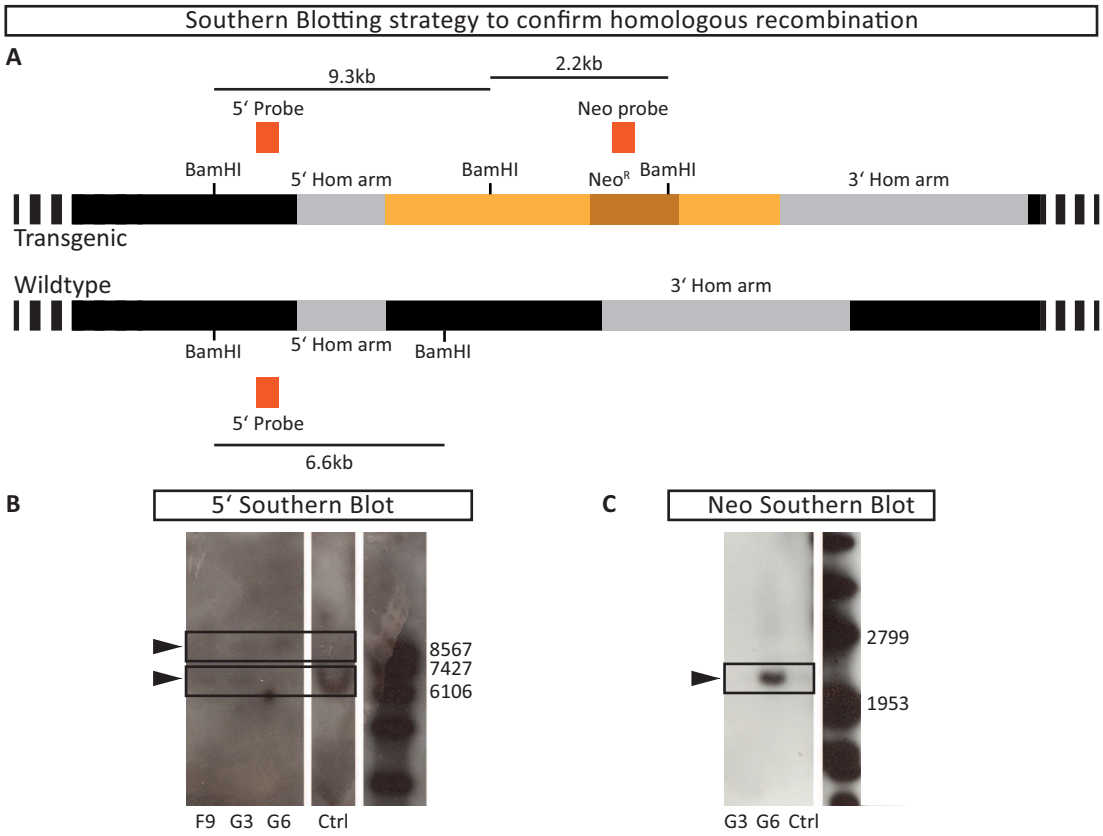

Figure 13: Verification of clones with successful homologous recombination by Southern blot technique.
A The strategy for both 5' terminus and neomycin Southern blots is indicated. For the 5' terminus BamHI restriction sites span a 9.3kb region in the transgenic allele, and a 6.6kb region in the wildtype. BamHI restriction sites also flank the neomycin gene, marking a 2.2kb region.
B While for clone F9 a recombined 5' terminus could not be detected, clone G3 and G6 were deemed positive for insertion of the 5' end of the transgenic construct as they expose a faint 9.3kb band. All 3 clones and the wildytpe control show a 6.6kb band reflecting the wildtype locus. **C** Of subsequently tested clones G3 and G6 for single insertion of the construct into the genome, only G6 was positive for neomycin detection as indicated by the 2.2kb band. No band was detected for clone G3 and the wildtype negative control.

transgenic construct into the genome. BamHI restriction sites also flank the neomycin gene, marking a 2.2kb region, which contains the binding sequence for the internal neomycin probe. For wildtype alleles no detectable fragment was expected (fig.13).

The Southern blot for verifying the 5' terminus resulted in expected wildtype bands at 6.6kb for all three tested clones, including the wildtype control. For clone F9 no recombined 5' terminus could be detected, for clone G3 and clone G6 though bands at 9.3kb confirmed expected homologous recombination of the construct at the 5' end. Hence, clone G3 and G6 were subsequently tested for single insertion of the construct. Neomycin detection yielded an expected band at 2.2kb for clone G6, but not for clone G3 (fig.13).

Successful recombination at the 3' homology arm could not be confirmed. Southern blot did not result in detection of an according fragment, nor did various attempts on amplifying a DNA region spanning the 3' homology arm by long-range PCR yield any product. For the time being it was decided to proceed with clones of confirmed 5' recombination and single insertion.

4.1.3 Confirmation of the *lacZ* expression pattern by whole mount Xgal staining

Clone G6 positively tested for proper 5' terminus and single insertion was subjected to tetraploid aggregation performed by Dr Heiner Schrewe and Karol Macura (Department of Developmental Genetics, Max-Planck-Institute for Molecular Genetics). Chimera generated by this technique already are mostly derived from C57Bl6 ES cells. Successively, the strain was expanded by further crossing F_0 mice to C57BL/6J wildtype mice. To verify the expression pattern of the *Osr1* promotor-driven *lacZ* reporter gene, from the transgenic Osr1-MFA allele, embryos of stage E12.5 were genotyped for genomic eGFP as this gene is included in the Osr1-MFA construct. Heterozygous specimen were subsequently subjected to whole mount Xgal staining. Analysis was performed by comparison with a whole mount RNA *in situ* staining for *Osr1* transcript [Stricker et al., 2006] (fig.14).

Xgal stainings showed a *lacZ* expression pattern similar to *Osr1* expression in wildtype embryos of same developmental stage visualized by RNA in situ hybridization. In fore and hindlimbs overlapping signals were detected in interdigital regions of the autopod and in a more complex pattern in zeugopod and stylopod. Matching expression patterns are also represented by signals in the embryo flank, the upper and lower jaw, tissue anterior and ventral of the eyes (fig.14).

The F_0 Osr1-MFA mice were crossed to the C57BL/6J wildtype background for at least six successive generations to obtain a transgenic mouse line with a uniform genomic C57BL/6J background.

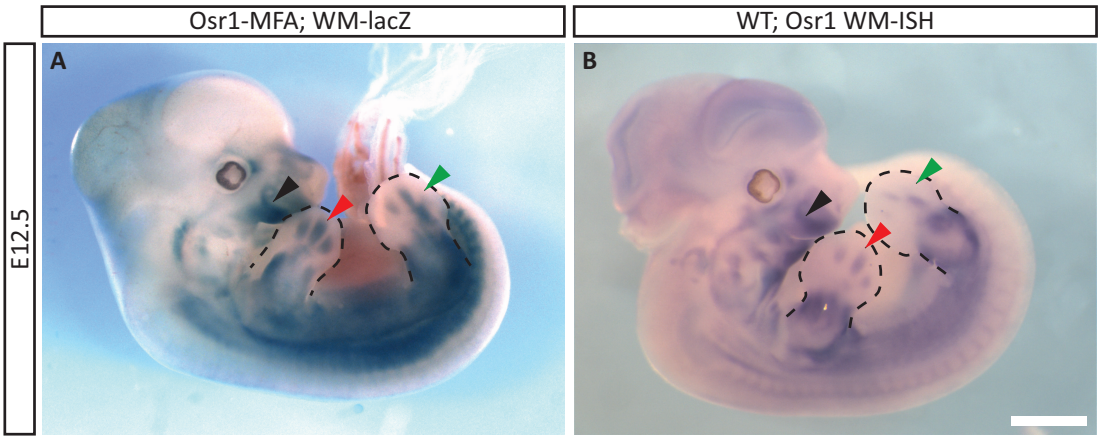

Figure 14: *LacZ* expression pattern of Osr1-MFA embryos reflects the *Osr1* expression pattern obtained by wildtype whole-mount *Osr1* RNA in situ hybridization.
Whole-mount *lacZ* stainings of Osr1-MFA embryos E12.5 (**A**) resembles the *Osr1* mRNA expression in wildtype embryos as indicated by whole-mount RNA *in situ* hybridization (**B**). With both techniques *Osr1* expression is detected in upper and lower jaw regions (black arrows) and e.g. in the interdigital regions in the forelimbs (red arrows) and the hindlimbs (green arrows). Images are representative for 3 independent experiments. Scale bar represents 1mm.

4.1.4 Generation of a conditional *Osr1* knock-out mouse line

By crossing Osr1-MFA mice with flippase (Flpe) deleters the MFA locus will be recombined obtaining a conditional allele for *Osr1* with a floxed exon 2. This is done

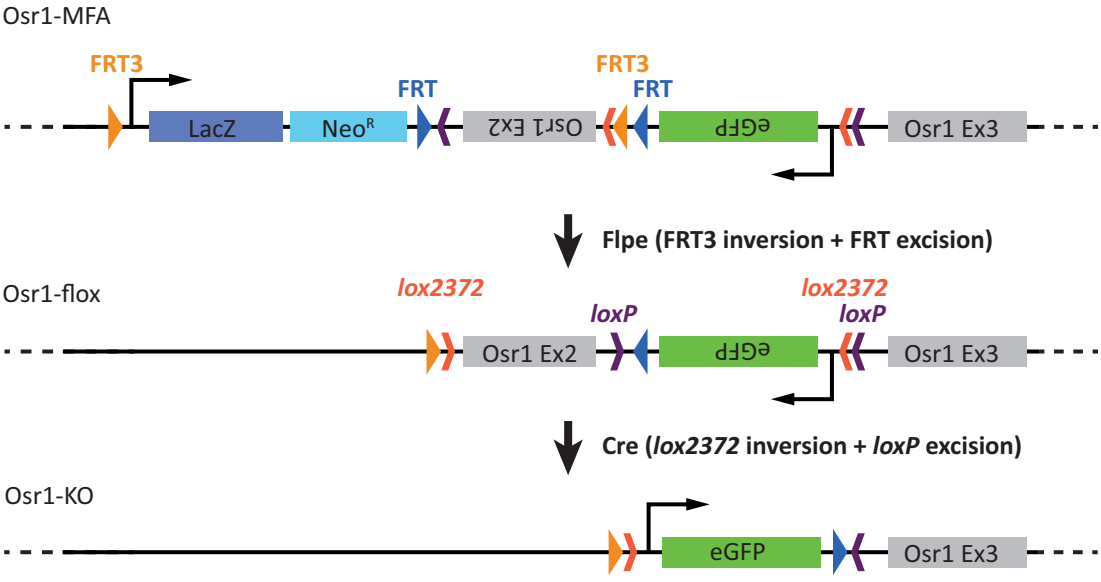

Figure 15: The Osr1-MFA locus can be recombined by Flpe recombinase to obtain a floxed exon 2.
On the Osr1-MFA allele *lacZ* and neomycin genes (sense orientation), and the *Osr1* exon 2/ eGFP cassette (antisense orientation), are flanked by a complex array of FRT and FRT3 elements (blue and yellow triangles). This enables flippase (Flpe) mediated recombination of the locus to yield a reinverted (sense orientation), floxed exon 2 (Osr1-flox). This allele features *lox2327* and *loxP* sites (red and purple arrows) to enable Cre mediated conversion of the allele to result in a knock-out eGFP reporter (Osr1-KO).

by two Flpe-mediated recombination steps. Due to a pair of inversely oriented FRT3 sites exon 2 is reinverted, hence regaining a functional *Osr1* gene. In a subsequent step, *lacZ* and neomycin are excised, which is enabled by a pair of FRT sites in the same orientation, spanning both genes. The resulting allele harbors a functional exon 2 and an inverted eGFP gene flanked by a combination of *lox2372* sites and *loxP* elements. This arrangement allows again a two-step recombination process mediated by Cre recombinase. Recombination of the *lox2372* sites inverts the exon 2/ eGFP cassette, subsequently exon 2 is excised by both *loxP* sites (fig.15).

After crossing Osr1-MFA mice with Flpe deleters, genomic DNA of offspring was tested for expected Flpe mediated recombination at the MFA locus. A PCR utilizing three primers was designed to enable discrimination between both loci. As a region for both forward primers exon 2 was chosen, as this region is distinct to both loci due to inverted orientations. One primer was oriented in sense, the other one in antisense direction. The reverse primer was located on the eGFP gene and was common to both loci. Expected product sizes of 1974bp for the MFA locus and 1463bp for the Flpe recombined locus were evaluated after agarose gel electrophoresis on a gel containing 1% agarose (fig.16).

Both products were extracted from the agarose gel and subjected to Sanger sequencing for verification of expected sequence.

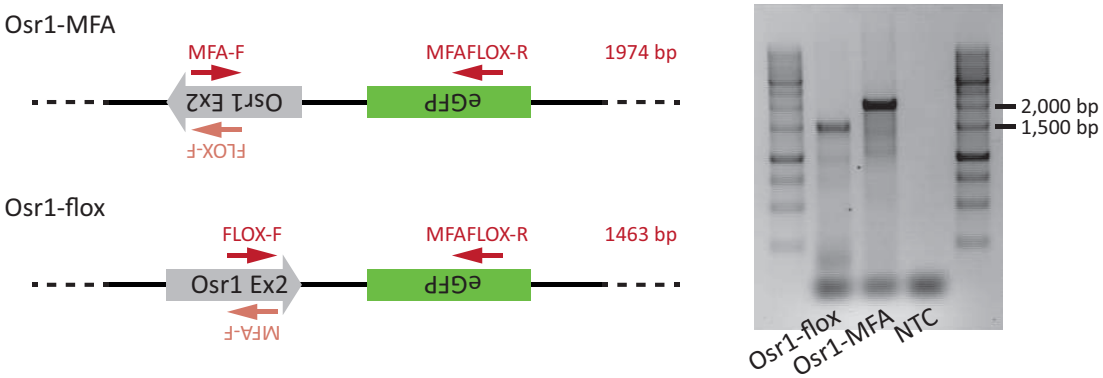

Figure 16: PCR confirmation of successful flippase mediated conversion of the Osr1-MFA allele to a conditional Osr1 allele (Osr1-flox).
Based on the orientation of exon 2 Osr1-MFA and Osr1-flox alleles can be distinguished utilizing PCR technique. In a reaction mix containing 3 primers the reverse primer (MFAFLOX-R) is common to both alleles, whereas one primer is specific to the Osr1-MFA locus (MFA-F) and another primer specific to the Osr1-flox locus (FLOX-F). For an Osr1-MFA template a product of 1974bp is amplified, the product for an Osr1-flox template measures 1463bp. No template DNA but bidistilled H_2O was added to the no template control (NTC) to exclude DNA contamination in the reaction mix. Agarose gel electrophoresis was performed using a 1% agarose gel and a GeneRuler™1kb DNA Ladder.

4.2 Postnatal *Osr1* expression

4.2.1 During adolescence *Osr1* is expressed in fibro/ adipogenic progenitors in muscle tissue

To assess the expression pattern of *Osr1* in postnatal muscle tissue, cryosections of muscle tissue were subjected to immunofluorescence stainings. Due to the lack of sufficiently working antibodies against murine OSR1, *Osr1* reporter mouse lines were used. The mouse strain *Osr1*$^{eGFP\text{-}CreERt2/+}$ (Osr1-GCE) expresses eGFP under the control of the *Osr1* promotor, the Osr1-MFA strain expresses β-galactosidase, respectively. Both reporter models express *Osr1* from only one allele, whereas the other allele functions as a knock-out reporter. However, no phenotype due to haploinsufficiency was reported for heterozygous *Osr1* knock-out mice (see Material 2.5.1).

Initially, *Osr1* expression in muscle tissue during the first three weeks of age was investigated. During this early postnatal stage muscle mass increases by muscle stem cells still being active. They proliferate and differentiate to fuse to muscle fibers, before they will turn quiescent after 3 weeks of age. After this time point, muscle satellite cells remain in their specific niche below the myofiber basal lamina and they only become reactivated in an injury situation. The expression of *Osr1* was studied in the three week time period after birth, which according to the activity of muscle progenitors can still be considered a developmental stage.

Reporter-positive cells were detected in the muscle interstitium indicated by staining against type IV collagen (COL4) to delineating muscle fibers of *tibialis anterior* muscle sections of neonatal (P0), 1 day (P1), 3 days (P3), 7 days (P7) and 14 days (P14) old mice (fig.17). The number of detectable Osr1+ interstitial cells decreases over time. After 3 weeks of age eGFP+ cells were not detected using this mouse model. To assess the identity of these cells a co-staining for PDGFRα, an accepted specific marker for fibro/ adipogenic progenitors (FAPs), was included (fig.17A-E). At P0 all *Osr1* reporter+ cells are positive for PDGFRα, which was also observed for P1 and P3. At P7 and P14 the number of eGFP+ FAPs cells have progressively decreased. While at P7 eGFP signal intensity has started to fade, a signal at the age of 21 days could not be detected anymore using this model.

To support these findings of a declining *Osr1* expression during the first three weeks of age RT-qPCR to quantify *Osr1* mRNA in whole muscle lysates of TA muscle specimen was performed (fig.17F). For this series Osr1-GCE mice at respective age were sacrificed and RNA extracted from dissected muscle samples. In line with the observation of the declining number of *Osr1* reporter+ cells within the first 3 weeks after birth relative *Osr1* transcript quantity drops to a basal level after 14 days of age.

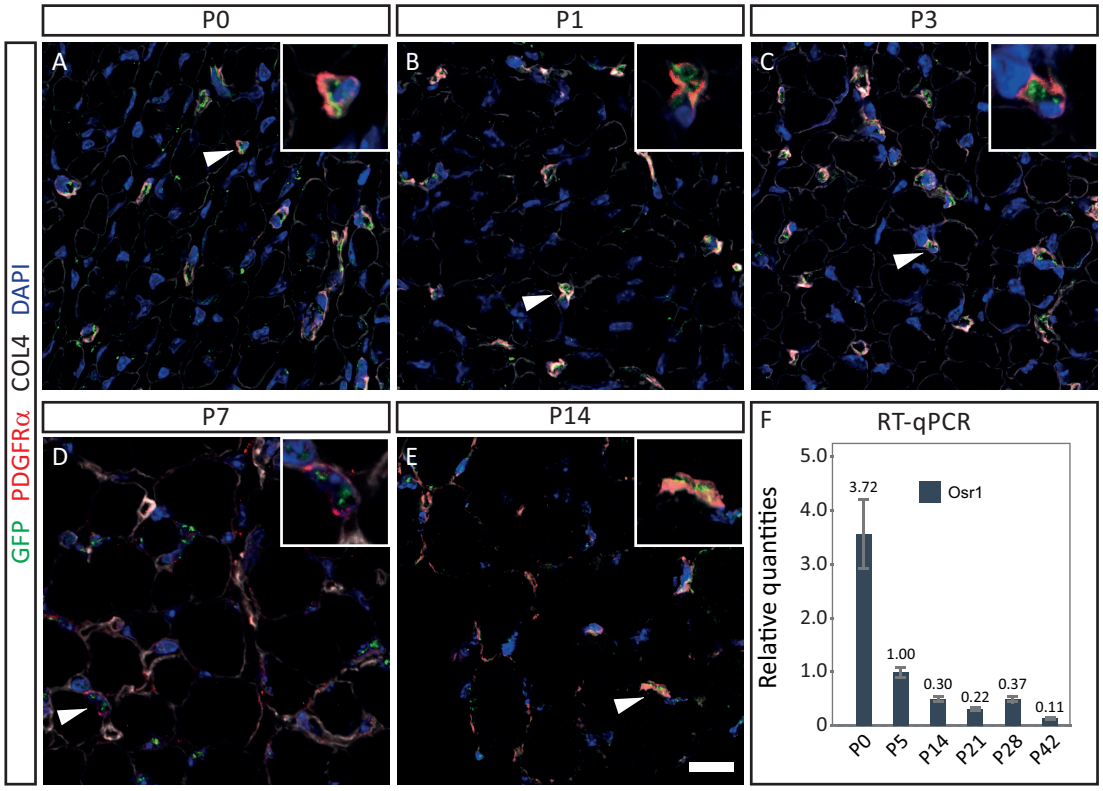

Figure 17: *Osr1* reporter expression declines during the first 3 weeks of age in *tibialis anterior* muscle tissue.
A-E Tibialis anterior muscles of Osr1-GCE reporter mice ($Osr1^{GCE/+}$) of postnatal stages P0, P1, P3, P7 and P14 were subjected to cryosectioning and subsequently to immunohistochemistry. Immunostaining was applied using anti-GFP (green), anti PDGFRα (red) and anti-COL4 (white). Nuclei were stained by DAPI (blue). Images are representatives of 2 independent experiments. Scale bar indicates 20µm.
F RT-qPCR of whole muscle lysates of $Osr1^{GCE/+}$ *tibialis anterior* muscle resembles declining *Osr1* mRNA quantities in tissues of different postnatal stages. For relative quantification of *Osr1* normalization to GAPDH was performed, error bars show standard deviation. The displayed series was a single experiment.

For quantification of Osr1+ FAPs during the first three weeks of juvenile phase, and further confirmation of the identity of *Osr1* expressing cells, fluorescence-activated cell sorting (FACS) was performed using 7 days old Osr1-lacZ reporter mice Osr1-MFA (fig.18, 19). Muscle tissue of all hindlimb muscles was processed to single cell suspensions and stained for cell type specific markers using according fluorophore-coupled antibodies.

In a stepwise process single alive cells were sorted using FACS. By initially separating cells by forward and sideward light scatter, that is by particle size and complexity, debris were excluded. Successive separation by area and height properties of the forward scatter enabled exclusion of cell doublets (fig.18A). Remaining single cells were selected for alive cells only. Previously added propidiumiodide (PI) to the cell suspension can pass defected cell membranes and intercalated into the DNA, hence

marking dead cells (fig.18B). From this pool of single alive cells hematopoietic cells positive for CD45 and Ter119 were negatively selected (fig.18C). Separating the remaining cells (lin–) by stem cell markers CD34 and Sca-1, juvenile tissue presents four distinct cell populations, as previously reported [Mitchell et al., 2010, Pannérec et al., 2013]. A population CD34-/ Sca-1– features osteogenic and chondrogenic differentiation potential *in vitro*. CD34+/ Sca-1– cells are myogenic, and CD34+/ Sca-1+ contain fibro/ adipogenic progenitors. An additional population exhibits a

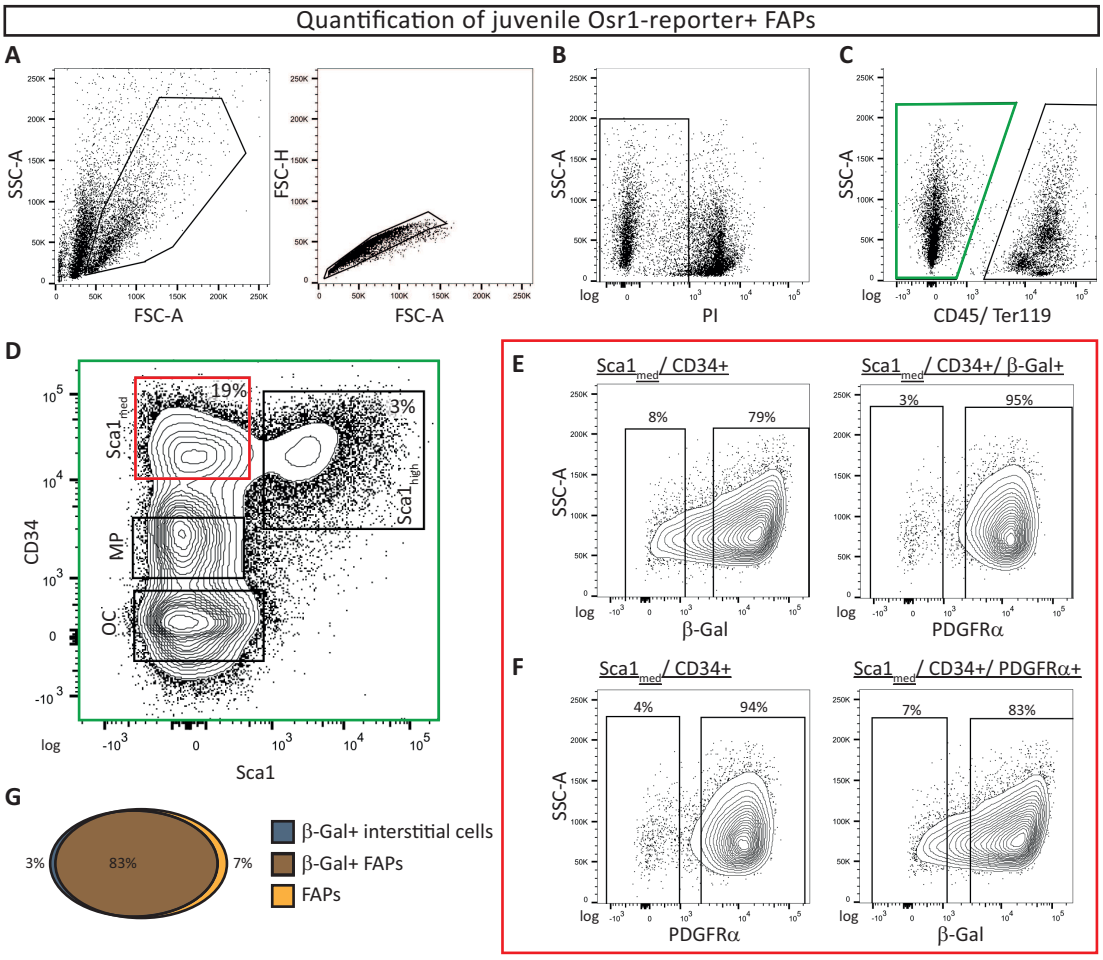

Figure 18: FACS acquired distribution and quantification of *Osr1* reporter+ cells in a transient juvenile muscle cell population.
From cell suspensions of all hindlimb muscles obtained from 1 week old Osr1-MFA mice cell debris and doublets were excluded by light scattering (**A**). Negative selection for dead cells (PI+) yielded alive single cells (**B**), of which only non-hematopoietic cell types (CD45–/ Ter119–) were selected (**C**). Separation of the remaining cells by CD34 and Sca-1 presented an osteo-/ chondrogenic (CD34–/ Sca-1–; OC), a myogenic (CD34+/ Sca-1–; MP) and two FAP-containing populations (CD34+/ Sca-1_{med} and CD34+/ Sca-1_{high}) (**D**). The transient juvenile population CD34+/ Sca-1_{med} contains 79% of *Osr1* reporter+ cells of which 95% are positive for FAP marker PDGFRα (**E**). Vice versa, this transient population consists of 94% PDGFRα+ cells of which 83% express *Osr1* reporter *lacZ* (**F**). Venn diagram summarizes 83% of cells double positive for *Osr1* reporter and FAP marker PDGFRα , 3% only express *Osr1* reporter *lacZ*, and 7% only PDGFRα in the transient juvenile cell population CD34+/ Sca-1_{med} (**G**). Plots are representatives of 3 independent experiments.

medium intensity Sca-1 property (Sca-1_{med}) and is positive for CD34 (fig.18D). This population was reported to be detectable only during the first 3 weeks after birth during the juvenile phase [Pannérec et al., 2013]. While the medium shift in Sca-1 signal intensity is merely marginally determined, this is due to the fluorescence of Sca-1 antibody coupled Alexa-700 dye. A clear separation and display of a medium Sca-1 property can be achieved using FITC coupled FACS antibodies [Mitchell et al., 2010].

This cell population is present only during the first 3 weeks of age in the mouse, and also contains cell types with fibrogenic and adipogenic potential. It accounts for 19% of all lin– cells at P7. Investigating this population for *Osr1* expression by *Osr1* reporter *lacZ*, 79% of these cells express *Osr1*, while by 95% almost all are PDGFRα+, the only specific marker known so far for fibro/ adipogenic progenitors in muscle tissue (fig.18E). Vice versa, 94% of this Sca-1_{med} population is positive for FAP marker PDGFRα, and 83% of these Sca-1_{med} FAPs are *Osr1* reporter+ (fig.18F).

A similar analysis was performed to investigate the CD34+/ Sca-1+ population. However, at P7 this population accounts for merely 3% of all lin– cells. Of this small fraction only 54% cells are expressing *Osr1* reporter βgal. Half of these, 49%, are

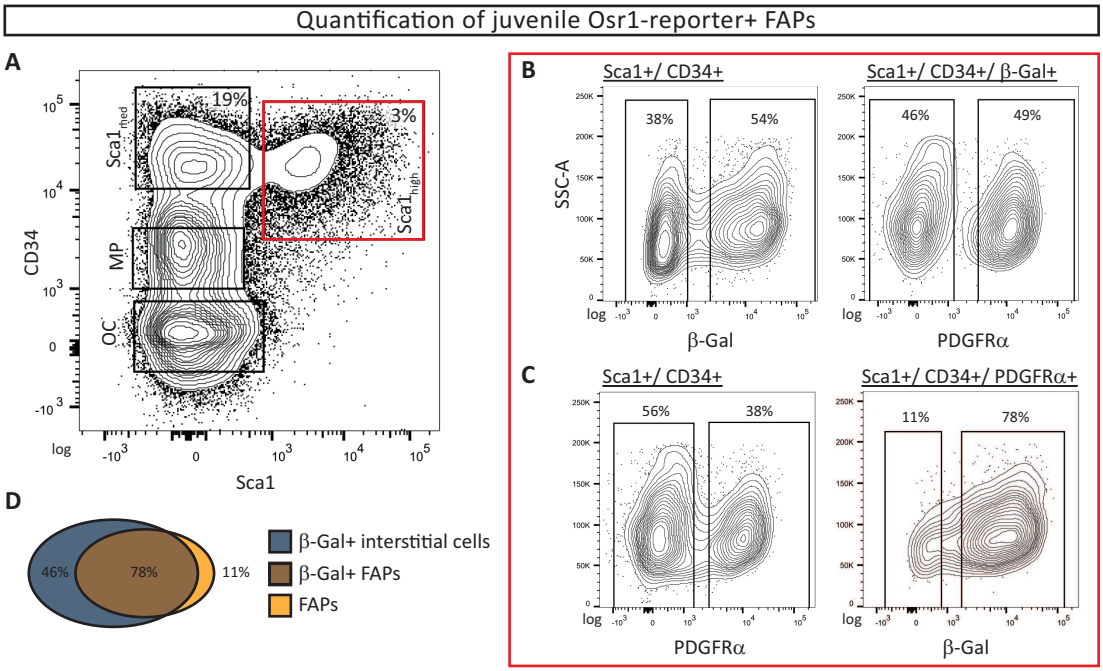

Figure 19: FACS acquired distribution and quantification of *Osr1* reporter+ cells in a cell population containing fibro/ adipogenic progenitors.
The FAP containing population CD34+/ Sca-1+ ($Sca1_{high}$) of 1 week old Osr1-MFA mice (**A**) consists of 54% *Osr1* reporter+ cells, of which 49% are positive for FAP marker PDGFRα (**B**). Likewise, 38% of this population are PDGFRα, and of these 78% express *Osr1* reporter *lacZ* (**C**). In summary, 78% of all FAPs express *Osr1* reporter *lacZ*, 11% are *Osr1* reporter–. However, 49% of the CD34+/ Sca-1+ population express *Osr1* reporter *lacZ*. Plots are representatives of 3 independent experiments.

FAPs, determined by marker PDGFRα. And while 38% of the entire CD34+/ Sca-1+ population are FAPs, 78% of these FAPs are expressing *Osr1* reporter βgal (fig.19).

While by 95% the majority of *Osr1* reporter+ cells in the Sca-1_{med} population are positive for FAP marker PDGFRα, the CD34+/ Sca-1+ population contains *Osr1* reporter+ cells that are negative for PDGFRα, 46%, hence do not expose a FAP identity.

For additional characterization of juvenile Osr1+ cells, an overlap with PW1 expressing interstitial progenitors (PICs) was investigated. Reportedly, more than 90% of CD34+/ Sca-1_{med} cells are positive for PIC marker PW1. Given almost 80% of the CD34+/ Sca-1_{med} population expresses *Osr1* reporter *lacZ*, a high overlap of juvenile Osr1+ and juvenile PICs is implied. Semiquantitative reverse transcription PCR detecting *Osr1* mRNA was performed on RNA extracted from FACS isolated cell populations including PW1+ portions of CD34+/ Sca-1_{med} (Sca-1_{med} PICs) and CD34+/ Sca-1_{high} (Sca-1_{high} PICs) cells. *Osr1* transcript is highly abundant in RNA yielded from Sca-1_{med} PICs, and a medium abundance was detected in Sca-1_{high} PICs. *Osr1* is neither transcribed by satellite cells nor by the PW1– portion of CD34+/ Sca-1_{high} cells (fig.20), which is reportedly PDGFRα–. This experiment was performed by Luigi Formicola, UPMC (Paris, France).

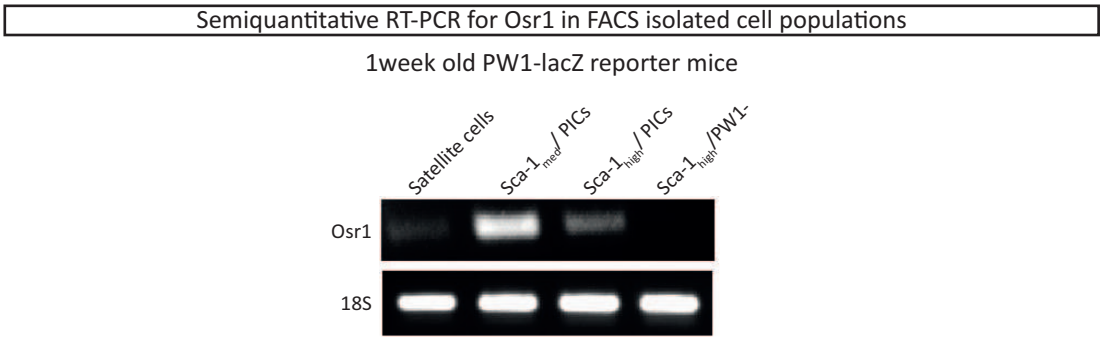

Figure 20: *Osr1* is expressed by Sca-1_{med} and Sca-1_{high} PICs.
Cell populations were isolated from hindlimbs of 1 week old PW1-lacZ reporter mice by FACS, RNA extracted and reverse transcribed. *Osr1* cDNA was PCR amplified using *Osr1* qPCR primers (Osr1-qPCR-F; Osr1-qPCR-R) during 25 PCR cycles, and products separated on a 1.5% agarose gel. Amplification of 18S RNA was used as a loading control. This is a single experiment.

In order to further characterize the identity of *Osr1* reporter+ cells, muscle tissue of 1 week old Osr1-lacZ reporter mice (Osr1-MFA) was subjected to histochemistry. Cryosections of *tibialis anterior* and *gastrocnemius* muscles were stained against β-galactosidase to visualize *Osr1* expression, and cell type specific markers (fig.21, 22). For quantification *Osr1* reporter+ cells and according cell types were counted and compared (fig.23).

An Xgal staining provides an overview on the amount of *Osr1* reporter+ cells on

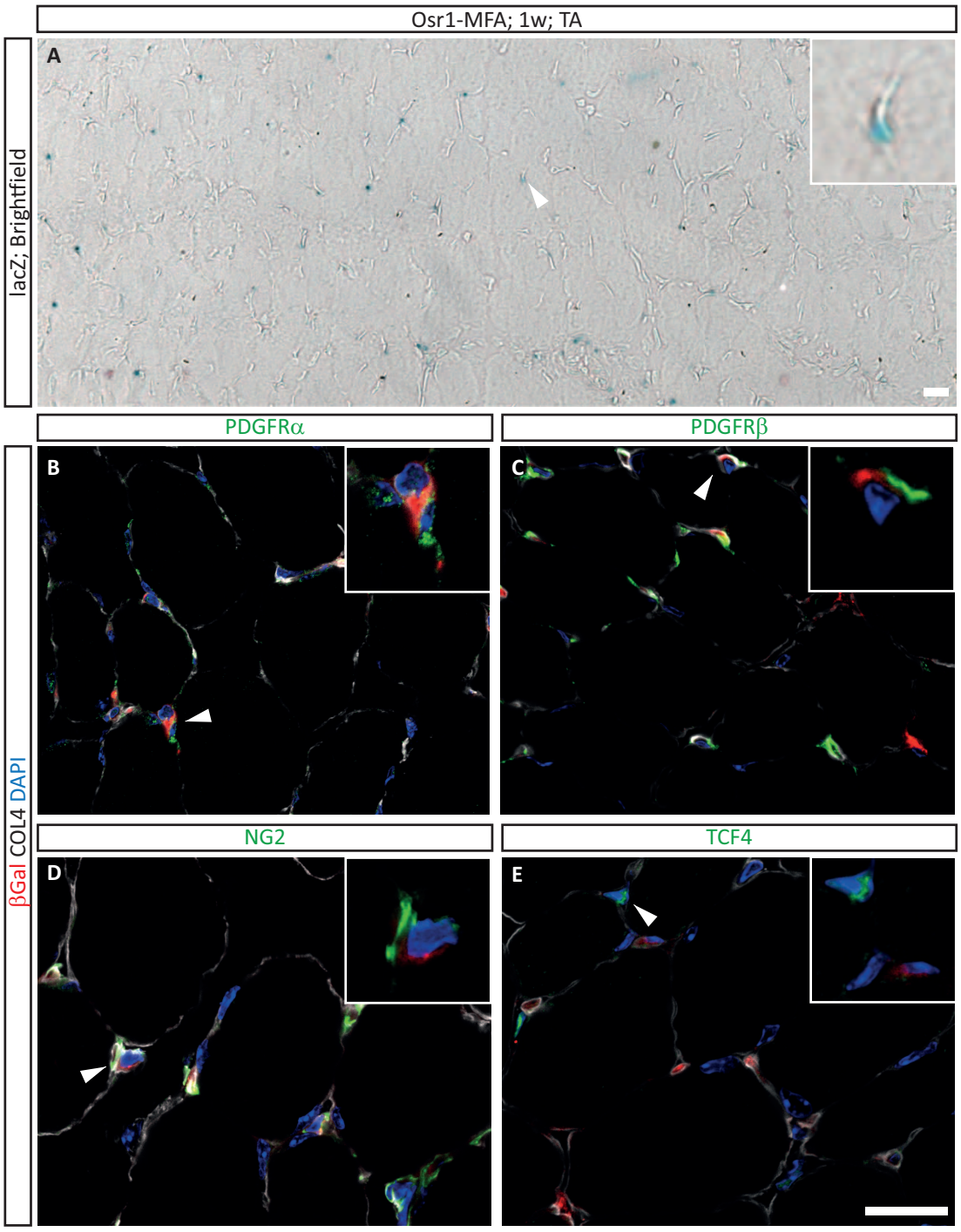

Figure 21: Histochemical stainings of *tibialis anterior* cryosections of 1 week old Osr1-MFA mice.

A X-gal staining of *tibialis anterior* (TA) sections of 1 week old Osr1-MFA mice labels lacZ+ *Osr1* reporter cells. **B-E** Immunofluorescent stainings include anti-β-GAL to indicate *Osr1* reporter expression (red), anti-COL4 (white) to indicate tissue context and DAPI as a nuclear staining (blue). Co-stainings with markers (green) for FAPs (PDGFRα), pericytes (PDGFRβ, neural/glial antigen 2 (NG2)) and interstitial fibroblast marker TCF4 were performed for cell type identification (**B-E**). Arrowheads mark magnified inlayed details. Inlays of immunofluorescence images do not include COL4 layer. Images are representatives of 3 independent experiments. Scale bar indicates 10µm.

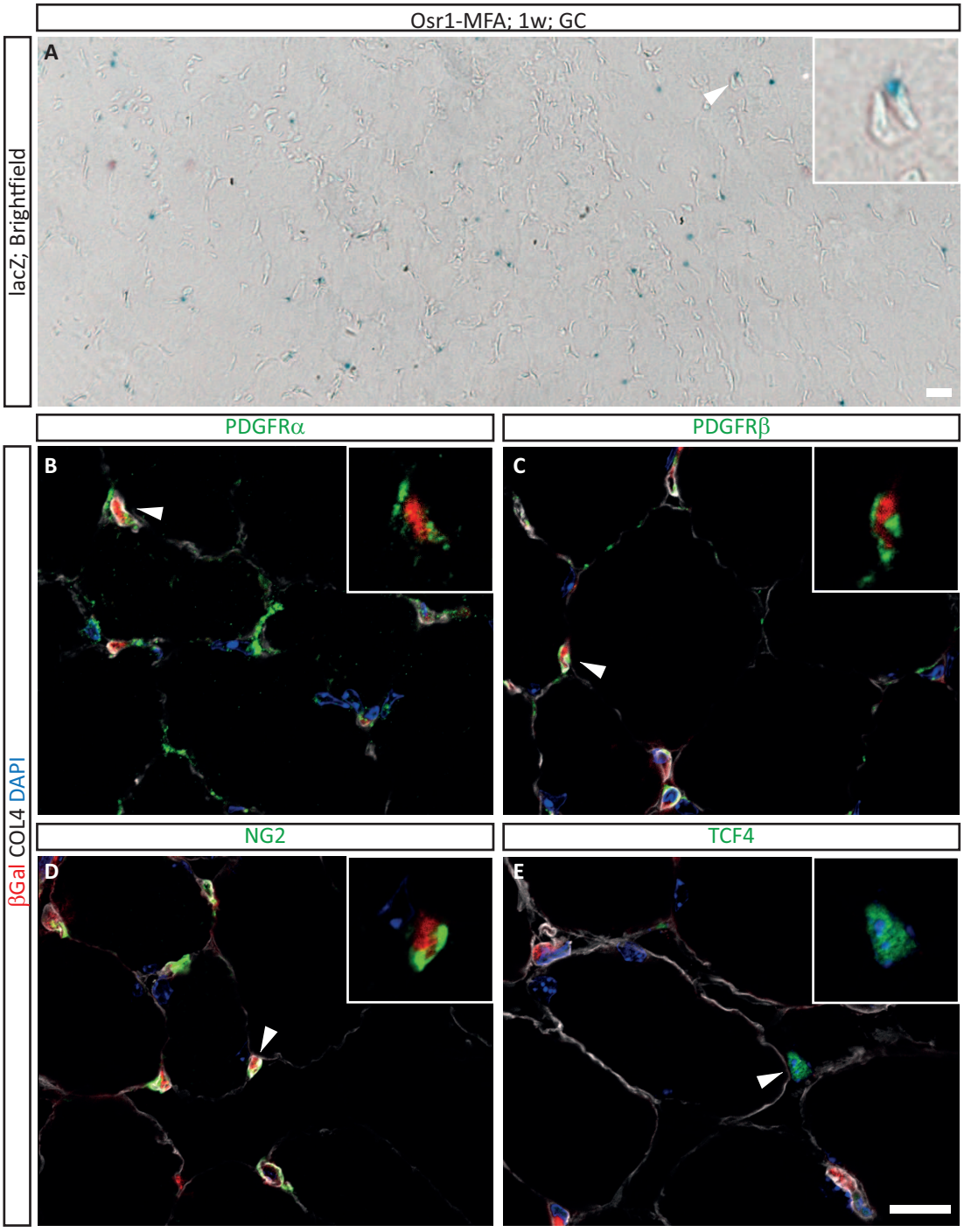

Figure 22: Histochemical stainings of *gastrocnemius* cryosections of 1 week old Osr1-MFA mice.
A X-gal staining of *gastrocnemius* (GC) muscle sections of 1 week old Osr1-MFA mice labels lacZ+ *Osr1* reporter cells. **B-E** Immunofluorescent stainings include anti-β-GAL to indicate *Osr1* reporter expression (red), anti-COL4 (white) to indicate tissue context and DAPI as a nuclear staining (blue). Co-stainings with markers (green) for FAPs (PDGFRα), pericytes (PDGFRβ, neural/glial antigen 2 (NG2)) and interstitial fibroblast marker TCF4 were performed for cell type identification. Arrowheads mark magnified inlayed details. Inlays of immunofluorescence images do not include COL4 layer. Image are representatives of 3 independent experiments. Scale bar indicates 10µm.

the sections of the *tibialis anterior* muscle (fig.21A). This amount is in coherence with the amount of eGFP+ cells of immunohistochemical stainings on sections of 7 days old Osr1-GCE reporter mice (also see fig.17). Co-immunostainings of Osr1-lacZ reporter and FAP marker PDGFRα indicate *Osr1* expression in FAPs (fig.21B). 84% of all *Osr1* reporter+ cells expose a PDGFRα signal. However, while β-galactosidase and PDGFRα signals predominantly colocalize, cells only positive for PDGFRα or β-galactosidase were detected to a small amount as well. To investigate whether *Osr1* reporter+ cells show a pericyte cell identity co-stainings with PDGFRβ and NG2 were performed (fig.21C, D). Of all *Osr1* reporter+ cells 56% were positive for PDGFRβ+, and a small portion of 35% exhibit an NG2 signal. Cells only positive for β-galactosidase in these stainings were detected as well. By immunostaining against TCF4 interstitial fibroblasts are marked. *Osr1* reporter+ cells that co-express TCF4 were not observed at this stage.

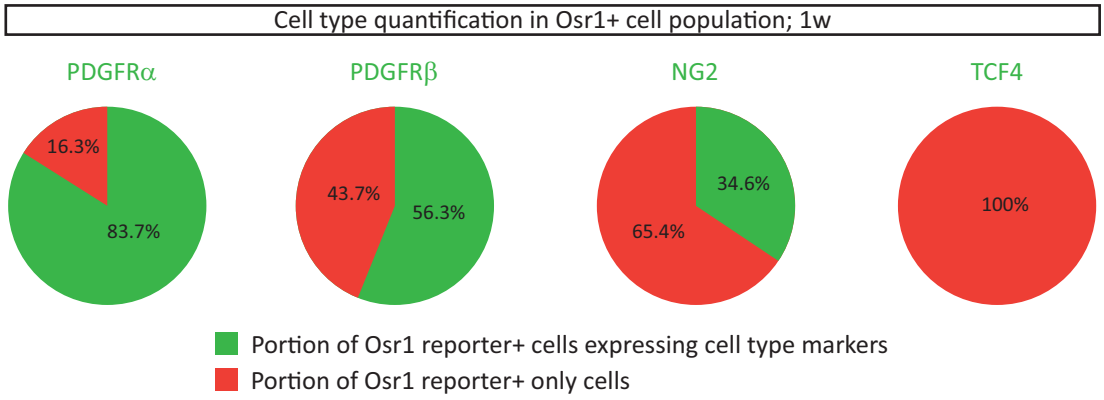

Figure 23: The majority of *Osr1* reporter+ cells in 1w old muscle are FAPs.
For quantification of *Osr1* reporter+ cells and cells double positive for *Osr1* reporter and respective marker were counted on sections of the *tibialis anterior* muscle. 8 fields of view for each of 2 replicates were counted and averaged.

Unpublished studies on embryonic *Osr1* mutants revealed a muscle patterning phenotype in the *gastrocnemius* muscle, but notably milder in the *tibialis anterior* muscle [Vallecillo García, 2016]. Hence, the same cell type characterization by immunohistochemistry was performed on cryosections of the *gastrocnemius* muscle (fig.22). Differences for cell type identity of *Osr1* expressing cells in both muscles were not observed.

4.2.2 Neonatal *Osr1* reporter+ FAPs can differentiate to TCF4+ interstitial fibroblasts and intramusculuar adipocytes during adolescence

Osr1+ cells are mainly expressing PDGFRα, but also PDGFRβ. Both receptors are present on progenitor or stem cell-like cell types that embrace differentiation potential as per definition.

To investigate the fate of neonatal Osr1+ cells and their differentiation potential, cell fate tracking studies were performed using Osr1-ROSA26mTmG lineage tracer mice (see fig.11). These mice ubiquitously express a membraneous tomato fluorophore (mTOM), unless recombined by the inducible *Osr1* promotor driven Cre recombinase for cells will be labeled by a membraneous eGFP (mGFP). As this is the result of a genomic recombination the labeling will be permanent and persistent across potential differentiation steps, which enables tracking of cell fate. This genomic labeling is also inherited to daughter cells during proliferation.

Neonates of this strain were tamoxifen induced, thus Osr1+ cells labeled, and *tib-*

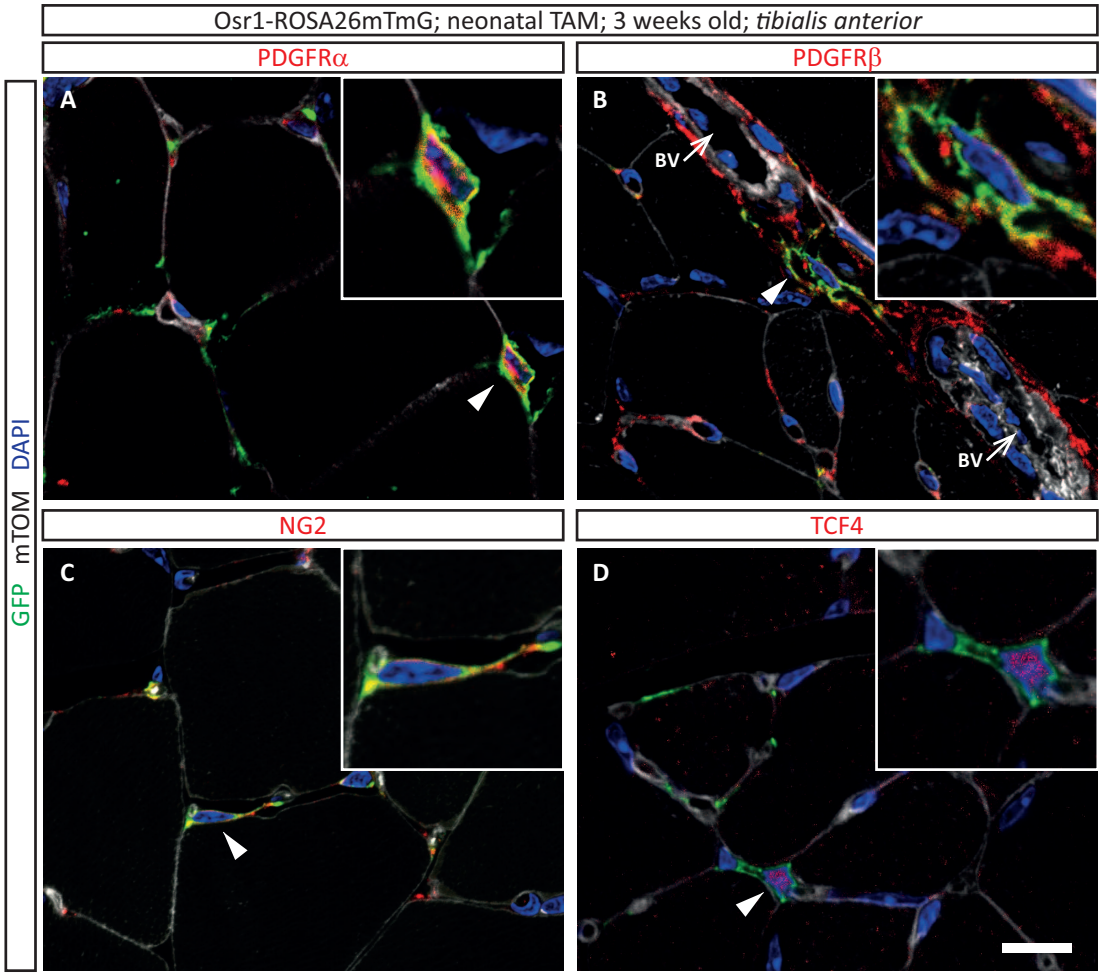

Figure 24: Neonatal Osr1+ cells possess differentiation potential for FAPs, pericytes and interstitial fibroblasts, but are not myogenic.
A-D Using cryosections of *tibialis anterior* muscle dissected from Osr1-ROSA26mTmG lineage tracer mice induced at P0 and P1, fate of Osr1+ cells at the age of 3 weeks was studied applying immunohistochemistry. By anti-GFP tracked cells were labeled (green), tomato indicates tissue context (white) and nuclei were stained by DAPI (blue). Co-stainings with markers (red) for FAPs (PDGFRα), pericytes (PDGFRβ, neural/glial antigen 2 (NG2)) and interstitial fibroblast marker TCF4 were performed for cell type identification. Arrowheads mark magnified inlayed details, arrows (BV) indicate blood vessels. Images are representatives of 3 independent experiments. Scale bar indicates 10µm.

ialis anterior muscle analyzed at the age of 3 weeks. At this stage *Osr1* expression could not be detected in Osr1-GCE GFP reporter mice. By immunofluorescence stainings for FAP marker PDGFRα, pericyte markers PDGFRβ and NG2, and interstitial fibroblast marker TCF4 differentiation potential of neonatal Osr1+ cells for these cell types was investigated (fig.24). For quantification traced cells and respective cell types were counted and numbers compared (fig.25).

In the muscle interstitium over 70% of FAPs are mGFP labeled, hence descendants of neonatal Osr1+ cells (fig.24A, 25). PDGFRβ+ pericytes were detected mainly in close proximity to larger blood vessels. Of these pericytes 26% could be tracked back to a formerly *Osr1* expressing origin (fig.24B, 25). NG2+ cells were predominantly localized in the muscle interstitium, with only 9% being mGFP+ (fig.24C, 25). While at the age of 1 week *Osr1* reporter+ cells expressing TCF4 were not observed (see fig.21, 22), at the age of 3 weeks a portion of 41% of TCF4+ cells indicate former *Osr1* expression as they were neonatally labeled (fig.24D, 25).

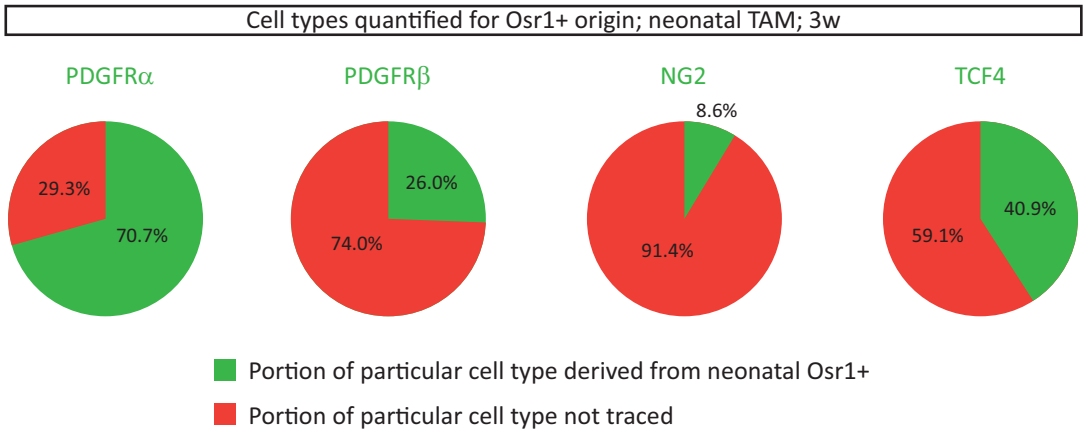

Figure 25: The majority of FAPs ate the age of 3 weeks originate from neonatal Osr1+ cells.
For quantification all cells positive for each cell type corresponding marker and the portion of cells double positive for marker and tracer labeling GFP were counted on sections of the *tibialis anterior* muscle. 8 fields of view for each of 2 replicates were counted and averaged.

Moreover, morphologically identifiable muscle fiber contours do not expose an mGFP labeling but are entirely mTOM positive. Hence, they did not arise from formerly *Osr1* expressing cells, confirming the non-myogenic potential of postnatal Osr1+ cells (fig.24).

The differentiation potential of neonatal Osr1+ cells was also investigated for more mature cell types including adipocytes, smooth muscle and endothelial cells (fig.26). Regardless the very low abundance of intramuscular fat cells in adolescent mice, adipocytes could be detected by stainings against the lipid droplet associated protein perilipin (PLINA/B). These adipocytes were localized mainly in close proximity to blood vessels. Adipocytes positive for mGFP labeling indicates adipogenic differen-

tiation potential of neonatal Osr1+ cells (fig.26A). Descendants of early postnatal Osr1+ cells can also be found next to blood vessels, but they do not show a myofibroblast identity. Myofibroblasts are marked by alpha smooth muscle actin (αSMA) (fig.26B). Likewise, cells positive for CD31, a commonly accepted marker for endothelial cells, do not show mGFP labeling, neither in capillaries (fig.26C) nor in larger blood vessels (fig.26D). Therefore, endothelial cells are not derived from neonatal Osr1+ cells.

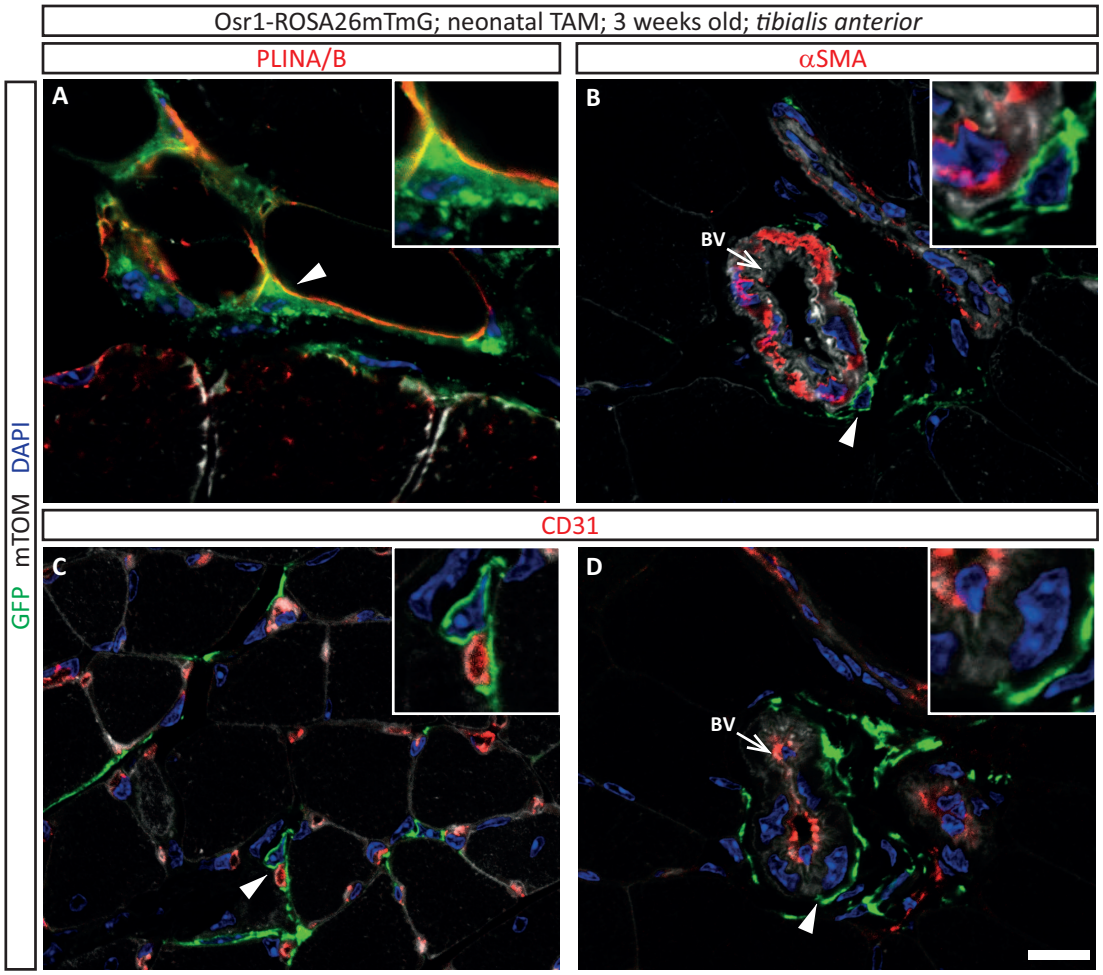

Figure 26: Neonatal Osr1+ cells are adipogenic, but have no differentiation potential for myofibroblasts or endothelial cells.
A-D Using TA muscle cryosections of Osr1-ROSA26mTmG lineage tracer mice induced at P0 and P1, fate of Osr1+ cells at the age of 3 weeks was studied applying immunohistochemistry. By anti-GFP tracked cells were labeled (green), mTOM indicates tissue context (white) and nuclei were stained by DAPI (blue). Co-stainings with markers (red) for mature adipocytes (PLINA/B)(A), myofibroblasts (αSMA)(B) and endothelial cells (CD31) were performed for cell type identification. Endothelial cells were investigated in capillaries (C) and large blood vessels (D). Arrowheads mark magnified inlayed details. Images are representatives of 3 independent experiments. Scale bar indicates 20µm.

In a parallel cell fate tracking approach, utilizing a different lineage tracer mouse model, neonatal Osr1+ cells were labeled and their fate was analyzed at adult stage.

The mouse model used, Osr1-ROSA26lacZ, harbors an inactivated *lacZ* gene cassette in the ROSA26 locus. This *lacZ* gene can be persistently activated by a Cre recombinase, such as the inducible *Osr1* promotor driven Cre. Comparable to the Osr1-ROSA26mTmG lineage tracer mouse model, cytoplasmic *lacZ* will become permanently expressed (see fig.10).

Mice of this Osr1-ROSA26lacZ strain were tamoxifen induced neonatally, and analyzed after 3 months at adult age. By immunohistochemistry on cryosections of the TA muscle tracked cells positive for β-galactosidase mainly expose a FAP identity as indicated by staining for PDGFRα. Muscle fibers, morphologically visualized by basal lamina staining by COL4, do not show cytoplasmic β-galactosidase, which confirms non-myogenic properties of neonatally *Osr1* expressing cells (fig.27).

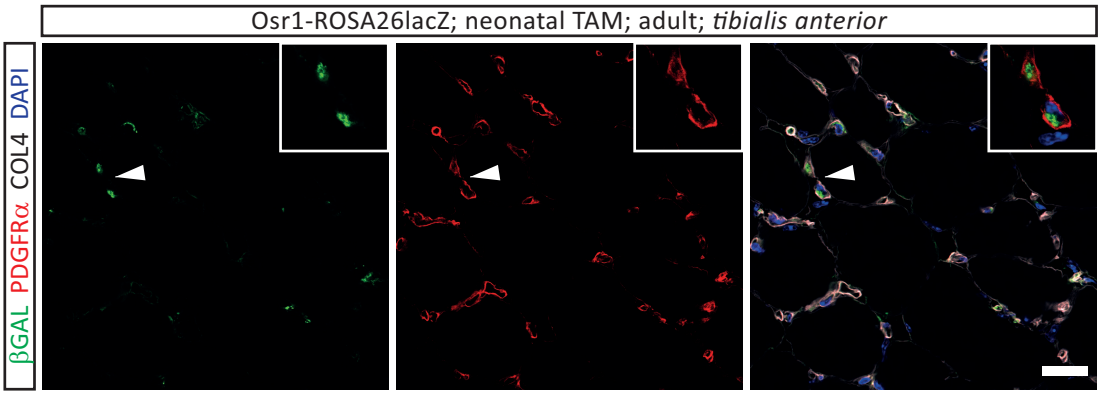

Figure 27: FAPs in adult TA muscle tissue are descendents of neonatal Osr1+ cells. Osr1-ROSA26lacZ lineage tracer mice were tamoxifen induced at P0 and P1 and analyzed in adult age. Immunohistochemistry was performed on cryosections of TA muscle using anti-βGAL (green), anti-PDGFRα (red), and DAPI (blue). Muscle basal lamina is marked by COL4 (white). Arrowheads mark magnified inlayed details. Images are representatives of 3 independent experiments. Scale bar indicates 20µm.

4.2.3 *Osr1* is sparsely expressed in FAPs in healthy adult homeostatic muscle tissue

By utilizing Osr1-GCE reporter mice to assess the expression of *Osr1* during the first 3 weeks after birth, eGFP signal was not detected at the age of 3 weeks and later. However, by RT-qPCR basal level *Osr1* mRNA quantities were detected (fig.17). To further investigate *Osr1* expression in adult mice, Osr1-lacZ reporter mice (Osr1-MFA) were subjected to histological stainings.

To assess potential *Osr1* expression in healthy adult muscle tissue, the *tibialis anterior* and *gastrocnemius* muscle from adult Osr1-lacZ reporter mice Osr1-MFA at the age of 2 to 6 months were subjected to histological stainings on cryosections (fig.28, 29).

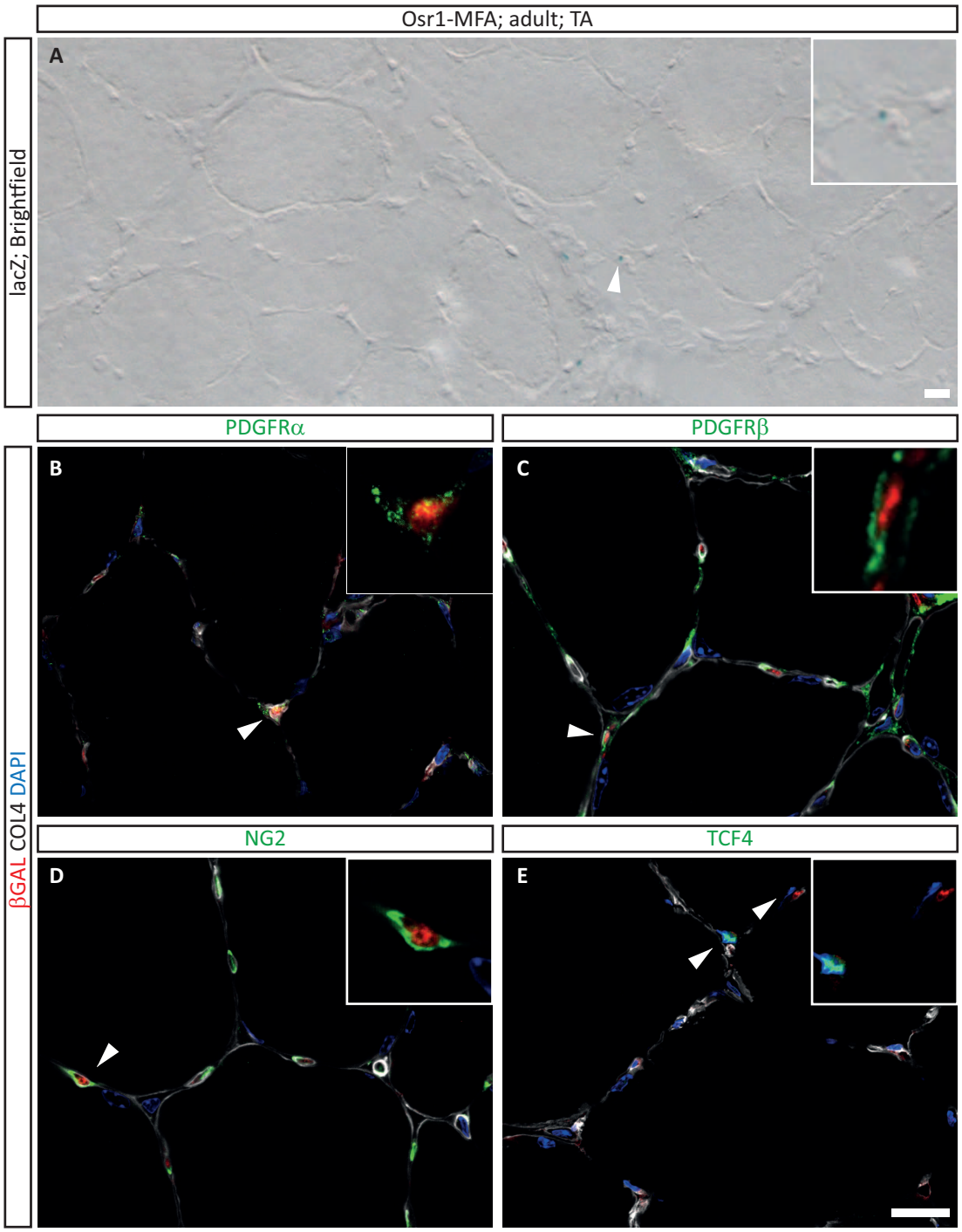

Figure 28: Adult *tibialis anterior* muscle tissue contains only sporadic Osr1+ cells.
A Brightfield imaging of TA muscle cryosections after Xgal staining reveals *Osr1* reporter+ cells sparsely distributed across the tissue. **B-E** *Osr1* reporter+ cells were stained by anti-βGAL (red), co-stainings with markers (green) for FAPs (PDGFRα), pericytes (PDGFRβ, neural/glial antigen 2 (NG2)) and interstitial fibroblast marker TCF4 were performed for cell type identification. Tissue context is visualized by anti-COL4 staining (white), nuclei were stained using DAPI (blue). Arrowheads mark magnified inlayed details. Images are representatives of 3 independent experiments. Scale bars indicates 20µm.

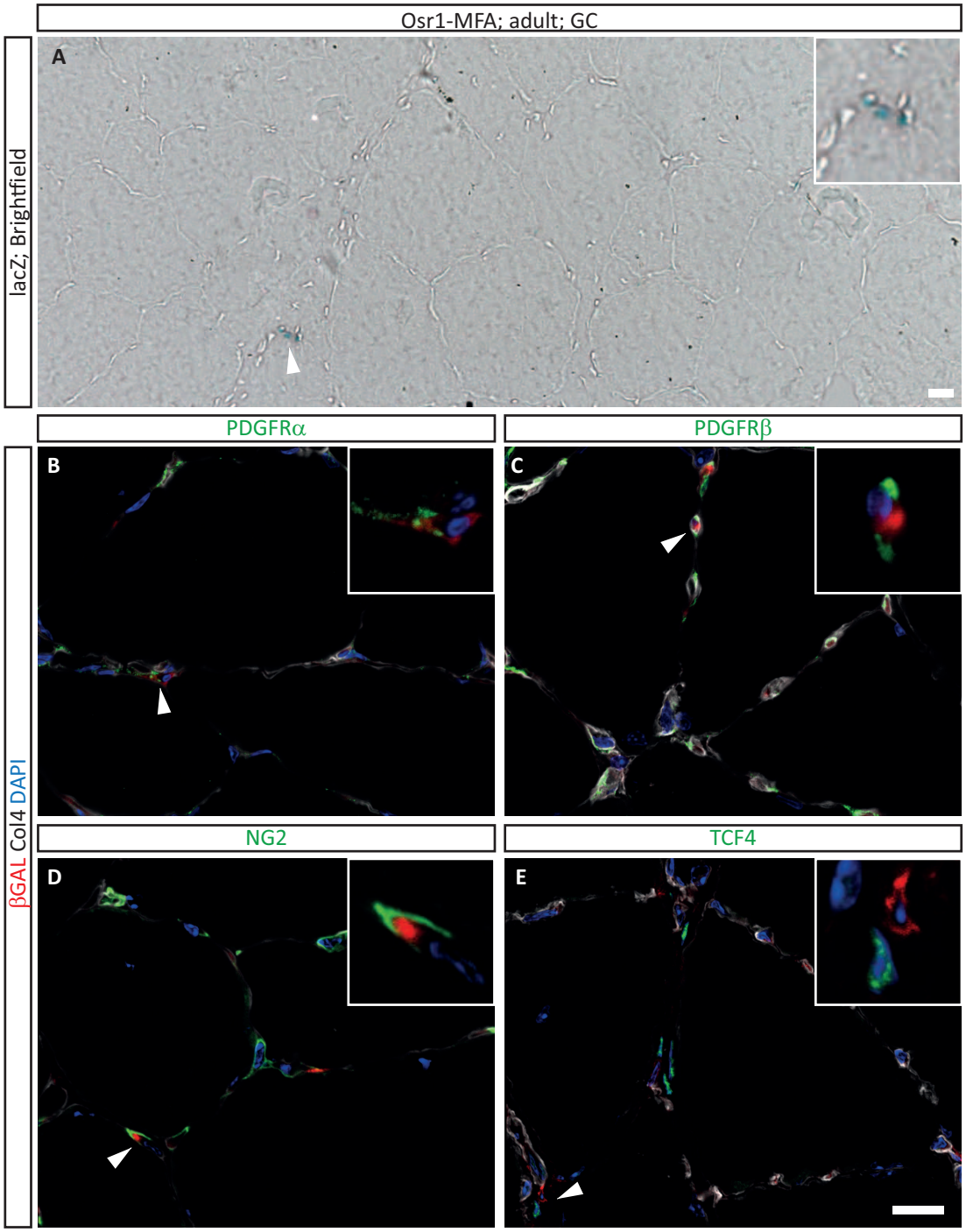

Figure 29: Adult *gastrocnemius* muscle tissue contains only sporadic Osr1+ cells.
A Brightfield imaging of GC muscle cryosections after Xgal staining reveals *Osr1* reporter+ cells sparsely distributed across the tissue. **B-E** *Osr1* reporter+ cells were stained by anti-βGAL (red), co-stainings with markers (green) for FAPs (PDGFRα), pericytes (PDGFRβ, neural/glial antigen 2 (NG2)) and interstitial fibroblast marker TCF4 were performed for cell type identification. Tissue context is visualized by anti-COL4 staining (white), nuclei were stained using DAPI (blue). Arrowheads mark magnified inlayed details. Images are representatives of 3 independent experiments. Scale bars indicates 20µm.

X-gal stainings on sections of the *tibialis anterior* muscle indicate *Osr1* expression in generally very few cells, either closely located to blood vessels and in muscle

interstitial cells (fig.28A). For cell type identification of these cells immunohistochemical stainings for FAP markers (PDGFRα), pericytes (PDGFRβ, NG2) and interstitial fibroblasts (TCF4) were performed in addition to immunofluorescent stainings for β-galactosidase. Predominantly, *Osr1* expressing cells resident in the muscle interstitium are positive for FAP marker PDGFRα (fig.28B), few show PDGFRβ or NG2 labeling (fig.28C, D), indicating pericyte identity. As during juvenile stages, expression of *Tcf4* is exclusive with Osr1-lacZ expression (fig.28E). Similar results were obtained for the *gastrocnemius* muscle (fig.29A-E).

To further characterize Osr1+ cells, *Osr1* expression in PW1+ interstitial cell populations (PICs) was investigated. PDGFRα+ and PDGFRα– PIC subsets, satellite cells and Sca-1+/ PW1– cells were isolated from adult PW1-lacZ reporter mice, and subjected to semiquantitative reverse transcription PCR. *Osr1* transcript abundance was detected in PDGFRα+ PICs, but not in PDGFRα– PICs, satellite cells or Sca-1_{high} PW1– cells (fig.30). This experiment was performed by Luigi Formicola, UPMC (Paris, France).

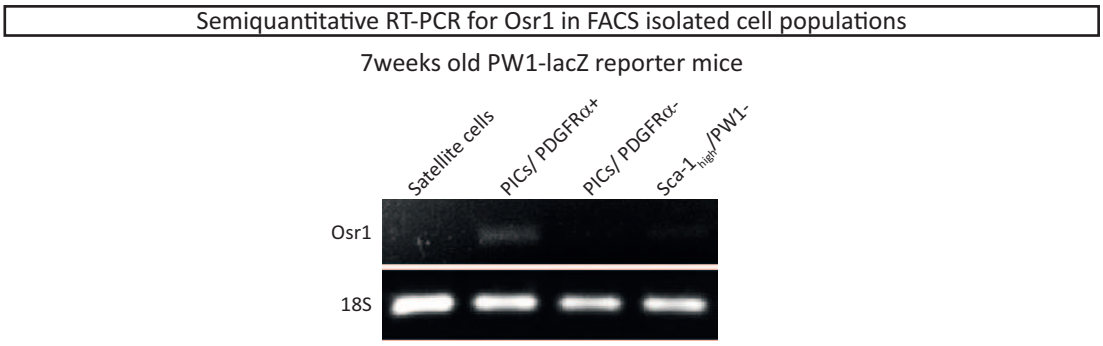

Figure 30: *Osr1* is expressed by PDGFRα+ PICs.
Cell populations were isolated from hindlimbs of 7 weeks old PW1-lacZ reporter mice by FACS, RNA extracted and reverse transcribed. Osr1 cDNA was PCR amplified using *Osr1* qPCR primers (Osr1-qPCR-F; Osr1-qPCR-R) during 25 PCR cycles, and products separated on a 1.5% agarose gel. Amplification of 18S RNA was used as a loading control. The image is representative of 2 independent experiments.

4.3 *Osr1* expression during muscle regeneration after injury

Muscle injury causes critical changes in the tissue and the stem cell niche. During an immediate initial pro-inflammatory stage immune cells infiltrate the tissue and remove cellular debris. Resident cell types and myogenic progenitors are activated, clearance progresses and during the following anti-inflammatory stage a pro-myogenic environment is generated to facilitate final regeneration. This regenerative process requires a coordinated interplay of all cell types involved.

4.3.1 Osr1+ cells accumulate after muscle injury

In the course of regeneration myogenesis and muscle development is required. The observation of upregulated *Osr1* expression during the developmentally active stage of juvenile muscle growth indicated an involvement of *Osr1* expression during muscle regeneration. Moreover, *Osr1* is expressed in FAPs during the first 3 weeks after birth,

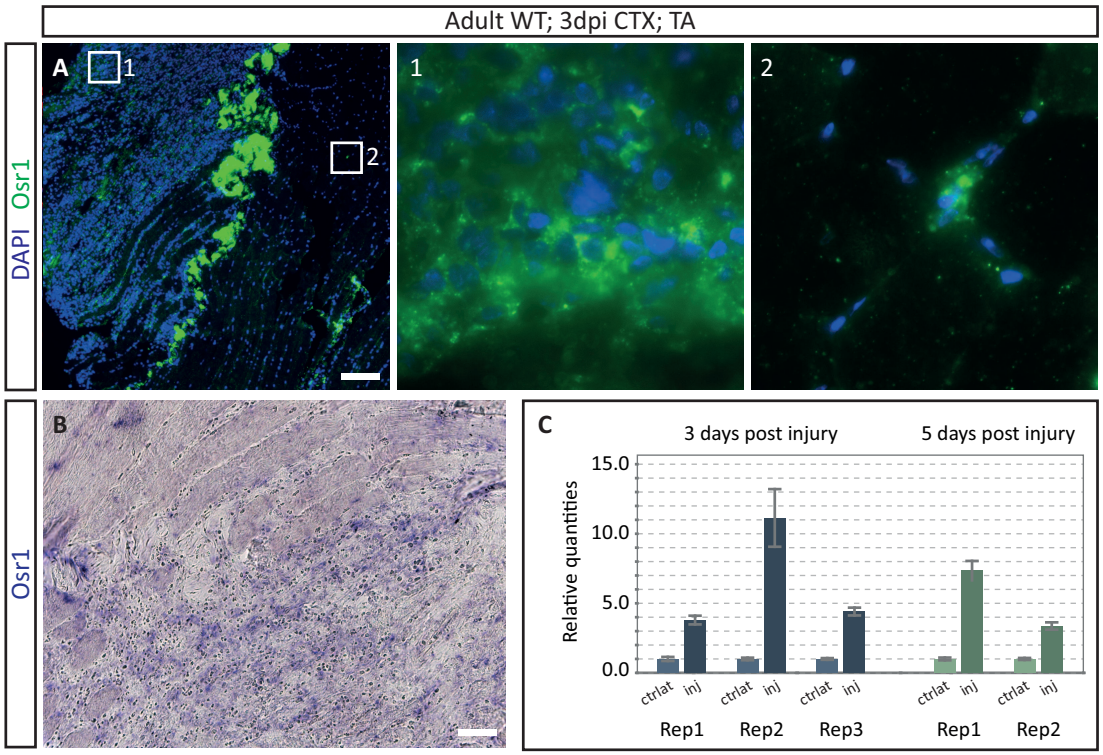

Figure 31: *Tibialis anterior* (TA) muscle tissue after cardiotoxin induced injury exposes an increased abundance of *Osr1* transcribing cells.
A Paraffin sections of wildtype TA muscle 3 days after cardiotoxin (CTX) induced injury were subjected to fluorescent RNA in situ hybridization using a probe for *Osr1* mRNA (green). Nuclei were stained using DAPI (blue). Squares mark magnified regions in injured (1) and intact tissue (2). **B** BCIP-NBT based detection of *Osr1* mRNA after RNA in situ hybridization. **C** RT-qPCR quantification of *Osr1* mRNA in biological replicates (Rep) of cardiotoxin injured whole muscle lysates (inj), 3 and 5 days post injury, compared to corresponding contralateral control muscles (ctrlat). Relative quantification was performed by normalization to GAPDH, contralateral relative *Osr1* mRNA quantities were set to 1. Scale bars indicate 100µm, error bars standard deviation.

and sparsely in homeostatic adult muscle, while FAPs were reported to be actively involved during muscle regeneration after injury.

In a pilot experiment samples from cardiotoxin-injected (CTX) *tibialis anterior* muscles of adult wildtype mice were obtained from Delphine Duprez and analyzed 3 and 5 days post injury (dpi). Tissues were prepared for paraffin embedding and for RNA extraction, in parallel.

Fluorescent RNA in situ hybridization on paraffin sections was conducted to detect *Osr1* transcript. An increase in the number of *Osr1* transcribing cells in the regenerating region of the damaged tissue was observed, whereas in the intact region *Osr1* mRNA was detected in few sparse cells only. In addition, a histochemical RNA in situ hybridization utilizing a BCIP-NBT color reaction was performed to evaluate potential autofluorescent artifacts. A putative connective tissue layer crossing the

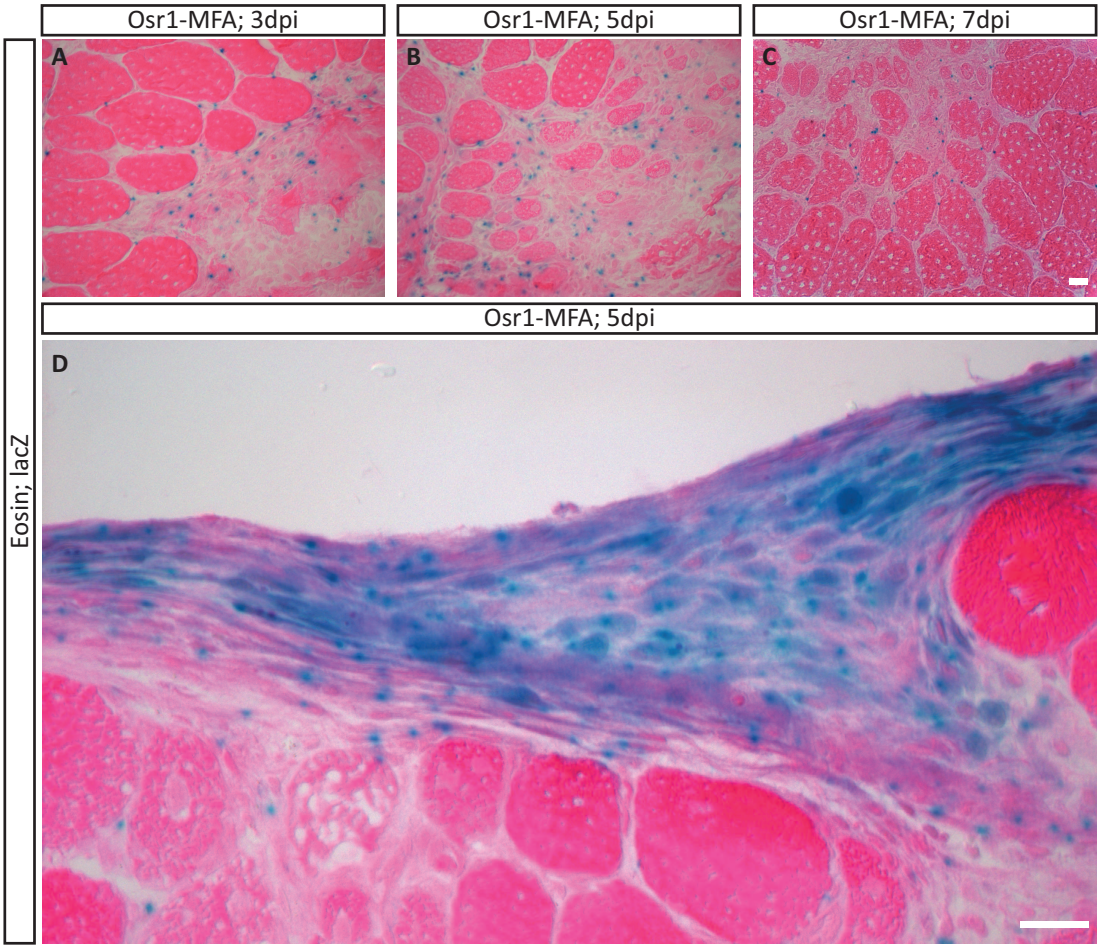

Figure 32: Number of *Osr1* reporter+ cells declines with progression of regeneration after injury.
A-C Cryosections of intramuscular regions of Osr1-MFA TA muscles 3, 5, and 7 days after freeze/pierce injury treatment were Xgal stained followed by eosin staining. Series images are representative of single biological replicates. **D** Epimysial region proximal to injured tissue of 5 days post injury. Images is representative of 2 independent experiments. Scale bar indicates 20µm.

tissue exhibits a strong green fluorescent signal which is not present after staining using BCIP-NBT. This appearance is concluded an autofluorescent artifact. Applying RT-qPCR on whole muscle lysate RNA extracts to quantify *Osr1* transcript levels confirms an increase on *Osr1* RNA amount normalized to the contralateral uninjured control (fig.31).

While CTX induced injury excludes mononucleated cells from damage [Couteaux and Mira, 1985, Couteaux et al., 1988, Harris et al., 2003], a mechanically applied injury model was considered for further investigations to mimick naturally occuring injuries. Applying tissue damage by piercing the *tibialis anterior* muscle with a syringe needle cooled in liquid nitrogen (freeze/ pierce injury), muscles of Osr1-lacZ reporter mice Osr1-MFA were injured and analyzed 3, 5 and 7 days after treatment. On cryosections Xgal staining indicates numerous *Osr1* reporter+ cells in the region of damaged tissue 3dpi. The same can be observed at 5dpi, where newly regenerating muscle fibers are already recognizable. At 7dpi muscle regeneration has further progressed, and the number of *Osr1* expressing cells decreases (fig.32A-C). In epimysial regions of these tissues, representing presumable temporary fibrotic scarring, *Osr1* reporter+ cells are highly abundant at 5dpi (fig.32D).

In juvenile muscle, *Osr1* expression is mainly found in the majority of juvenile Sca-1_{med} FAPs (see fig.18, 19). To test whether this juvenile population is still present in the adult, and whether expanding FAPs after injury are derived from juvenile FAPs, lineage tracing utilizing the Osr1-ROSA26lacZ mouse model was conducted. This model contains the Osr1-GCE cassette which encodes for the inducible

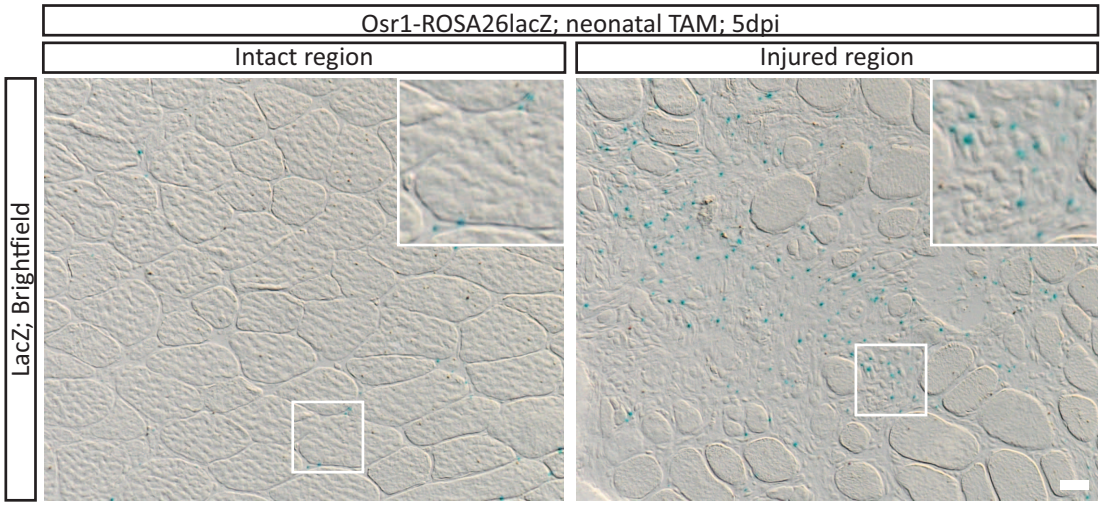

Figure 33: Neonatal Osr1+ cells expand in the adult after muscle injury.
Neonatal Osr1-ROSA26lacZ pups were tamoxifen induced at P0 and P1, and in adult age injured by freeze/ pierce treatment. Regenerating TA muscles were analyzed 5 days post injury. Neonatally traced cells were stained by Xgal and imaged. Squares indicate regions of inlayed magnifications. Images are representatives of 3 independent experiments. Scale bar represents 20µm.

Cre recombinase driven by the *Osr1* promotor, and the *lacZ* gene cassette in the ROSA26 locus for permanent genetic labeling (see fig.10). Osr1-ROSA26lacZ mice were tamoxifen induced at P0 and P1, hence cells expressing *Osr1* during the first 2 days after birth were permanently labeled by *lacZ* expression. Once grown into adult mice, these animals were subjected to freeze/ pierce injury application and analyzed 5 days post injury for lacZ+ cells. Regenerating muscle tissue was cryosectioned, and subjected to Xgal staining. Intact muscle tissue shows traced cells in the muscle interstitium, while damaged tissue regions expose an accumulation of lacZ+ cells (fig.33). In these cells *Osr1* was expressed during P0 and P1.

Scarcity of Osr1+ cells in healthy muscle and abundance of Osr1+ cells after injury indicates proliferative expansion of the Osr1+ cell pool. In order to elucidate proliferation as a potential cause for the increase in the number of *Osr1* reporter+ cells immunofluorescent staining for the proliferation marker Ki67 was conducted. Ki67 is expressed and abundant throughout all active phases of the cell cycle, but not in G0 phase which marks resting or quiescent cells. Osr1-MFA mice were injured and analyzed 3 days post injury. Cryosections of the regenerating *tibialis anterior* were subjected to Xgal and subsequent immunofluorescence stainings. *Osr1* reporter+ cells in the damaged area of the tissue are predominantly positive for Ki67, hence are proliferating (fig.34).

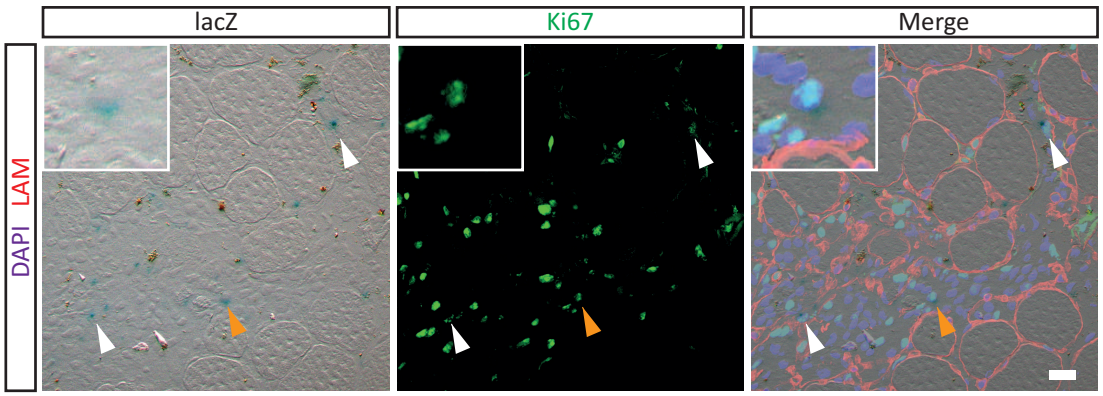

Figure 34: *Osr1* reporter+ cells in injured tissue proliferate.
Cryosection of adult Osr1-MFA *tibialis anterior* muscles 3 days after freeze/ pierce injury treatment were stained using Xgal, imaged, and subsequently subjected to immunohistochemistry to mark proliferating cells by anti-Ki67 (green). Tissue context is visualized by staining for Laminin (red), nuclei were stained using DAPI (purple). After confocal imaging both images were overlayed and merged. White arrowheads mark cells double positive for Xgal and Ki67, orange arrowheads indicate magnified inlay region. Images are representatives of 2 independent experiments. Sale bar indicates 20µm.

4.3.2 Most but not all *Osr1* reporter+ cells after injury are PDGFRα+

TCF4+ muscle connective fibroblasts were reported to expand after muscle injury and provide a temporary fibrosis consisting of extracellular matrix [Murphy et al., 2011, Mann et al., 2011]. An overlap in the identity of Osr1+ cells after injury with TCF4+ muscle connective tissue fibroblasts was investigated utilizing the Osr1-GFP reporter strain Osr1-GCE. Immunohistochemistry on cryosections of *Osr1*$^{GCE/+}$ *tibialis anterior* muscle 5dpi showed *Osr1* reporter GFP and *Tcf4* expressed exclusively (fig.35). GFP+/ TCF4+ cells were not observed, indicating distinct cell identities.

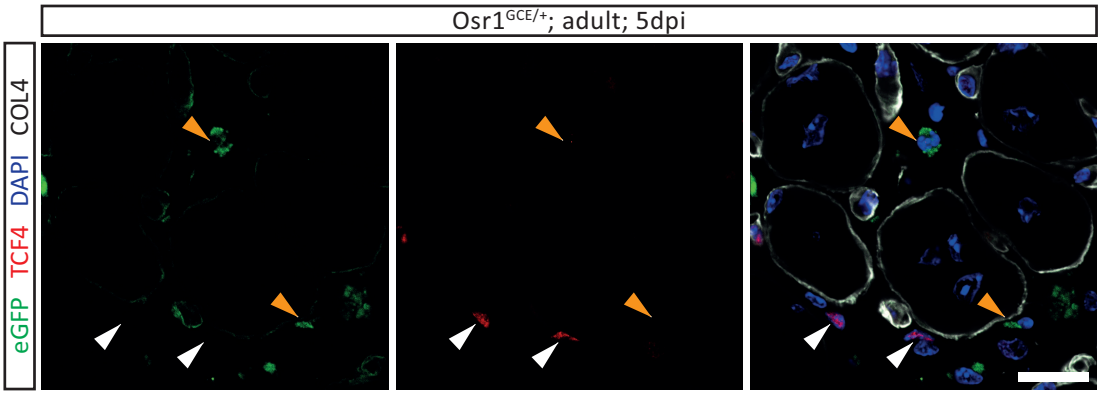

Figure 35: After injury *Osr1* and *Tcf4* are expressed exclusively.
Cryosections of *Osr1*$^{GCE/+}$ TA muscle 5 days after freeze/ pierce injury treatment was subjected to immunohistochemistry to detect endogenous eGFP expression (green; orange arrowheads) and TCF4+ (red; white arrowheads) cells. Co-staining against collagen 4 (white) indictes tissue context, nuclei were stained using DAPI (blue). This image is representative of single biological replicate. Scale bar represents 20µm.

To approach further cell type characterization and quantification of *Osr1* expressing cells in damaged tissue, FACS analysis was conducted. Having observed a population false positive for fluorescent β-galactosidase substrate C_{12}FDG in wildtype C57BL/6j mice, sorting gates in the FACS setup were adjusted accordingly. The gate for selection of C_{12}FDG signals was set for a minimal inclusion of C_{12}FDG+ cells in wildtype mice, then applied to the cell pool of Osr1-MFA reporter mice 3 days after injury. All remaining events were considered β-glactosidase– (fig.36).

Using this setup injured adult *tibialis anterior* muscles of Osr1-MFA reporter mice 3 days post freeze/ pierce injury were subjected to FACS analysis (fig.37). By light scattering cell debris and aggregates were excluded from further analyses (fig.37A), PI– single cells furthermore included as alive cells (fig.37B). Cells of the immune response having infiltrated the damaged tissue, such as macrophages, and other hematopoietic cells were detected by staining against CD45, and were excluded from the cell pool. Same accounts for erythroid cells, marked by Ter119 (fig.37C). A portion of 1.7% *lacZ* reporter+ was detected in this hematopoietic cell population. The remaining

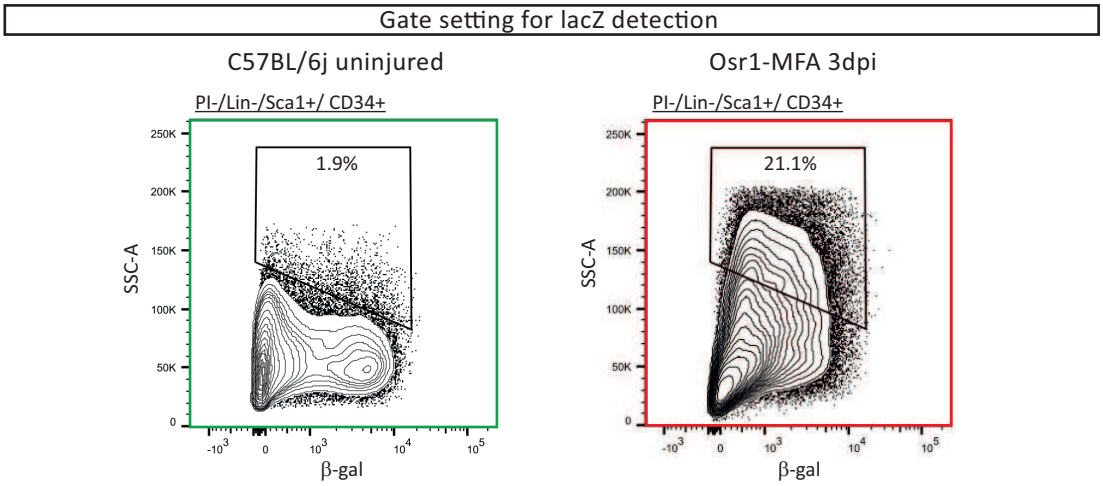

Figure 36: FACS gate setting for *lacZ* detection in injured Osr1-MFA cells.
Single cell suspensions from TA muscles of 4 uninjured wildtype C57BL/6j and 4 injured Osr1-MFA 3 days post injury were generated and subjected to FACS analysis. Green fluorescent signal of C_{12}FDG, mediated by βgalactosidase conversion of the substrate, was measured in the PI–/Lin–/Sca1+/CD34+ population of wildtype cells, set as negative reference and adapted to βgalactosidase+ Osr1-MFA cells.

cells were separated by Sca1 versus CD34, both markers for subsets of stem cells (fig.37D). This results in a separation of cell populations with osteo-/ chondrogenic potential (CD34–/ Sca1–), myogenic progenitors (CD34+/ Sca1–) and a cell pool containing FAPs (CD34+/ Sca1+). The osteo/ chondrogenic cell population contains 7.8% *lacZ* reporter+ events, the myogenic population 3.2%. The FAPs containing cell population was also further investigated for *Osr1* reporter expressing cells, which is indicated by a percentage of 21%. Of these 21% *Osr1* reporter expressing cells 85% are positive for FAP marker PDGFRα (fig.37E). Investigating the FAP containing population (CD34+/ Sca1+) for PDGFRα, 42% are positive for this FAP marker. Of these FAPs 39% are positive for *Osr1* reporter *lacZ* (fig.37F). In summary, analysis of whole muscle tissue cells of injured mice 3 days post injury indicates 39% of all FAPs expressing *Osr1* reporter. 7% of *Osr1* reporter+ cells do not expose a FAP identity as they are PDGFRα–.

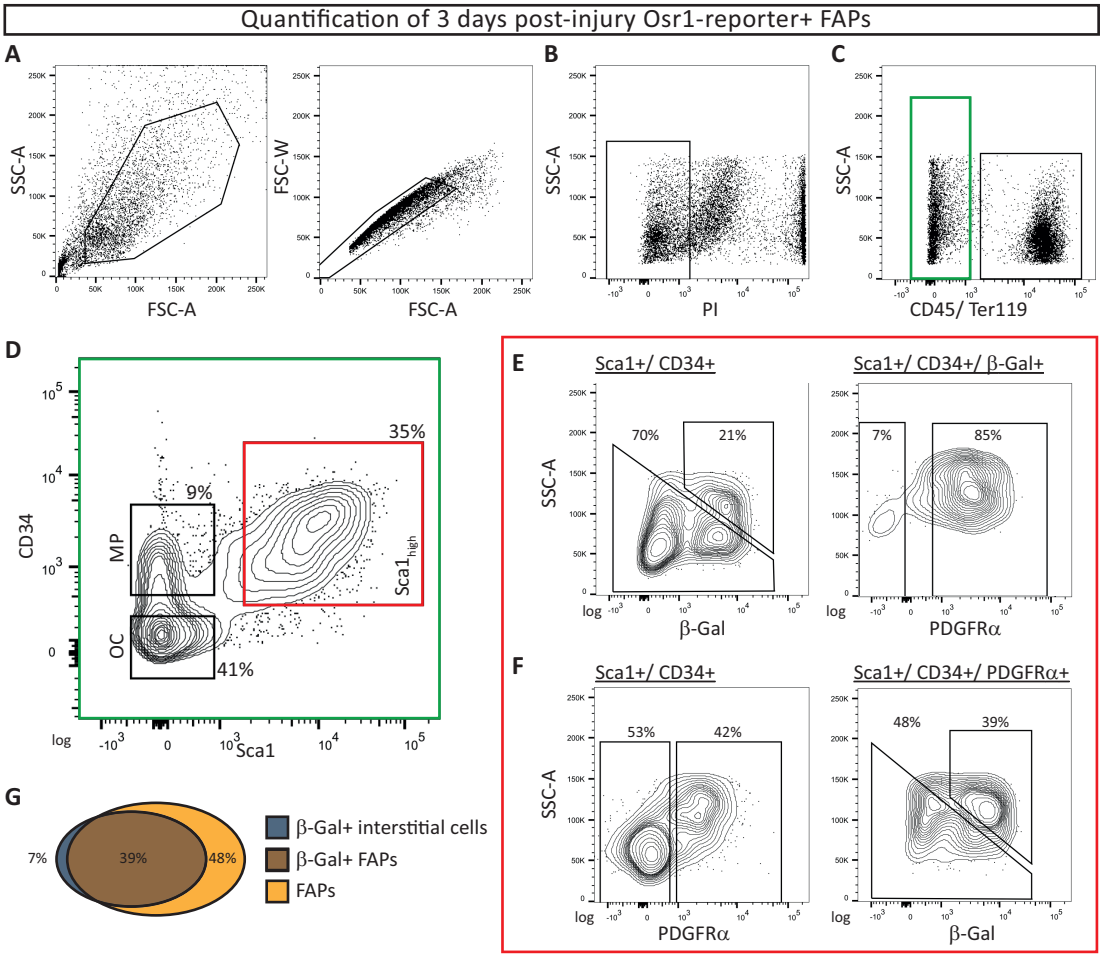

Figure 37: FACS acquired distribution and quantification of *Osr1* reporter+ cells in TA muscles of Osr1-MFA mice 3 days post injury.
A From cell suspensions of 6 injured TA muscles 3 days post injury cell debris and doublets were excluded by light scattering. **B** Negative selection for dead cells (PI+) yielded alive single cells, of which only non-hematopoietic cell types (CD45–/ Ter119–) were selected (**C**). **D** Separation of the remaining cells by CD34 and Sca-1 presented an osteo-/ chondrogenic (CD34–/ Sca-1–), a myogenic (CD34+/ Sca-1–) and a FAP-containing population (CD34+/ Sca-1+). **E** This CD34+/ Sca1+ population contains 21% *Osr1* reporter+ cells, of which 85% are positive for FAP marker PDGFRα. **F** Vice versa, 42% of the CD34+/ Sca1+ population express FAP marker PDGFRα of which 39% are *Osr1* reporter+. **G** Venn diagram summarizes 39% of cells double positive for *Osr1* reporter and FAP marker PDGFRα , 7% only express *Osr1* reporter *lacZ*, and 48% only PDGFRα. Plots are representatives of 3 independent experiments.

4.3.3 Muscle injury triggers activation of *Osr1* expression in FAPs

In healthy intact muscle tissue only few, sparse cells show *Osr1* expression, whereas after tissue damage an increase in Osr1+ cells was detected. To investigate whether this increase is the consequence of an expansion of those sporadic Osr1+ cells or of an activation of *Osr1* expression in cells that did not express *Osr1* before injury, cell fate tracking experiments were conducted (fig.38). Osr1-ROSA26lacZ and Osr1-ROSA26mTmG lineage tracer mice were tamoxifen induced for 5 consecutive days 1 week before injury, thus lineage-labeling Osr1+ cells in healthy muscle was conducted

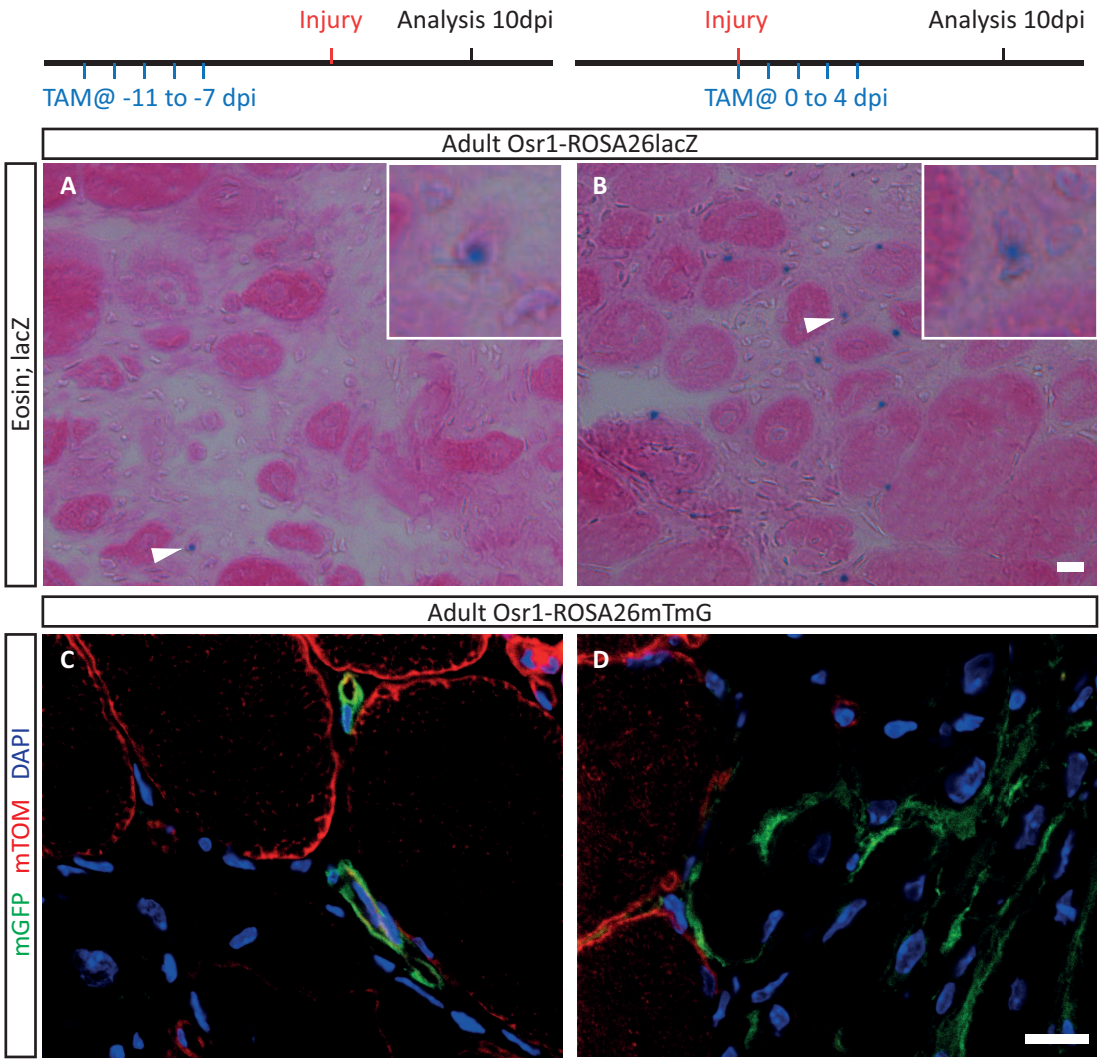

Figure 38: Activation of *Osr1* expression is triggered by muscle injury.
Adult lineage tracer mice (Osr1-ROSA26lacZ; Osr1-ROSA26mTmG) were tamoxifen induced for 5 consecutive days to lineage-trace Osr1+ cells in healthy tissue, and after further 7 days injured by freeze/ pierce method. In parallel, mice of the corresponding strains were injured followed by 5 days of tamoxifen induction to lineage-trace Osr1+ cells post injury. TA muscles were analyzed 10 days post injury. **A, B** Cryosections after Xgal and eosin staining of Osr1-ROSA26lacZ lineage tracers induced before (left) and after (right) injury. Images are representatives of 3 independent experiments. **C, D** Confocal imaging of cryosections of Osr1-ROSA26mTmG specimen, after additional DAPI (blue) nuclear staining. Traced cells are mGFP+, mTOM indicates tissue context. Single experiment. Scale bars indicate 20µm.

(fig.38A, C). In parallel, mice of both strains were subjected to injuries and tamoxifen induced day 0 to day 4 after injury (fig.38B, D). For both setups, mice were analyzed 10 days post injury.

Histochemical staining methods on cryosections of tissue induced before application of injury hardly show an increase in labeled cells in the region of injury. However, labeling of cells expressing *Osr1* after injury results in a remarkable increase in the number of labeled cells. This indicates an activation of *Osr1* expression triggered by

injury, in cells in proximity to damaged tissue.

4.3.4 Fate of activated Osr1+ cells in the course of regeneration

For studying the fate of cells expressing *Osr1* during regeneration after injury, cell fate tracking was conducted using lineage tracer mouse lines. Mice were mechanically injured, tamoxifen induced for 5 consecutive days from the day of injury on, to label cells expressing *Osr1* and analysed at two different times during regeneration.

First, Osr1-ROSA26lacZ mice were analyzed 10 days post injury to investigate possible fusion of Osr1+ cells with regenerating muscle fibers. Immunofluorescent staining on cryosections of injured *tibialis anterior* muscle using anti-βGAL to mark cytoplasmic β-galactosidase and anti-LAM to stain muscle fiber basal laminas did reveal no labeled muscle fibers. Thus, as in development, *Osr1* expressing cells do not fuse to muscle fibers in the course of regeneration (fig.39).

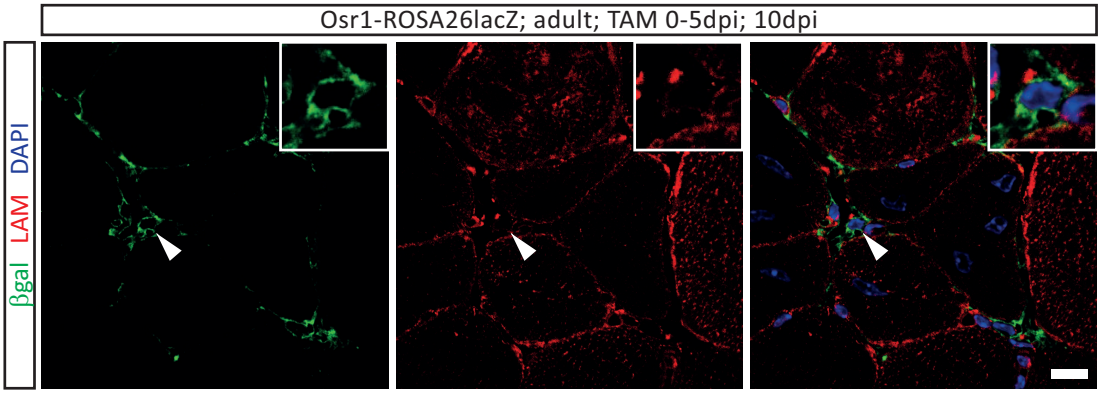

Figure 39: Injury activated Osr1+ cells are not myogenic in the course of regeneration. Osr1-ROSA26lacZ mice were injured by freeze/ pierce technique, tamoxifen induced at the time of injury and 4 consecutive days, and analyzed 10 days after injury. Cytoplasmic βGAL (green) was detected solely in interstitial cells, not in muscle fibers as indicated by Laminin (red). Nuclei were stained using DAPI (blue). Arrowheads mark magnified inlayed details. Images are representatives of 2 independent experiments. Scale bar indicates 10µm.

Osr1-ROSA26mTmG lineage tracer mice were used to study the fate of Osr1+ cell progeny 10 days post injury in regard to pericytes and interstitial fibroblasts. For analyses of regenerating *tibialis anterior* muscle cryosections were subjected to immunohistochemistry. While labeled cells were stained using anti-GFP, co-stainings for pericytes (PDGFRβ, NG2) and interstitial fibroblasts were conducted. Few labeled cells colocalize with PDGFRβ and with NG2, hence few descendant cells expose a pericyte identity (fig.40A, B). However, while TCF4+ *Osr1* expressing cells in healthy homeostatic muscle could not be observed (see fig.28, 29), neither at early stage during regeneration (fig.35), Osr1+ cells after tissue damage have differentiation potential to TCF4+ interstitial fibroblasts in the course of tissue regeneration (fig.40C).

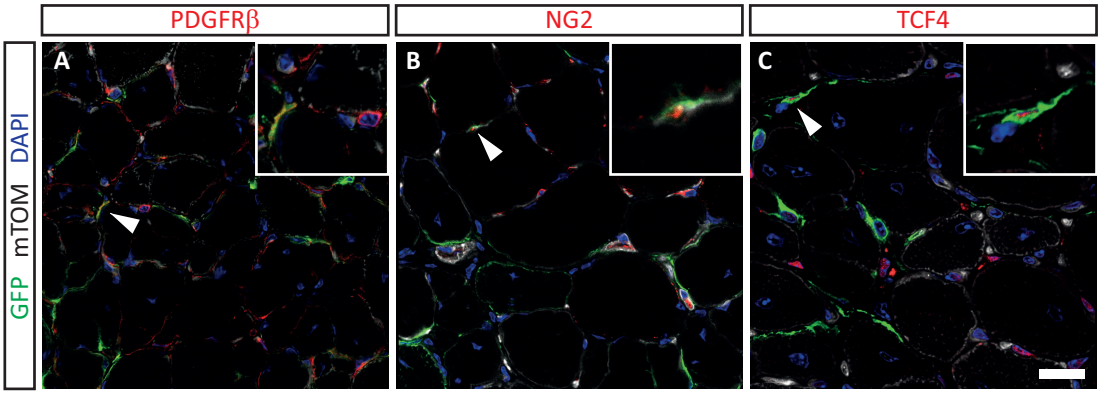

Figure 40: Cell fate of injury activated Osr1+ cells 10 days post injury.
Using cryosections of Osr1-mTmG lineage tracer mice induced at the time of injury and 4 consecutive days, fate of Osr1+ cells at 10 days post injury was studied applying immunohistochemistry. By anti-GFP tracked cells were labeled (green), mTOM indicates tissue context (white) and nuclei were stained by DAPI (blue). Co-stainings with markers (red) for pericytes (PDGFRβ, NG2) and interstitial fibroblast marker TCF4 were performed for cell type identification. Arrowheads mark magnified inlayed details. Images are representatives of 2 independent experiments. Scale bar indicates 20µm.

The fate of cells expressing *Osr1* after injury was also investigated at a stage of terminal regeneration, 4 weeks after tissue damage. Tibialis anterior muscle of Osr1-ROSA26mTmG was subjected to immunohistochemistry, using anti-GFP to stain for labeled cells. Regenerated regions can be identified by fibers featuring centrally located nuclei, that is myonuclei did not terminally migrate peripheral, yet. In these regions of the tissue, lineage traced cells are accumulated in the muscle interstitium (fig.41B or D). This observation implies at least not all FAPs positive for Osr1 after injury undergo apoptosis in the course of regeneration. Co-stainings using anti-PDGFRα and anti-PDGFRβ show labeled cells remaining resident in the muscle interstitium as FAPs or pericytes, respectively (fig.41A, B).

By co-stainings with anti-CD31, a specific marker for endothelial cells, blood vessel capillaries were identified. These structures are damaged by mechanical injury as well, and regenerate subsequently. While Osr1+ cell descendants are often located in close proximity to blood vessel capillaries (fig.41C1), sporadic tracked cells potentially exposing an endothelial cell type identity were detected (fig.41C2). In co-stainings for TCF4 tracked cells having become interstitial fibroblasts are observable (fig.41D), as it was shown above already at 10 days post injury.

To further evaluate the fate of cells expressing *Osr1* during regeneration the origin of FAPs, pericytes and connective tissue fibroblasts was assessed quantitatively. Lineage tracer mice Osr1-ROSA26mTmG were subjected to injury and tamoxifen induced during the first 5 days. 4 weeks post injury immunohistochemistry on cryosections was performed for cell type markers PDGFRα, PDGFRβ and TCF4. Cells positive for each marker and cells double positive for marker and tracer labeling were counted and

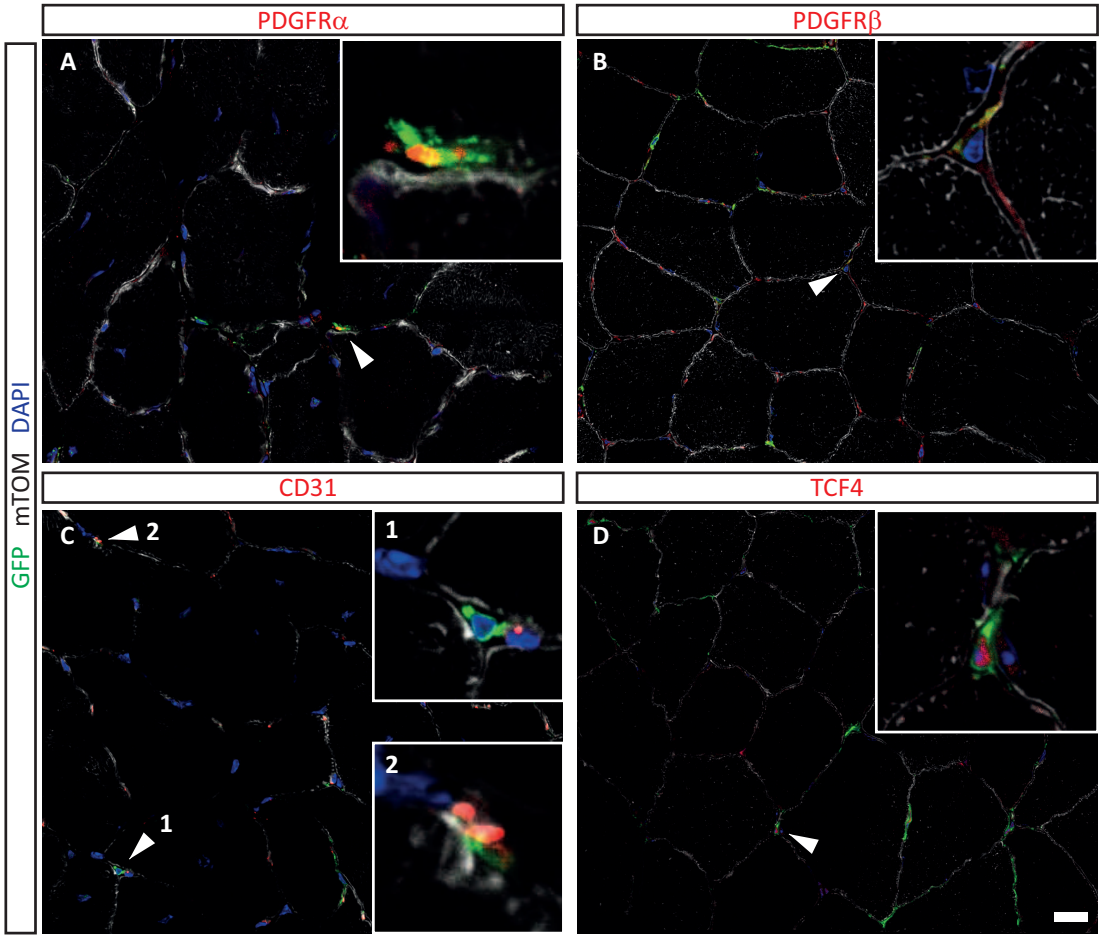

Figure 41: Cell fate of injury activated Osr1+ cells 28 days post injury.
Using cryosections of Osr1-mTmG lineage tracer mice induced at the time of injury and 4 consecutive days, fate of Osr1+ cells at 28 days post injury was studied applying immunohistochemistry. By anti-GFP tracked cells were labeled (green), mTOM indicates tissue context (white) and nuclei were stained by DAPI (blue). Co-stainings with markers (red) for FAPs (PDGFRα), pericytes (PDGFRβ), endothelial cells (CD31) and interstitial fibroblast marker TCF4 were performed for cell type identification. Arrowheads mark magnified inlayed details. Images are representatives of 4 independent experiments. Scale bar indicates 20µm.

the numbers compared (fig.42). In the regenerated region 68% of all PDGFRα+ and 33% of all PDGFRβ cells show GFP signals, indicating an origin in Osr1+ cells. While Osr1+ cells 5 days after injury do not express *Tcf4* (see fig.35), 4 weeks after injury 43% of all TCF4+ cells are positive for membraneous GFP. This observation implies that Osr1+ cells can acquire TCF4+ fibroblast identity in the course of progressing regeneration.

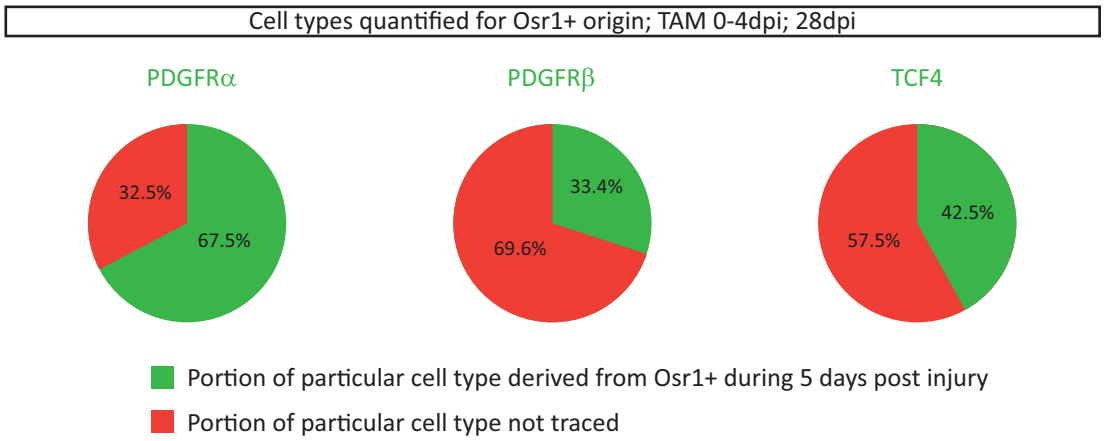

Figure 42: Cell fate of injury activated Osr1+ cells 28 days post injury.
For quantification all cells positive for each cell type corresponding marker and the portion of cells double positive for marker and tracer labeling GFP were counted. 8 fields of view for each of 2 replicates were counted and averaged.

4.4 *Osr1* expression during fatty infiltration in the course of muscle regeneration after injury

Based on the observed adipogenic capacities of neonatal Osr1+ cells and the strong adipogenic potential of FAPs [Uezumi et al., 2010] their involvement in muscular fat formation during muscle regeneration after injury was studied. Intramuscular injection of glycerol is a commonly accepted model for fatty infiltration in muscle tissue. Glycerol dissolves muscle fiber membranes, thus leading to muscle injury. In the course of following regeneration it furthermore drives the adipogenic differentiation of tissue resident progenitor cells, hence fat formation.

Initially, wildtype mice were injected and investigated histologically 14 days later. Cryosections stained by H&E displayed newly regenerated fibers including centrally located nuclei. In between the fibers caverns are recognizable, containing hematoxylin stained nuclei (fig.43). These caverns are adipocytes that had contained large lipid droplets whose lipid was washed out by the ethanol dilution series required for eosin staining. This result is in coherence with the reported characterization of this injury model for fatty accumulation [Pisani et al., 2010].

By cell lineage tracing adipogenic potential of Osr1+ cells after glycerol induced injury was investigated *in vivo*. Osr1-ROSA26mTmG lineage tracer mice were subjected to glycerol injury, and tamoxifen induced day 0 to day 4. Analysis took place 5 days and 14 days post injury.

Cryosections of regenerating *tibialis anterior* muscle were subjected to immunfluorescent staining, utilizing anti-GFP to mark traced cells and anti-PLINA/B to identify

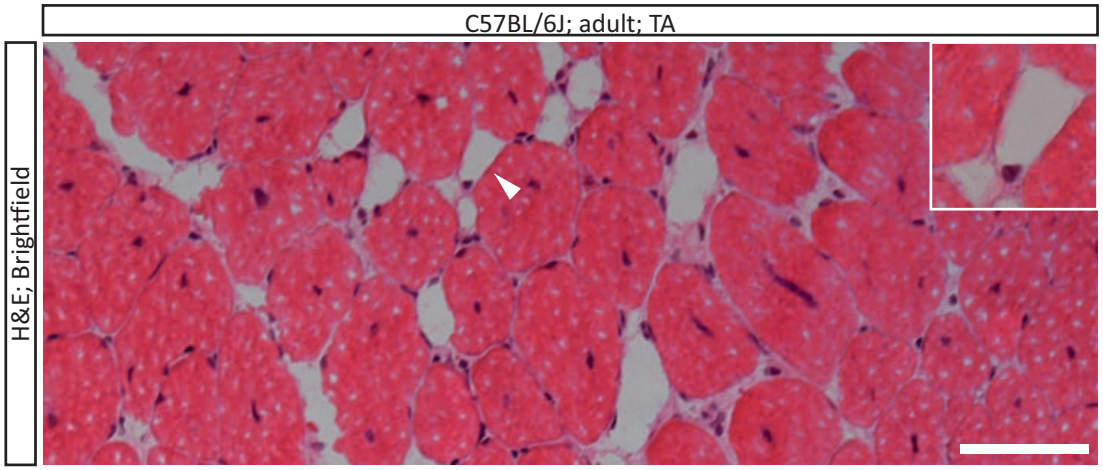

Figure 43: Histological confirmation of glycerol induced muscle injury and fatty infiltration. Glycerol was administered intramuscularly into the TA muscle of adult C57BL/6J mice and analyzed 14 days after treatment. Cryosections subjected to H&E staining show centrally located myonuclei and interstitial adipocytes (arrowhead and magnified inlay). Images are representatives of 3 independent experiments. Scale bar indicates 100µm.

adipocytes.

On day 5 after glycerol injection the damaged area of the tissue shows accumulated tracked mGFP+ cells, confirming an activation of *Osr1* expression triggered by glycerol induced muscle injury. Lipid droplet containing adipocytes, as indicated by a staining of lipid droplet membranes by perilipin, could not be observed. On day 14 post injury, muscle fibers have partially regenerated, identifiable by fibers exposing a centrally located nucleus. Tracked cells stained by mGFP are residing in the muscle interstitium, in proximity to lipid droplet containing adipocytes stained for perilipin. However, a colocalization of traced cells and perilipin was not observed, hence adipogenic potential of Osr1+ cells after glycerol induced injury is limited in this injury model for fatty infiltration (fig.44).

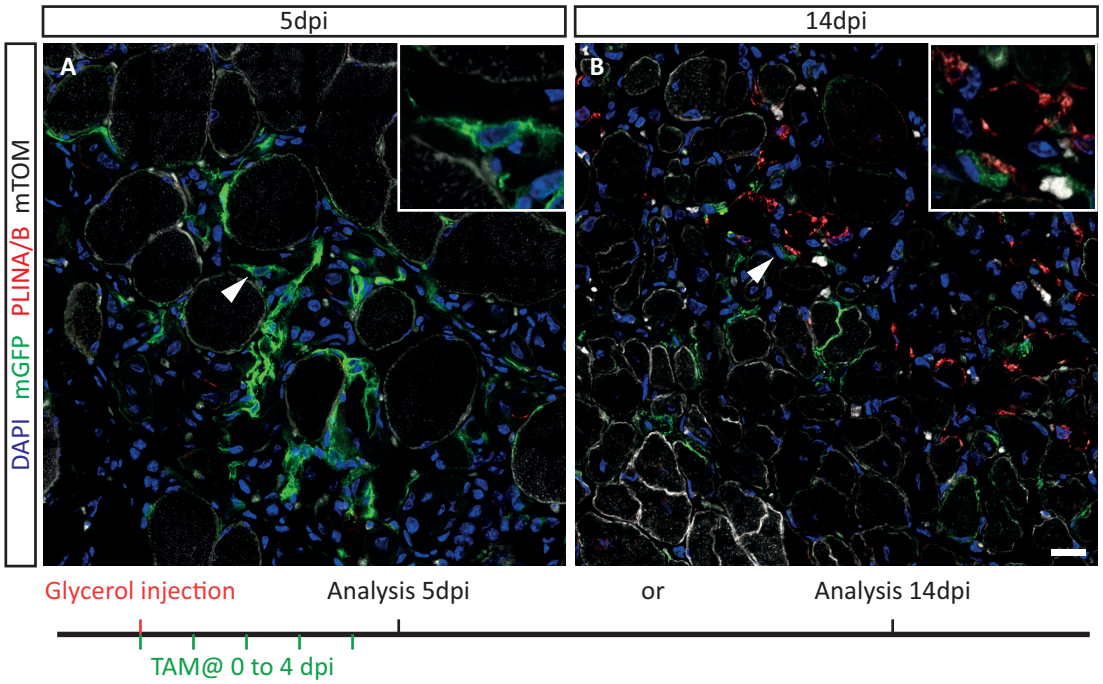

Figure 44: Injury induced Osr1+ cells show limited adipogenic potential in the course of fatty infiltration after glycerol injection.
Osr1-ROSA26mTmG lineage tracer mice were glycerol injected, followed by tamoxifen induction for 5 consecutive days. Regenerating TA muscles were analyzed 5 days (**A**) and 14 days (**B**) post injury. By anti-GFP tracked cells were labeled (green), tomato indicates tissue context (white) and nuclei were stained by DAPI (blue). Co-stainings with anti-PLINA/B were performed to identify lipid droplet containing adipocytes. Images are representatives of 3 independent experiments, respectively. Scale bar indicates 20µm.

4.5 Functional studies of a conditional *Osr1* knock-out *in vivo* during muscle regeneration

Investigations of the effect of an *Osr1* knock-out on muscle regeneration after mechanically induced injury were approached utilizing a mouse line generated by crossing Osr1-GCE mice with Osr1-flox mice. The mouse model $Osr1^{GCE/fl}$ enables inducible recombination of the *Osr1* locus at the *loxP* flanked exon 2, in cells that express *Osr1* promotor driven Cre recombinase from the other allele. However, the generation of this mouse model was completed at the final stage of this PhD thesis, hence, studies were limited to initial analyses.

$Osr1^{GCE/fl}$ were injured by freeze/ pierce technique, and knock-out induced by tamoxifen on the day of injury and 4 additional consecutive days. The aim was to cause a knock-out in cells experiencing an activation of *Osr1* expression in the regions of tissue damage. The mice were sacrificed on day 5 post injury and regenerating *tibialis anterior* muscles processed for cryosectioning.

Initially, successful recombination in injured tissue was tested. 3 cryosections of 50µm thickness were trimmed from the tissue and DNA extracted from the specimen. This DNA was subjected to a PCR to detect excision of exon 2 by forward and reverse primers spanning this region. Additionally, the reverse primer was located on the inverted eGFP gene, which was flipped in the course of Cre mediated recombination of the locus. This way a PCR product was amplified only in case of a successfully recombined *Osr1* locus (fig.45).

While this PCR product was obtained from $Osr1^{GCE/fl}$ mice, $Osr1^{GCE/+}$ specimen

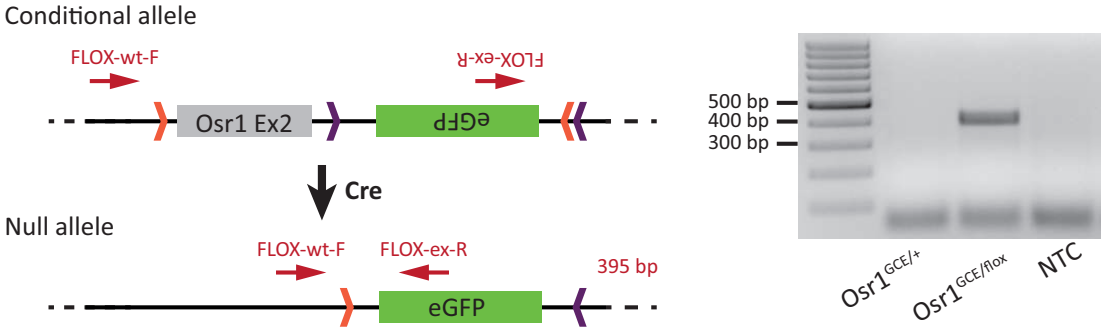

Figure 45: *Lox2372* flanked Exon 2 in $Osr1^{GCE/fl}$ is recombined after injury and successive tamoxifen induction.
Successful recombination of the *lox2372* site (orange) flanked cassette containing exon 2 and eGFP after Cre recombination was tested by PCR. DNA extracted from muscle tissue 5 days post injury, after tamoxifen induction for 5 consecutive days, was used as template. Using a forward primer (FLOX-wt-F) located 5' of exon 2 and its upstream *lox2372* site, and a reverse primer (FLOX-ex-R) 3' of the *lox2372* site downstream, a PCR product of 395bp was amplified only in case of successful Cre recombination. This product was extracted from the 2% agarose gel and subjected to Sanger sequencing. GeneRuler™100bp DNA Ladder was loaded onto the gel as size reference.

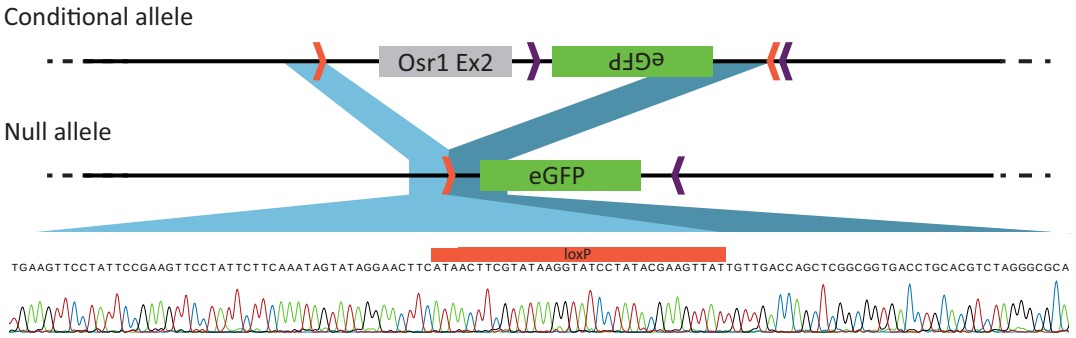

Figure 46: Sequencing analysis of the PCR product amplified after tamoxifen induced recombination of *Osr1*$^{GCE/fl}$ specimen.
Sequence of the product obtained by PCR with primers spanning the 5' terminal *lox2372* site (red arrows) of the potentially Cre recombined region shows successful recombination. Projecting the sequence of the resulting null allele on the originating floxed allele (blue area) confirms inversion of the cassette containing eGFP and exon 2. The sequence downstream of the *loxP* site (red box) on the null allele is reverse complement to the corresponding sequence in the conditional allele (dark blue).

did not yield a product, as expected. The PCR product was extracted from the agarose gel and sequenced by Sanger method. Analysis of the sequence confirmed successful excision of exon 2 from the *Osr1* locus (fig.46).

Cryosections fixed in 4% PFA and mounted using Fluoromount-G™ exhibit abnormal aggregates located at the sites of muscle fibers that are not present in control tissues, as assessed by brightfield imaging (fig.47). Capturing of these aggregations on the sections for histological analyses by H&E staining, Direct Red 80 (Sigma-Aldrich)

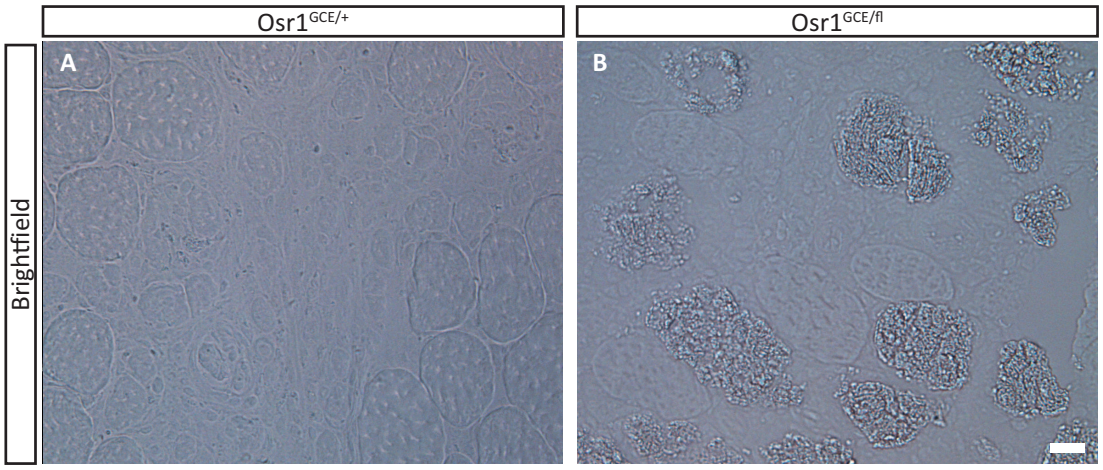

Figure 47: Conditional *Osr1* knock-out shows abnormal aggregates inside muscle fibers after injury.
Osr1$^{GCE/+}$ (**A**) and *Osr1*$^{GCE/flox}$ (**B**) were injured by freeze/ pierce technique, tamoxifen induced at the time of injury plus 4 consecutive days, and regenerating TA muscles analyzed 5 days post injury. Cryosections were fixed and imaged. Scale bar indicates 20µm. Images are representatives of 2 independent experiments.

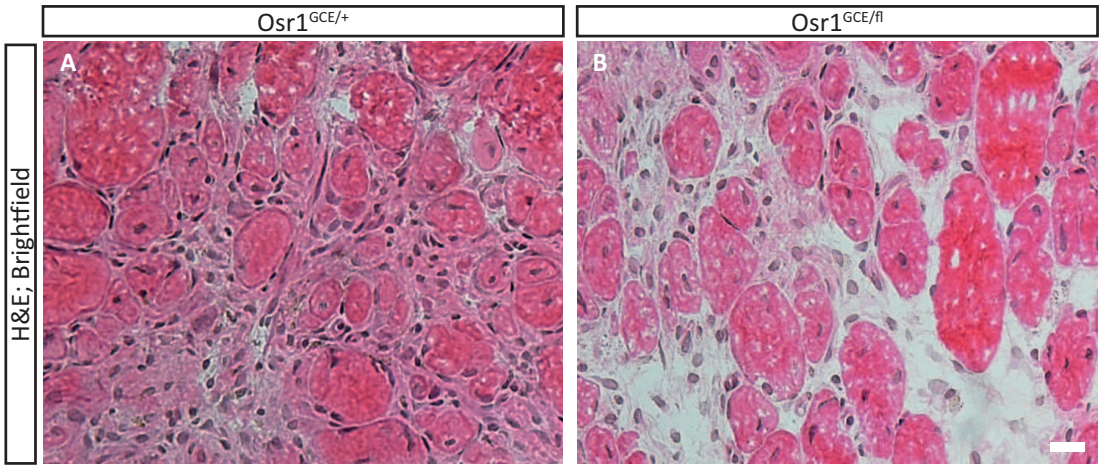

Figure 48: *Osr1* deficiency has reduced tissue density early during regeneration.
Osr1$^{GCE/+}$ (**A**) and *Osr1*$^{GCE/flox}$ (**B**) were injured by freeze/ pierce technique, tamoxifen induced at the time of injury plus 4 consecutive days, and regenerating TA muscles analyzed 5 days post injury. Cryosections were fixed, stained by hematoxylin and eosin, and imaged. Scale bar indicates 20µm. Images are representatives of 2 independent experiments.

or Masson-Goldner trichromic staining was not possible as they got presumably flushed off the tissue sections during ethanol washing steps required. Rigorous fixation of the sections adding 1% glutaraldehyde did not solve this issue.

However, H&E staining indicated a reduced tissue density at the site of injury (fig.48).

To characterize this potential phenotype addressing the question, whether cellular or extracellular components were dissolved from the tissue, cryosections were subjected to immunofluorescent stainings. By staining for collagen type VI (COL6), a major component of the extracellular matrix, was marked. Remarkable differences to control tissue were not determined (fig.49A, B). Furthermore, potential reduction in the abundance of macrophages in the regenerating tissue was investigated. Infiltration of macrophages into injured muscle is part of the early immune response after injury. Immunofluorescent stainings for pro-inflammatory macrophage specific marker CD68 showed a strong decrease in the number of CD68+ cells on *Osr1*$^{GCE/fl}$ tissue sections compared to control (fig.49C, D).

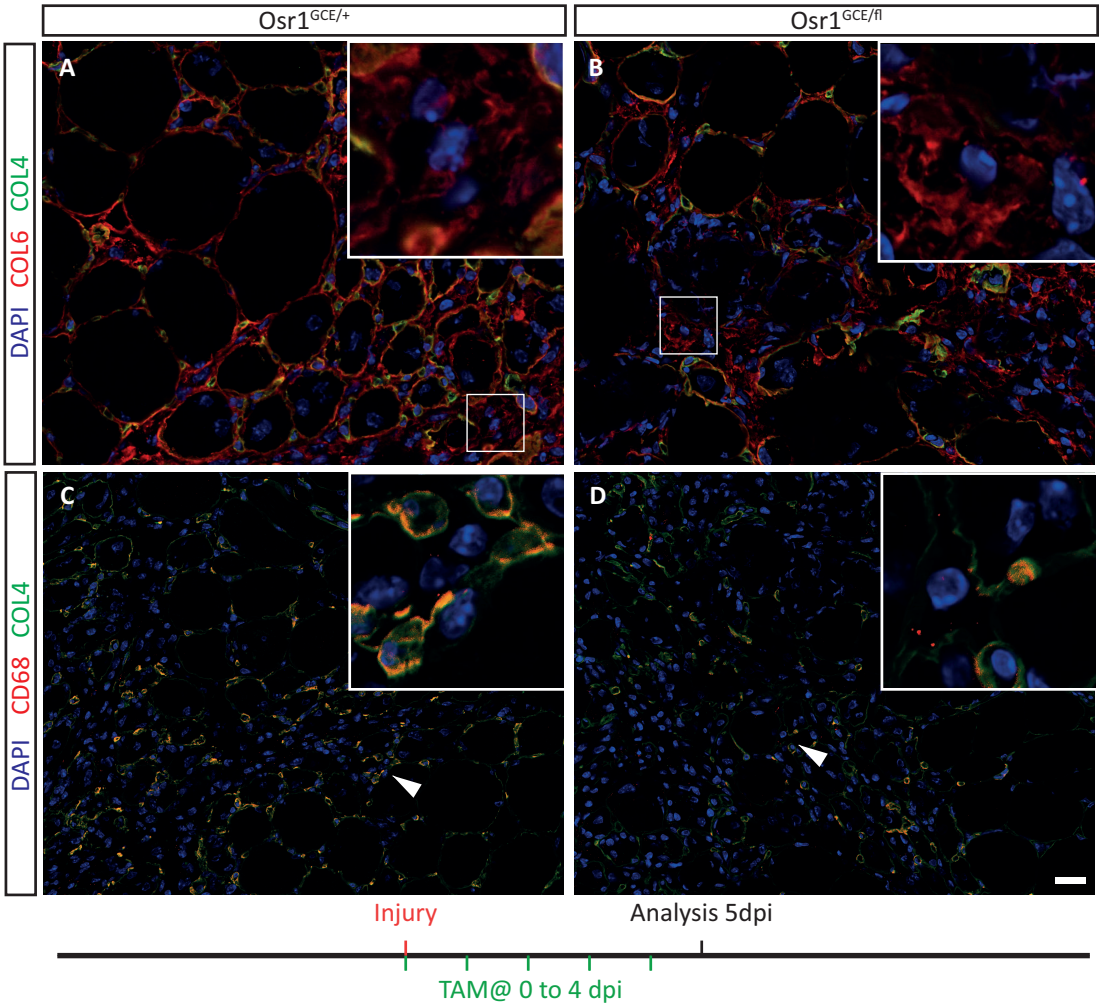

Figure 49: Conditional *Osr1* knock-out mice expose an immune-related phenotype during regeneration after injury.
Osr1$^{GCE/+}$ and *Osr1*$^{GCE/fl}$ were injury treatment by freeze/ pierce technique, tamoxifen induced at the time of injury plus 4 consecutive days to induce Cre mediated knock-out of *Osr1*, and regenerating TA muscles analyzed 5 days post injury. Immunofluorescent stainings for COL6 and CD68 mark extracellular matrix and macrophages, respectively (red). COL4 (green) staining marks basal lamina for visualization of tissue context, nuclei were stained using DAPI (blue). Images are representatives of 2 independent experiments. Scale bar indicates 20µm.

This decrease was evaluated by quantification of macrophages after knock-out of *Osr1*. CD68+ cells were counted on immunostained cryosections of *Osr1*$^{GCE/+}$ control animals and *Osr1*$^{GCE/fl}$ mutants. Specimen of both strains were mechanically injured, followed by tamoxifen induction for 5 consecutive days and analyzed at 5 dpi. *Osr1* mutants show a significant reduction in pro-inflammatory macrophage abundance to 54.9%.

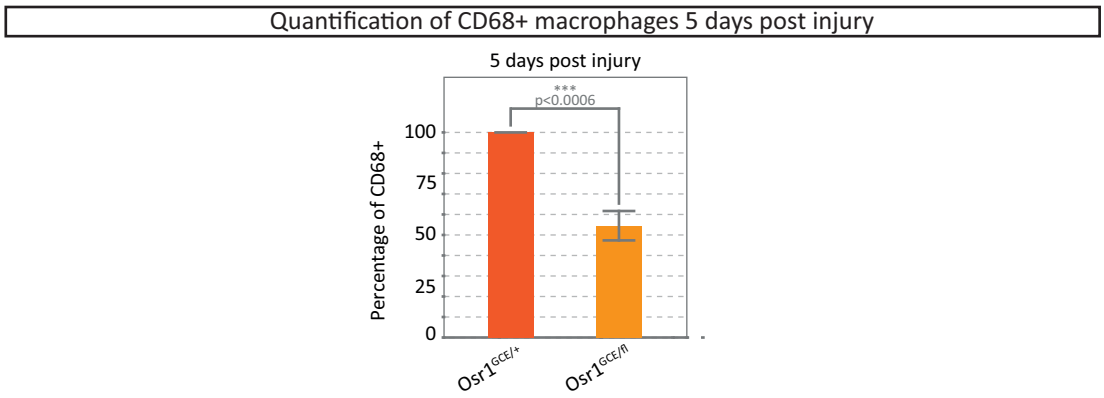

Figure 50: *Osr1* deficiency results in a reduced abundance of pro-inflammatory macrophages after injury.
Macrophages were quantified on confocal images of immunostainings. CD68+ cells on 3 fields of view of each 2 control specimen and 2 knock-out mice were counted. Averages were calculated by unpaired t-test, and control was set as 100% baseline. Error bars represent standard error of the mean.

5 Discussion

Juvenile muscle growth and muscle regeneration represent developmentally active postnatal stages that require a coordinated interplay of various cell types. Both processes involve activity of a distinct set of cell types. While postnatal muscle growth does not involve cells of the immune system, an innate immune response including a variety of immune cells is a major characteristic of the regenerative process. However, both phases have in common activated muscle stem cells interacting with connective tissue fibroblasts. Recent findings demonstrate the presence of fibro/ adipogenic progenitors (FAPs) in both juvenile growth and regeneration. While FAPs fulfill important functions during muscle regeneration, their role during postnatal muscle growth is still unclear.

The role of *Osr1* in muscle development was characterized in prenatal stages [Vallecillo García, 2016], but whether *Osr1* is expressed postnatally was not elucidated, yet. Moreover, lethality of *Osr1* deficiency at early fetal stage impeded investigations on the function of *Osr1* in postnatal age *in vivo*.

5.1 Validation of the conditional *Osr1* mouse model

Mouse models are widely used tools to perform functional gene studies. Due to high similarities in anatomy, physiology and genetics they allow for conclusions in human as well. In contrast to *in vitro* studies they enable to include the tissue context, and potential interactions with and influences by the cellular environment.

Osr1 deficiency is lethal during the early fetal stage in the mouse [Wang et al., 2005]. For investigating the function of *Osr1* in adult mice, the generation of a mouse model that enables a conditional *Osr1* knock-out was intended. The so-called "multi-functional" targeting construct [Economides et al., 2013] used furthermore offered the functionality of a gene reporter, by expressing *lacZ* under the control of the *Osr1* promotor.

Verification of successful targeting was performed by subjecting genomic DNA of embryonic stem cell clones to Southern blotting technique. While recombination at the 5' homology region and single insertion into the genome was confirmed, recombination at the 3' homology arm could not be validated. By Southern blotting a fragment containing the 3' homology arm was neither detected for the recombined locus nor for the wildtype allele. The probe region does not contain repetitive sequences, but is flanked by interspersed and simple repeats. These circumstances might have hampered probe binding by potential formation of secondary structures. Several independent attempts in amplifying DNA spanning the 3' homology arm by

long-range PCR did not yield a product, neither for targeted clones nor for wildtype. Likewise, repetitive regions on the 3' homology arm possibly led to an aborted PCR reaction.

Transgenic mice carrying the multi-functional allele express *lacZ* driven by the *Osr1* promotor. After Xgal stainings of embryos and comparison with the literature matching expression patterns were confirmed. However, on the targeting construct the *lacZ* gene is located in between the neomycin gene and the 3' homology arm. Hence, specific *lacZ* expression from the *Osr1* locus does not necessarily validate successful recombination of the 3' region, which is required for the conditional mouse model as this region contains the respective *loxP* element. Flippase mediated recombination of the locus results in a floxed exon 2 by reinversion of *Osr1* exon 2. This recombination was confirmed by Sanger sequencing. Moreover, a functional expression of OSR1 was indirectly verified by crossing to Osr1-GCE mice. Given the Osr1-GCE allele is essentially a knock-out of *Osr1*, expression from the transgenic allele is required for survival of the specimen. However, the *eGFP* gene inserted in between exon 2 and exon 3 might reduce the transcript level of *Osr1* due to an impairment of splicing efficiency, leading to a so-called hypomorphic effect. Matings of $Osr1^{GCE/+}$ with $Osr1^{fl/fl}$ mice yield specimen with an $Osr1^{GCE/fl}$ genotype at a remarkably lower frequency than Mendelian rules suggest. This observation implies a hypomorphic effect and lethality of mice with an $Osr1^{GCE/fl}$ genotype due to insufficient *Osr1* expression from the floxed allele. A possible decrease in *Osr1* mRNA could be tested by quantitative PCR analyses on specimen at embryonic stage E13.5, a stage prior to lethality due to Osr1 deficiency.

Cre mediated excision of exon 2 in $Osr1^{GCE/fl}$ mice was confirmed by sequencing of a PCR product spanning this exon. Further validation of the conditional knock-out can be achieved by RT-PCR to evaluate a transcriptional downregulation, or by Western blot to demonstrate depletion of OSR1 on protein level.

Summarizing, in the course of this thesis two novel genetic tools were generated that enable studies of *Osr1* expression in mice. The Osr1-MFA mouse model functions as an Osr1-lacZ reporter that allows for studying *Osr1* expression in mice at prenatal as well as at adult stages. Here, this reporter mouse model was extensively used to identify Osr1+ cells in adult mice in order to perform cell type characterizations via immunohistochemistry and FACS analyses. Furthermore, genetic recombination of the Osr1-MFA mouse resulted in the Osr1-flox mouse model. This model was available at the end of this thesis and was utilized for initial functional studies of *Osr1*.

5.2 *Osr1* expression marks a transiently active juvenile fibro/ adipogenic progenitor population

Osr1 is expressed in skeletal muscle tissue during the first 3 weeks after birth of a mouse. This period constitutes the juvenile or adolescent phase of the mouse. *Osr1* transcriptional activity decreases during this stage, as shown by reporter gene expression and quantitative RT-PCR. Still, it has to be verified whether the dynamics of *Osr1* mRNA or GFP abundance reflects abundance of actual OSR1 protein, or whether a temporal shift distorts the results. Post-transcriptional regulatory processes like 5'-capping or micro-RNA mediated decay can lead to increased half-life or rapid degradation of mRNA, thus alter the ratio mRNA/ protein abundance. In a global quantification approach to assess mammalian gene expression control, it was demonstrated that particularly genes encoding for transcription factors show unstable mRNAs and proteins, corresponding to few hours [Schwanhäusser et al., 2011]. However, particularly the transcription factor *Osr1* was not included in this genome-wide study. Short half-lives of *Osr1* transcript and protein would argue against a temporal shift, and rather support conform dynamics of declining *Osr1* expression presented here and actual endogenous OSR1. Immunohistochemistry using antibodies against OSR1 could confirm this assumption, however, there is no antibody suitable for immunolabeling on tissue sections available.

A muscle interstitial transient cell population (Sca-1_{med}) present only during the juvenile phase was reported [Pannérec et al., 2013, Mitchell et al., 2010]. More than 90% of these cells express the cell stress mediator PW1 and are referred to as juvenile PW1-expressing interstitial progenitors (Sca-1_{med} PICs). These Sca-1_{med} PICs show a high expression of mesenchymal marker PDGFRα. In coherence, all Osr1+ cells early after birth are resident in the muscle interstitium, the majority are PDGFRα+ (fig.17), and *Osr1* is highly expressed specifically in Sca-1_{med} PICs (fig.20). This indicates a matching identity of Sca-1_{med}/ PDGFRα+ PICs and juvenile Osr1+ cells in the muscle. In addition, adipogenic potential of neonatal Osr1+ cells was observed by lineage tracing *in vivo*. The same potential was demonstrated for isolated Sca-1_{med}/ PDGFRα+ PICs *in vitro*.

While not all Sca-1_{med} PICs are PDGFRα+, a small fraction is PDGFRα– and shows myogenic differentiation potential *in vitro* [Pannérec et al., 2013]. Hence, PICs represent a mixed population. Osr1+ cells are exclusively non-myogenic, as demonstrated by lineage tracing experiments. The minor portion of 8% of Sca-1_{med} cells negative for *Osr1* expression are therefore considered Sca-1_{med}/ PDGFRα– PICs.

This consideration qualifies *Osr1* expression as an exclusive marker for juvenile FAPs, while juvenile PICs comprise a mixed cell population of PDGFRα+ fibro/

adipogenic and PDGFRα– myogenic progenitors.

Osr1 was proposed as a marker for irregular connective tissue during embryogenesis [Stricker et al., 2012]. Cells expressing both *Osr1* and *Tcf4* were observed at developmental stage E11.5 and E13.5 in limb connective tissue [Vallecillo García, 2016]. Nevertheless, despite their localization in the muscle interstitium, juvenile Osr1+ cells in the muscle do not express muscle connective tissue fibroblast marker *Tcf4*. Previous studies demonstrate a direct repression of TCF activity by OSR1 *in vitro* [Otani et al., 2014], supporting the observation of exclusive expression of both genes. However, Osr1+ cells can give rise to TCF4+ cells during postnatal muscle growth. 41% of TCF4+ cells detected at 3 weeks of age were derived from neonatal Osr1+ cells. These data validate fibrogenic capacities of progenitor-like juvenile Osr1+ cells. While in part they differentiate to TCF4+ fibroblasts and lipid droplet containing adipocytes, they also remain resident in the muscle interstitium after postnatal muscle growth. The vast majority of PDGFRα+ muscle interstitial cells, 70%, are descendants of neonatal Osr1+ cells. These cells were defined as fibro/ adipogenic progenitors (FAPs).

Juvenile Osr1+ cells were also detected as PDGFRβ+ and NG2+, assumed markers for pericytes [Birbrair et al., 2013a]. Given 83% of Osr1+ cells are positive for PDGFRα but also 56% positive for PDGFRβ and 34% for NG2, cells double-positive or triple-positive for these mesenchymal markers is implied. This assumption is supported by characterizations of PICs. PICs show a strong expression of *Pdgfr*α but also a weaker expression of *Pdgfr*β and *Ng2* [Pannérec et al., 2013]. Moreover, endothelial differentiation potential, as it is attributed to pericytes, was not observed for neonatal Osr1+ cells *in vivo*. Hence, pericytic identity of juvenile Osr1+ cells is not concluded.

Osr1 expression declines in the course of adolescence, whereas PDGFRα and PW1 expression in this cell population remains static and further persistent in the adult. Expression of *Osr1* in these cells is limited to the developmentally active phase of postnatal muscle growth, hence serves as an indicator for an active state. In summary, these data demonstrate that *Osr1* is the first unique marker for transient juvenile progenitors with fibrogenic and adipogenic capacities in an activated state.

The transient juvenile population Sca-1_{med} is not detectable anymore after the age of 3 weeks [Pannérec et al., 2013]. The fate of these cells, whether they undergo apoptosis, further differentiate or if they become FAPs in the adult, showing a Sca-1_{high} property, remained elusive. A lineage tracing approach demonstrates 70% of adult FAPs are derived from neonatal Osr1+ cells. If the remaining 30% are evolved from cells expressing *Osr1* prenatally requires further confirmation. The data presented here provide first evidence of juvenile Sca-1_{med} FAPs, at least in part, maturate to Sca-1_{high} FAPs in the adult.

5.3 Hypothetical function of Osr1+ cells during postnatal muscle growth

Muscle is either constituted of fast twitch fibers, of slow twitch fibers or of mixed fiber types, depending on the major function of the muscle. While the *gastrocnemius* muscle consists of a mix of fast and slow twitch fibers, the *tibialis anterior* is composed of fast twitch fibers mainly [Lionikas et al., 2005]. It was demonstrated that TCF4 mediated gene regulation in fibroblasts provides cues to promote the formation of slow twitch fibers, and to repress expression of embMyHC, which characterizes a developmental fast fiber type [Rubinstein and Kelly, 2004] during myofiber maturation [Mathew et al., 2011]. In prenatal muscle development *Osr1* deficiency leads to a mispatterning in muscles such as the *gastrocnemius*, and less pronounced in the *tibialis anterior* muscle. The gastrocnemius muscle showed a higher abundance of Osr1+ cells than the *tibialis anterior* [Vallecillo García, 2016].

During postnatal muscle growth, *Osr1* and *Tcf4* expressions are exclusive in cells. This is in coherence with studies indicating a repression of TCF activity by OSR1 [Otani et al., 2014]. However, early postnatal Osr1+ cells can give rise to TCF4+ cells in the course of muscle growth. This indicates an altered potential of prenatal and postnatal Osr1+ cells. Supporting this conclusion, similar results for cell type characterizations of juvenile Osr1+ cells were obtained for both the *gastrocnemius* muscle and the *tibialis anterior*.

To investigate the functional role of *Osr1* during postnatal muscle growth, a conditional knock-out at neonatal stage would provide clarification. Using the $Osr1^{GCE/flox}$ mouse model *Osr1* can be knocked out exclusively in Osr1+ cells. Possibly altered myofiber maturation by repression of *Tcf4* by OSR1 could be studied. If OSR1 is repressing differentiation of juvenile FAPs into TCF4+ fibroblasts, a delayed maturation could result. This would be indicated by a prolonged presence of embMyHC in myofibers.

Utilizing *Osr1* expression as a marker for activated FAPs during juvenile muscle growth also would enable ablation of FAPs from the tissue. A widely-used model for cell ablation is provided by the transgenic mouse model $R26R^{DTA}$ [Wu et al., 2006]. This model carries the gene for diphteria toxin A (DTA) in the ubiquitously active ROSA26 locus, inactivated by a preceding floxed stop codon. This codon is floxed out by Cre recombinase for DTA being expressed to kill and ablate the cell. By crossing the Osr1-GCE mouse to this $R26R^{DTA}$ model, Osr1+ cells could be ablated at neonatal stage by tamoxifen induction and the effect on juvenile muscle growth studied in absence of juvenile FAPs.

Summarizing, *Osr1* expression allows for the identification of exclusively activated

FAPs in juvenile muscle with high fidelity. Expression of *Osr1* is attributed to embryonic and fetal developmental processes including myogenesis [Vallecillo García, 2016, Tena et al., 2007, Wang et al., 2005, James et al., 2006], whereas there are no reports describing *Osr1* expression in the adult.

In contrast, PDGFRα as an accepted marker for adult FAPs not only plays important roles during embryogenesis, but also during adult age. PDGFRα+ cells are distributed throughout the adult central nervous system, contributing to adult neurogenesis [Rivers et al., 2008]. Functionally, PDGFRα signaling is involved in pancreatic β-cell proliferation [Chen et al., 2011].

Hence, PDGFRα expression is an inappropriate marker for manipulating particularly FAPs in a complex organism. Although further studies of *Osr1* expression in tissues of the adult are required, *Osr1* expression is hypothesized to be a suitable marker for specifically targeting active juvenile FAPs.

5.4 *Osr1* expression might be required for maintenance of muscle homeostasis in the adult

In adult homeostatic muscle tissue *Osr1* expression was detected in very scarce cells, with no differences between *gastrocnemius* and *tibialis anterior* muscle. These Osr1+ cells are predominantly PDGFRα+, but also PDGFRβ and NG2+ cells were detected. These characteristics were also assigned to Sca-1+/ PDGFRα+ PW1-expressing interstitial cells (adipoPICs) in the adult [Pannérec et al., 2013]. Reportedly, PDGFRα and PW1 are not dynamically expressed, but rather statically mark FAPs also in the state of quiescence in the adult [Joe et al., 2010, Uezumi et al., 2010, Mitchell et al., 2010, Pannérec et al., 2013].

It was demonstrated *in vitro* and *in vivo* that FAPs can give rise to fibroblasts that produce collagens providing extracellular matrix (ECM) [Uezumi et al., 2011, Joe et al., 2010].

While healthy adult skeletal muscle has a slow turnover, with 1-2% of myonuclei being replaced per week observed in the rat [Schmalbruch and Lewis, 2000], satellite cells need to be activated to differentiate and fuse to fibers for providing new nuclei [Morgan and Partridge, 2003]. Slow turnover is also elicited after microtrauma inflicted by day-to-day wear [Chargé and Rudnicki, 2004]. Activation of satellite cells comes in line with changes in the composition of the niche. TCF4+ fibroblasts were suggested to provide signals critical for satellite cell activation after muscle injury [Murphy et al., 2011]. The activation of *Osr1* expression in scarce FAPs can have different reasons and functions. In the course of muscle turnover *Osr1* expression in FAPs might be activated to promote changes to the niche for satellite cell activation.

This hypothesis can be further validated by investigating activated satellite cells in the immediate environment of Osr1+ FAPs. Activated satellite cells can be identified by expression of *Pax7* in addition to myogenic regulatory factors *MyoD* or *Myf5* during at least 12 hours after activation. Quiescent satellite cells do not express these factors [Cooper et al., 1999].

Alternatively, FAPs could sparsely activate *Osr1* expression as a regulatory requirement for collagen production in order to maintain the niche including quiescent state of satellite cells. In this case, a PDGFRα conditional knock-out of *Osr1* would result in an increased number of Pax7+/MyoD+ or Pax7+/Myf5+ activated satellite cells.

5.5 *Osr1* is expressed in activated FAPs after injury

Muscle injuries disturb the homeostatic balance of healthy adult muscle. Following damage an immediate immune response takes place. Tissue resident granulocytes and M1 activated macrophages release pro-inflammatory signals, for further immune cells are recruited. Simultaneously these macrophages remove necrotic debris by phagocytosis to clear the tissue. During this early stage of regeneration, within the first 3 days post injury (dpi) in the mouse, FAPs are activated. They proliferate and accumulate at the injured site, reaching a peak abundance at 3 dpi [Heredia et al., 2013]. FAPs not only can give rise to collagen producing fibroblasts, they also effectively phagocytize debris in injured tissue [Heredia et al., 2013]. Moreover, TCF4+ fibroblasts expand, with a maximum number observed 5 dpi [Murphy et al., 2011]. These fibroblasts transiently deposit collagenous ECM to stabilize the tissue and to regulate satellite cell expansion [Murphy et al., 2011]. Satellite cells are the major contributor to regenerating muscle fibers. They become activated early after injury, expand in parallel to TCF4+ fibroblasts, and start to fuse to regenerating myofibers at 7 days after injury [Murphy et al., 2011].

An accumulation of Osr1+ cells was observed 3 dpi, coinciding with activated and proliferating FAPs. Identity of Osr1+ cells and FAPs not only overlaps by matching temporal and spatial properties in the early phase of regeneration. In fact, accounting for 85% of CD34+/ Sca-1+/ PDGFRα+ cells the vast majority of *Osr1* expressing cells are FAPs 3 dpi, as detected by FACS using Osr1-lacZ reporter mice. In regenerated muscle 28 dpi, 68% of PDGFRα+ FAPs had expressed *Osr1* during the first five days following injury, as demonstrated by lineage tracing. This is in further support of FAP specific *Osr1* expression. However, there is an apparent discrepancy of 17% between Osr1+ FAPs early during regeneration (85%) and FAPs at proceeded regeneration having expressed *Osr1* during the first 5 days after muscle damage (68%). Osr1+ FAPs not only remain resident in the tissue at completed regeneration. As progenitors with multiple differentiation potential they also give rise to PDGFRα– cell

types such as fibroblasts or adipocytes.

While 85% of CD34+/ Sca-1+/ Osr1+ cells are also PDGFRα+, the identity of the remaining 15% PDGFRα–/ Osr1+ cells requires further clarification. LacZ expression was detected by FACS via β-galactosidase mediated conversion of C_{12}FDG substrate to a fluorescent product. Thus, minimal abundance of β-galactosidase can produce an intense signal. In addition, β-galactosidase has a long half-life *in vivo* of >20 hours [Bachmair et al., 1986]. Hence, the remaining 15% of apparently PDGFRα– /Osr1+ cells might be already differentiated cell types, such as PDGFRα– fibroblasts, containing remainders of β-galactosidase. This hypothesis could be tested by FACS isolation of Osr1-lacZ+ cells followed by evaluation of *Tcf4* expression on transcriptional level by RT-PCR. In addition, by using the Osr1-GCE mouse Osr1+ cells could be isolated by FACS. By RT-PCR for *Tcf4* or anti-TCF4 immunostainings on cytospun cells, the identity of TCF4+ fibroblasts could be excluded.

In injured muscle tissue, Osr1+ cells expressing *Tcf4* were not observed at 5 dpi (fig.35), however, Osr1+ cells can give rise to TCF4+ fibroblasts. 42% of all TCF4+ cells in regenerated muscle 28 days after injury are originating from Osr1+ cells (fig.41D, 42). This demonstrates that Osr1+ after muscle injury are progenitors of TCF4+ fibroblasts.

Osr1-lacZ reporter+ cells were also observed highly abundant in the epimysial region at 5 dpi (fig.32D). In healthy adult muscle, this region is reportedly populated by TCF4+ fibroblasts [Mathew et al., 2011,Murphy et al., 2011]. During regeneration after injury, fibroblasts establish temporary fibrotic scarring of the tissue by ectopic ECM production at this stage [Mann et al., 2011]. In regenerating muscle tissue Osr1+ cells are TCF4–, as demonstrated by identification of Osr1+ cells by Osr1-reporter eGFP. While endogenous eGFP is directly detectable via its fluorescence, signal intensity is proportional to eGFP abundance, indicating a reasonable expression of *Osr1* in TCF4– cells exclusively. Epimysial Osr1-lacZ+ cells were detected on cryosections of Osr1-lacZ reporter mice by β-galactosidase mediated conversion of Xgal to an indigo dye. Likewise in FACS detected lacZ+ cells, positive signal might result from stable β-galactosidase remainders in cells already differentiated to TCF4+ fibroblasts. Yet, whether *Osr1* and *Tcf4* expressions are mutually exclusive in the epimysial region as observed in injured regions of the muscle, and whether Osr1+ cells are TCF4+ fibroblast progenitors in this distinct tissue context, requires further confirmation.

In the course of regeneration the majority of Osr1+ cells remain resident in the interstitium as PDGFRα+ FAPs. However, in the regenerated muscle 33% of all detected PDGFRβ+ cells are derived from cells that had expressed *Osr1* early after injury. PDGFRβ is considered a marker for pericytes, whereas PDGFRα+ adipoPICs,

representing the FAP population, are co-expressing PDGFRβ. To further investigate a pericyte identity, endothelial fate of Osr1+ cells was investigated. Pericytes were reported to contribute to blood vessel and capillary formation [Birbrair et al., 2014]. In general, CD31+ endothelial cells were not derived from formerly Osr1+ cells, although scarce potential overlaps of CD31+ capillaries and traced cells were observed. Angiogenic potential is exclusively attributed to myogenic PDGFRα–/ Nestin+ type 2 pericytes, not to adipogenic PDGFRα+/ Nestin– type 1 pericytes.

Given Osr1+ cells are non-myogenic in prenatal development, juvenile muscle growth and during regeneration in the adult, angiogenic type 2 pericyte identity is unlikely. Nevertheless, isolated Osr1+ cells subjected to differentiation in a revascularization model [Birbrair et al., 2014] and comparison to properties of angiogenic pericytes in this model could verify this conclusion.

A broad differentiation potential is attributed to FAPs. Depending on the environment they are incorporated into, they can differentiate to fibroblasts *in vitro* [Joe et al., 2010, Uezumi et al., 2011], or white ectopic fat in a glycerol induced model of fatty accumulation *in vivo* [Uezumi et al., 2010]. FAPs transplanted into a model of heterotropic ossification show osteogenic potential [Wosczyna et al., 2012], and after stimulation with BMP7 they can give rise to brown adipocytes [Schulz et al., 2011]. Particularly, bone is derived from the ventral part of the somites, brown adipocytes are thought to be derived from the myogenic lineage, which is in contrast to the assumed mesenchymal origin of FAPs. This highlights and emphasizes a mesenchymal stem cell-like character of FAPs, and raises the possibility of endothelial differentiation potential of FAPs in an environment promoting vascularization. Tracing Osr1+ cells in a model of ischemia [Birbrair et al., 2014] would further elucidate this potential for transdifferentiation into cells of a distinct lineage.

3 days after mechanically applied injury a minor portion of 7% Osr1+ cells was observed in the CD34–/ Sca-1– population. This population was reported to show osteogenic and chondrogenic differentiation potential *in vitro* [Joe et al., 2010]. In the context of osteogenic FAPs dependent on the environmental cues, it requires further clarification whether the used injury model promotes osteogenic or chondrogenic contribution. By lineage tracing of Osr1+ cells and identification of descendants using appropriate markers, such as Osterix for osteocytes or *Sox9* for chondrocytes, potential contribution to bone or cartilage tissues could be investigated.

5.6 *Osr1* expression marks non-adipogenic commitment of FAPs

After muscle injury FAPs are activated during an early time frame 24 to 48 hours later. This activation was associated with IL-4 signaling of granulocytes which also activates anti-inflammatory M2 macrophages that provide a pro-myogenic environment. As a

consequence, FAPs proliferate and expand in the damaged tissue, and reach a peak abundance at 3 dpi [Heredia et al., 2013]. TCF4+ fibroblasts proliferate delayed in time, attaining maximum abundance at 5 dpi [Murphy et al., 2011]. *Osr1* is highly expressed at 3 dpi and 5 dpi, as obtained by RT-qPCR on RNA from whole muscle lysates of injured tissue. Accumulated Osr1-lacZ reporter+ cells were observed already at 3 dpi, are preserved at 5 dpi and declined at 7 dpi. These dynamics of *Osr1* expression and abundance of Osr1+ cells in the course of regeneration reflect the properties of activated and proliferating FAPs. Moreover, the stability, thus a prolonged lifetime of intracellular β-galactosidase of at least 20 hours, implies a delay in the regression of Osr1-lacZ reporter+ cells between 3 dpi and 7 dpi. This is in further support of the conclusion that Osr1+ FAPs represent progenitors of TCF4+ fibroblasts, including fibroblasts located in the epimysial region of fibrotic scarring.

Previous studies of cellular dynamics of FAPs and TCF4+ fibroblasts utilized different models of injury. Macrophage mediated activation of FAPs was investigated after CTX induced injury [Heredia et al., 2013], by a similar approach applying NTX injury proliferation of FAPs was demonstrated [Joe et al., 2010]. Both studies show matching conclusions regarding the peak abundance of FAPs at 3 dpi. The injury models used implement myotoxins that harm myofibers, whereas mononucleated cell types such as FAPs and satellite cells are excluded from damage. TCF4+ fibroblast expansion was studied after chemically applied injury via $BaCl_2$ injection [Murphy et al., 2011]. This injury leaves the basal lamina intact, which envelopes single myofibers, in addition to mononucleated cells [Rogers et al., 2015, Otis et al., 2014].

In contrast, mechanical injury inflicted by a liquid nitrogen cooled needle is non-selective but causes damage regardless cell or tissue type. Muscle regeneration is an orchestrated process involving and requiring interactions of various cell types and tissue structures. Selectively inflicted damage to single components might alter activation time or rate of undamaged components. Whether chronological shifts in the activity of involved cell types, including intercellular coordination, is might occur is not clear. Hence, comparability in regard to temporally coordinated activation among the different injury models requires validation.

De novo expression of *Osr1* in FAPs is triggered by injury. It is hypothesized that this expression indicates a particular functional cell commitment. Adipogenic differentiation potential of FAPs was demonstrated by utilizing FACS isolated FAPs from healthy muscle tissue [Joe et al., 2010, Uezumi et al., 2010, Schulz et al., 2011, Wosczyna et al., 2012, Pannérec et al., 2013]. These FAPs are essentially quiescent and particularly prone to environmental cues and stimuli. A distinct cell or lineage commitment is not determined, yet. After transplantation into an environment that promotes ectopic fat formation, these quiescent FAPs were activated and immediately

pushed towards an adipogenic fate [Joe et al., 2010, Uezumi et al., 2010]. Likewise, *in vitro* differentiation assays involve factors to promote the desired fate [Pannérec et al., 2013, Joe et al., 2010, Uezumi et al., 2010, Schulz et al., 2011]. While these approaches give important insights into the general capacities of this cell type, they do not sufficiently account for the dynamic tissue context *in vivo* during regeneration. Quiescent FAPs engrafted into muscle that was previously injured by glycerol injection gave rise to ectopic fat *in vivo*.

In contrast, a strong contribution to fat formation by Osr1+ cells in this model of fatty accumulation was not observed. Osr1+ FAPs were labeled during the first 5 days after glycerol injection in 2 months old young adult mice. 14 days after injection, lipid droplet containing adipocytes have formed, however, the majority was not derived from Osr1+ FAPs.

While 90% of FAPs isolated from healthy muscle showed adipogenic potential in *in vitro* differentiation assays, this commitment was decreased to a frequency of 60% using isolated FAPs after CTX injury [Uezumi et al., 2010, Uezumi et al., 2011]. These data were suggested to indicate a loss of adipogenic potential during regeneration. However, FAPs isolated from CTX injured whole muscle include quiescent cells from intact regions of the tissue. While these quiescent cells might contribute to the adipogenic portion under adipogenesis promoting conditions *in vitro*, the remaining 40% might have already been committed to a fibrogenic fate or are maintained as FAPs.

These observations lead to the hypothesis that the onset of activation is a critical step for the cellular determination of multipotent FAPs at an early stage during regeneration. It is therefore proposed, that fibrogenic or adipogenic commitment of FAPs, once acquired, are mutually exclusive. However, reversibility of this commitment in the course of dynamically progressing regeneration needs further clarification. Early fibrogenic commitment could be indicated by inital and immediate expression of *Osr1*, and results in derived TCF4+ fibroblasts and remaining resident FAPs, but not in adipocytes.

5.7 Promotion of muscle regeneration by *Osr1*

Muscle injury is immediately followed by an immune response. During the first three days in the mouse granulocytes infiltrate the tissue to secrete pro-inflammatory signals which classically activate (M1) resident macrophages [Tidball, 1995, Brigitte et al., 2010, Tidball and Villalta, 2010]. These signals as well lead to an increased permeabilization of blood capillaries which facilitates recruitment of further immune cells [Ten Broek et al., 2010]. Simultaneously, fibrin and fibronectin extravasate from the circulation to form a primary matrix. This matrix serves as a scaffold

and anchorage site for both activated resident cells and infiltrating cells [Serrano and Muñoz-Cánoves, 2010]. Particularly, fibrin is additionally involved in clotting of blood [Suelves et al., 2002, Lluís et al., 2001]. Also, it accumulates in degenerating myofibers and provides cues for macrophages. These fibers are successively degenerated by pro-inflammatory M1 macrophages in order to enhance infiltration of further cells [Suelves et al., 2007]. While FAPs are already activated at this early phase of regeneration, they show phagocytic capacities 3 days post injury [Heredia et al., 2013]. Whether FAPs play a role during expansion, that is immediately after the onset of their activation and prior to their maximum abundance, is largely unknown. During the first 5 days post injury collagenous ECM is also excessively produced by TCF4+ fibroblasts [Murphy et al., 2011]. This matrix promotes satellite cell expansion required for fiber repair. With progression of regeneration, and with the switch from pro- to anti-inflammatory immune response, further matrix formation is inhibited. Already present depositions of fibrin are proteolyzed by plasmin proteases [Lluís et al., 2001, Suelves et al., 2002, Suelves et al., 2007]. Plasmin is introduced to the site of injury as a precursor plasminogen (Plg). This precursor requires activation by either tissue-type plasminogen activator (tPA) or urokinase-type plasminogen activator (uPA) for conversion into a functional enzyme. Furthermore, plasmin activates collagenases in the tissue that directly degrade ECM produced by fibroblasts. Inhibition of matrix formation during progressing regeneration is mandatory to prevent the development of fibrosis, that is ecoptic extracellular matrix deposition.

To investigate the functional relevance of *Osr1* for the regenerative process after muscle injury, a conditional knock-out was studied. Osr1-flox mice were crossed to the Osr1-GCE strain to generate a mouse model Osr1$^{GCE/flox}$. Osr1-GCE mice carry the GCE cassette on one allele. This cassette is knocked into the *Osr1* locus and expresses eGFP and inducible Cre under the control of the *Osr1* promotor, while *Osr1* is disrupted. Hence, Osr1$^{GCE/flox}$ mice allow for an inducible Cre mediated knock-out of *Osr1* on the floxed allele, exclusively in Osr1+ cells, resulting in a homozygous knock-out Osr1$^{GCE/-}$.

Mechanically applied injury was followed by tamoxifen induction of Cre mediated knock-out for the following 5 days. Analysis was performed at 5 dpi during early regeneration. Brightfield imaging of cryosections displayed excessive clotting within myofibers at the site of injury. After histochemical H&E staining the tissue showed loose consistency. A strikingly similar phenotype was reported for uPA deficient mice [Suelves et al., 2007], as well as for Plg mutants [Lluís et al., 2001, Suelves et al., 2002]. Both mutant strains feature a loss of functional plasmin protease during regeneration, whereby fibrin depositions that prime degenerating muscle fibers were not degraded. These depositions remain in fibers as clots. Furthermore, impaired

recruitment of pro-inflammatory macrophages was observed in both strains [Suelves et al., 2007]. Coherently, *tibialis anterior* muscle of conditional *Osr1* knock-out mice showed a significant reduction in CD68+ pro-inflammatory macrophages at 5 dpi. While satellite cells, macrophages and bone marrow-derived cells were reported to express uPA [Lluís et al., 2001], expression in FAPs requires elucidation.

These data lead to the hypothesis that *Osr1* in activated FAPs early during muscle regeneration directly or indirectly regulates the production of uPA. Subsequently, uPA converts plasminogen to plasmin protease at the site of injury, which in turn can degrade fibrin depositions in degenerating myofibers (fig.52). In support of this hypothesis, transcriptome analyses of *Osr1* deficient embryos at developmental stage E13.5 show a downregulation of *Plau*, the gene encoding for uPA, in embryonic FAPs (unpublished; in revision). Moreover, preliminary data revealed a strong expression of *Plau* in FACS isolated non-hematopoietic Sca-1_{high} cells 3 days after injury, as obtained by RT-qPCR. This Sca-1_{high} cell population contains FAPs. Whether *Plau* is expressed in adult Osr1+ FAPs, or downregulated in *Osr1* knock-out specimen, could be further confirmed by immunohistochemical stainings for Osr1-lacZ or Osr1-GFP reporter and uPA. Moreover, FACS isolated Osr1+ FAPs can be subjected to RT-qPCR for confirmation of *Plau* expression. In addition, *Plaur*, which encodes for the uPA receptor that acts as an attractant for uPA, is highly expressed in the hematopoietic population at 3 days post injury. This population mainly comprises immune cells, such as granulocytes and macrophages, at this early stage of regeneration. The model proposed here assigns a critical role to *Osr1* expression in FAPs during an early stage of regeneration by indirectly recruiting macrophages and controlling their phagocytic activity.

In uPA deficient mice necrotic myofibers persist and fibrotic tissue forms progressively. Fibrin stimulates collagen expression in fibroblasts, which is required at the early phase of regeneration to establish the transient ECM. Plasmin not only proteolyzes fibrin, which is necessary in the progression of regeneration to prevent ectopic fibrotic tissue formation, but also activates collagenases that directly degrade the transient ECM in the course of regeneration. In consequence, uPA deficiency leads to impaired muscle regeneration and fibrosis. By studying the impact of a conditional knock-out of *Osr1*, induced during the first 5 days after injury, at progressed regeneration like 28 dpi, the observation of aberrant muscle regeneration and fibrosis would further support this hypothesis. Bone-marrow of wildtype mice engrafted at the site of injury in uPA deficient mice ameliorated the long-term regeneration defect [Suelves et al., 2007]. A similar rescue experiment in conditional *Osr1* knock-out mice could further verify a compensation of the phenotype due to uPA expressing bone-marrow derived cells.

In summary, *Osr1* expression is the first exclusive and unique marker for an activated mesenchymal stem cell-like cell type referred to as fibro/ adipogenic progenitors (FAPs). FAPs are a population of non-myogenic progenitors resident to the muscle interstitium. Juvenile FAPs are present in the tissue during postnatal muscle growth showing a distinct Sca-1_{med} signature. The vast majority of these FAPs express *Osr1*. While their fate after the juvenile phase was not clear, lineage tracing based on *Osr1* expression contributed to a better understanding of their destiny. Partially, if not entirely, juvenile FAPs give rise to FAPs in the adult. In homeostatic adult muscle FAPs showing a Sca-1_{high} property remain quiescent, but re-enter the cell cycle upon muscle injury and facilitate myogenic tissue repair. Muscle injury as well triggers *Osr1* expression in FAPs. Altogether, both juvenile FAPs and adult FAPs activated after injury express *Osr1* when situated in environments of ongoing myogenesis (fig.51).

Embryonic Osr1+ FAPs can differentiate to smooth muscle, adipocytes and fibroblasts [Vallecillo García, 2016], whereas in juvenile FAPs potential for smooth muscle was not observed. While juvenile FAPs can differentiate to adipocytes during the adolescent growth phase, activated FAPs after muscle injury show limited adipogenic differentiation in the *in vivo* tissue context. These observations indicate a successive loss in differentiation potential in the course of aging. Considering a common origin, these discrepancies can have two reasons. On the one hand, maturation of FAPs could alter cell differentiation potential, implied by distinct Sca-1 expression in juvenile and adult. On the other hand, differentiation potential could be decisively influenced and controlled by specific environmental cues depending on the tissue context. This reason would include the variance of Sca-1 properties in both populations.

Figure 51: Proposed model of FAP properties in regard to Osr1 and PDGFRα expression. *Osr1* is expressed in juvenile FAPs during the first 3 weeks of age. This juvenile FAP population is suggested to give rise to FAPs in the adult. Adult FAPs remain quiescent in homeostatic muscle tissue and do not express *Osr1*. After muscle injury FAPs re-enter the cell cycle and immediately activate *Osr1* expression. In the course of regeneration expression of *Osr1* is downregulated. FAPs are statically positive for surface marker PDGFRα, independent of the tissue context, whereas dynamic *Osr1* expression allows for identification of FAPs situated in an environment of ongoing myogenesis.

Quiescent FAPs in the adult show a *de novo* expression of *Osr1* after activation initiated by injury. These Osr1+ FAPs are not adipogenic in the complex and dynamic environmental context of regeneration in a model of ectopic fat formation, however, existence of Osr1– FAPs comprising an adipogenic portion of FAPs needs to be investigated. Instead, Osr1+ FAPs contribute to a large fraction of TCF4+ muscle connective tissue fibroblasts after mechanical injury. Therefore, it is concluded that *Osr1* expression indicates a non-adipogenic, pro-fibrogenic cell commitment acquired by FAPs at the time of initial activation. During regeneration they are potentially involved in the transient provision of extracellular matrix (ECM) which ensures effective tissue repair. This matrix enables myofiber degeneration by macrophages that allows for further infiltration of various cell types. *Osr1*-dependent expression of uPA, thus activation of plasmin proteases, could lead to the degradation of fibrin depositions. Subsequently, muscle degeneration would be inhibited and transient ECM

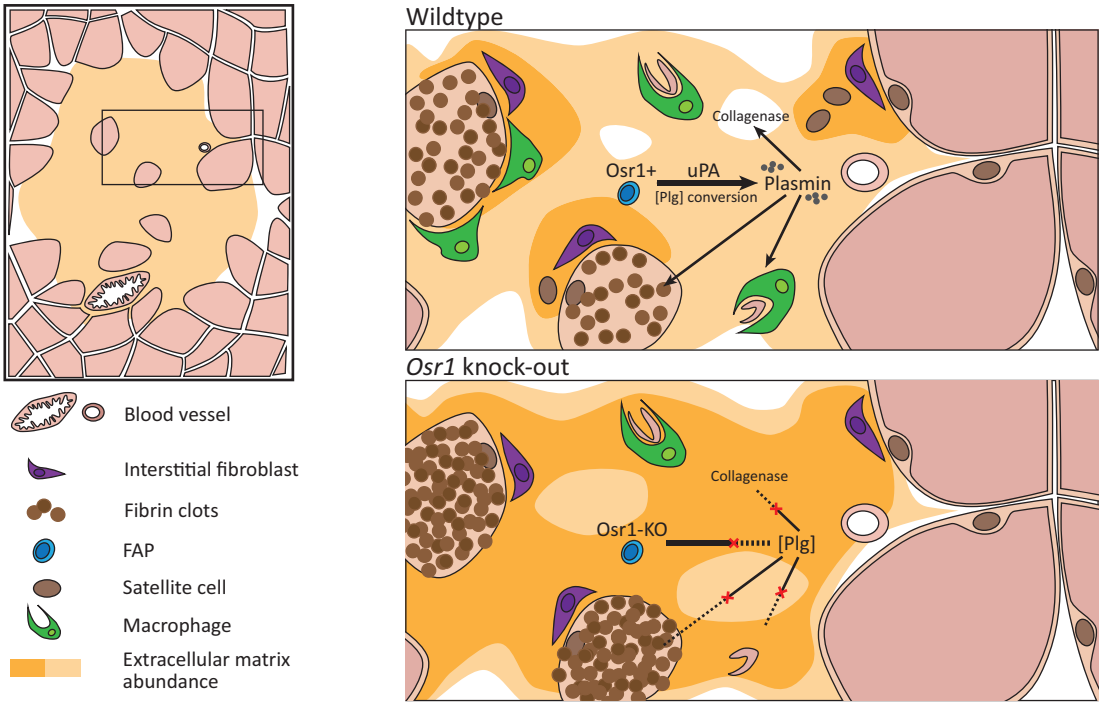

Figure 52: Proposed model of aberrant muscle regeneration caused by *Osr1* deficiency. Immediately after muscle injury fibrin extravasates from the circulation to clot blood and accumulate in degenerating myofibers. Infiltrating pro-inflammatory macrophages phagocytize degenerating myofibers causing a collateral damage which has pro-myogenic effects. Interstitial fibroblasts produce a collagenous transient extracellular matrix. Counteracting ectopic matrix formation, thus fibrosis, extravasated plasminogen (Plg) is converted to plasmin proteases (Plasmin) by urokinase-type plasminogen activator (uPA) enzymes. Plasmin activates collagenases that degrade matrix components, degrades fibrin and supports macrophage recruitment. *Osr1* expression in FAPs is suggested to regulate uPA synthesis. In Osr1 deficient FAPs (Osr1-KO) uPA would not be produced, resulting in inactivated plasmin Plg. Lacking in plasmin leads to progressive accumulation of fibrin in degenerating fibers and reduced macrophage abundance that clear the tissue from these fibers and other debris. In addition, decreased activation of collagenases leads to fibrosis.

accumulation progressively resolved. While uPA deficient mice showed severe fibrosis formation during the progression of regeneration and impaired tissue repair [Suelves et al., 2007], fibrosis would be prevented by *Osr1* expression in FAPs .

This model proposed here attributes a novel role to FAPs during an early phase of muscle regeneration based on the function of *Osr1* (fig.52). *Osr1* mediated gene regulation in FAPs could be crucially involved in modulating the pro-inflammatory immune response and controlling the progressive reduction of transient extracellular matrix. Hence, *Osr1* expression would be a critical component and indispensable in the course of effective regeneration.

6 References

[Allbrook et al., 1971] Allbrook, D. B., Han, M. F., and Hellmuth, A. E. (1971). Population of Muscle Satellite Cells in Relation To Age and Mitotic Activity. *Pathology*, 3(3):233–243.

[Ambrosio, 2008] Ambrosio, F. (2008). *Musculoskeletal Tissue Regeneration*.

[Andrae et al., 2008] Andrae, J., Gallini, R., and Betsholtz, C. (2008). Role of platelet-derived growth factors in physiology and medicine. *Genes & development*, 22(10):1276–312.

[Armand et al., 1983] Armand, O., Boutineau, A. M., Mauger, A., Pautou, M. P., and Kieny, M. (1983). Origin of satellite cells in avian skeletal muscles. *Archives d'anatomie microscopique et de morphologie expérimentale*, 72(2):163–81.

[Armulik et al., 2011] Armulik, A., Genové, G., and Betsholtz, C. (2011). Pericytes: Developmental, Physiological, and Pathological Perspectives, Problems, and Promises. *Developmental Cell*, 21:193–215.

[Arnold et al., 2007] Arnold, L., Henry, A., Poron, F., Baba-Amer, Y., van Rooijen, N., Plonquet, A., Gherardi, R. K., and Chazaud, B. (2007). Inflammatory monocytes recruited after skeletal muscle injury switch into antiinflammatory macrophages to support myogenesis. *J Exp Med*, 204(5):1057–1069.

[Bachmair et al., 1986] Bachmair, A., Finley, D., and Varshavsky, A. (1986). In vivo half-life of a protein is a function of its amino-terminal residue. *Science (New York, N.Y.)*, 234(4773):179–186.

[Banker and Engel, 2004] Banker, B. Q. and Engel, A. G. (2004). Basic reactions of muscle. In Engel, A. G. and Franzini-Armstrong, C., editors, *Myology Vol. 1*, pages 691–747. McGraw-Hill, New Yrok, 3 edition.

[Beauchamp et al., 2000] Beauchamp, J. R., Heslop, L., Yu, D. S. W., Tajbakhsh, S., Kelly, R. G., Wernig, A., Buckingham, M. E., Partridge, T. A., and Zammit, P. S. (2000). Expression of CD34 and Myf5 defines the majority of quiescent adult skeletal muscle satellite cells. *Journal of Cell Biology*, 151(6):1221–1233.

[Bentzinger et al., 2013] Bentzinger, C. F., Wang, Y. X., Dumont, N. a., and Rudnicki, M. a. (2013). Cellular dynamics in the muscle satellite cell niche. *EMBO reports*, 14(12):1062–72.

[Besançon et al., 1998] Besançon, F., Atfi, a., Gespach, C., Cayre, Y. E., and Bourgeade, M. F. (1998). Evidence for a role of NF-kappaB in the survival of hematopoietic cells mediated by interleukin 3 and the oncogenic TEL/platelet-derived growth factor receptor beta fusion protein. *Proceedings of the National Academy of Sciences of the United States of America*, 95(14):8081–6.

[Birbrair et al., 2013a] Birbrair, A., Zhang, T., Wang, Z.-M., Messi, M. L., Enikolopov, G. N., Mintz, A., and Delbono, O. (2013a). Role of pericytes in skeletal muscle regeneration and fat accumulation. *Stem cells and development*, 22(16):2298–314.

[Birbrair et al., 2013b] Birbrair, A., Zhang, T., Wang, Z.-M., Messi, M. L., Mintz, A., and Delbono, O. (2013b). Type-1 pericytes participate in fibrous tissue deposition in aged skeletal muscle. *American journal of physiology. Cell physiology*, 305(11):C1098–113.

[Birbrair et al., 2014] Birbrair, A., Zhang, T., Wang, Z.-M., Messi, M. L., Olson, J. D., Mintz, A., and Delbono, O. (2014). Type-2 Pericytes Participate in Normal and Tumoral Angiogenesis. *American Journal of Physiology Cell Physiology*, 307(84):C25–C38.

[Bjornson et al., 2012] Bjornson, C. R. R., Cheung, T. H., Liu, L., Tripathi, P. V., Steeper, K. M., and Rando, T. A. (2012). Notch signaling is necessary to maintain quiescence in adult muscle stem cells. *Stem Cells*, 30(2):232–242.

[Bodine et al., 2001] Bodine, S. C., Stitt, T. N., Gonzalez, M., Kline, W. O., Stover, G. L., Bauerlein, R., Zlotchenko, E., Scrimgeour, a., Lawrence, J. C., Glass, D. J., and Yancopoulos, G. D. (2001). Akt/mTOR pathway is a crucial regulator of skeletal muscle hypertrophy and can prevent muscle atrophy in vivo. *Nature cell biology*, 3(11):1014–1019.

[Bondjers et al., 2006] Bondjers, C., He, L., Takemoto, M., Norlin, J., Asker, N., Hellström, M., Lindahl, P., and Betsholtz, C. (2006). Microarray analysis of blood microvessels from PDGF-B and PDGF-Rbeta mutant mice identifies novel markers for brain pericytes. *FASEB journal : official publication of the Federation of American Societies for Experimental Biology*, 20(10):1703–5.

[Boonen et al., 2009] Boonen, K. J. M., Rosaria-Chak, K. Y., Baaijens, F. P. T., van der Schaft, D. W. J., and Post, M. J. (2009). Essential environmental cues from the satellite cell niche: optimizing proliferation and differentiation. *American journal of physiology. Cell physiology*, 296:C1338–C1345.

[Boppart et al., 2013] Boppart, M. D., Lisio, M. D., Zou, K., and Huntsman, H. D. (2013). Defining a role for non-satellite stem cells in the regulation of muscle repair following exercise. *Frontiers in Physiology*, 4 NOV(November):1–6.

[Brack et al., 2007] Brack, A. S., Conboy, M. J., Roy, S., Lee, M., Kuo, C. J., Keller, C., and Rando, T. A. (2007). Increased Wnt signaling during aging alters muscle stem cell fate and increases fibrosis. *Science (New York, N.Y.)*, 317(5839):807–10.

[Braun et al., 1992] Braun, T., Rudnicki, M. A., Arnold, H. H., and Jaenisch, R. (1992). Targeted inactivation of the muscle regulatory gene Myf-5 results in abnormal rib development and perinatal death. *Cell*, 71(3):369–382.

[Brigitte et al., 2010] Brigitte, M., Schilte, C., Plonquet, A., Baba-Amer, Y., Henri, A., Charlier, C., Tajbakhsh, S., Albert, M., Gherardi, R. K., and Chrétien, F. (2010). Muscle resident macrophages control the immune cell reaction in a mouse model of notexin-induced myoinjury. *Arthritis and Rheumatism*, 62(1):268–279.

[Caldwell et al., 1990] Caldwell, C. J., Mattey, D. L., and Weller, R. O. (1990). Role of the basement membrane in the regeneration of skeletal muscle. *Neuropathology and applied neurobiology*, 16(3):225–38.

[Chargé and Rudnicki, 2004] Chargé, S. B. P. and Rudnicki, M. a. (2004). Cellular and molecular regulation of muscle regeneration. *Physiological reviews*, 84(1):209–238.

[Chen et al., 2011] Chen, H., Gu, X., Liu, Y., Wang, J., Wirt, S. E., Bottino, R., Schorle, H., Sage, J., and Kim, S. K. (2011). PDGF signalling controls age-dependent proliferation in pancreatic β-cells. *Nature*, 478(7369):349–355.

[Chevallier et al., 1976] Chevallier, A., Kieny, M., and Mauger, A. (1976). Sur l'origine de la musculature de l'aile chez les Oiseaux. *C. R. Acad. Sci.*, (282):309–311.

[Chevallier et al., 1977] Chevallier, a., Kieny, M., and Mauger, a. (1977). Limb-somite relationship: origin of the limb musculature. *Journal of embryology and experimental morphology*, 41(1951):245–258.

[Cho et al., 1994] Cho, M., Hughes, S. M., Karsch-Mizrachi, I., Travis, M., Leinwand, L. a., and Blau, H. M. (1994). Fast myosin heavy chains expressed in secondary mammalian muscle fibers at the time of their inception. *Journal of cell science*, 107 (Pt 9:2361–2371.

[Christ and Ordahl, 1995] Christ, B. and Ordahl, C. (1995). Early stages of chick somite development. *Anatomy and embryology*, (November 1994):381–396.

[Cohn et al., 2002] Cohn, R. D., Henry, M. D., Michele, D. E., Barresi, R., Saito, F., Moore, S. A., Flanagan, J. D., Skwarchuk, M. W., Robbins, M. E., Mendell, J. R., Williamson, R. A., and Campbell, K. P. (2002). Disruption of Dag1 in differentiated skeletal muscle reveals a role for dystroglycan in muscle regeneration. *Cell*, 110(5):639–648.

[Collins et al., 2005] Collins, C. A., Olsen, I., Zammit, P. S., Heslop, L., Petrie, A., Partridge, T. A., and Morgan, J. E. (2005). Stem cell function, self-renewal, and behavioral heterogeneity of cells from the adult muscle satellite cell niche. *Cell*, 122(2):289–301.

[Cooper et al., 1999] Cooper, R. N., Tajbakhsh, S., Mouly, V., Cossu, G., Buckingham, M., and Butler-Browne, G. S. (1999). In vivo satellite cell activation via Myf5 and MyoD in regenerating mouse skeletal muscle. *Journal of cell science*, 112 (Pt 1:2895–2901.

[Coulter and Wieschaus, 1988] Coulter, D. E. and Wieschaus, E. (1988). Gene activities and segmental patterning in Drosophila: analysis of odd-skipped and pair-rule double mutants. *Genes & development*, 2(12 B):1812–1823.

[Couteaux and Mira, 1985] Couteaux, R. and Mira, J. C. (1985). *Molecular Basis of Nerve Activity*. W. de Gruyter, Berlin.

[Couteaux et al., 1988] Couteaux, R., Mira, J. C., and D'Albis, A. (1988). Regeneration of muscles after cardiotoxin injury. I. Cytological aspects. *Biology of the cell / under the auspices of the European Cell Biology Organization*, 62(2):171–82.

[Crisan et al., 2008] Crisan, M., Yap, S., Casteilla, L., Chen, C. W., Corselli, M., Park, T. S., Andriolo, G., Sun, B., Zheng, B., Zhang, L., Norotte, C., Teng, P. N., Traas, J., Schugar, R., Deasy, B. M., Badylak, S., Bühring, H. J., Giacobino, J. P., Lazzari, L., Huard, J., and Péault, B. (2008). A Perivascular Origin for Mesenchymal Stem Cells in Multiple Human Organs. *Cell Stem Cell*, 3(3):301–313.

[Dahlman et al., 2010] Dahlman, J. M., Bakkar, N., He, W., and Guttridge, D. C. (2010). NF-κB functions in stromal fibroblasts to regulate early postnatal muscle development. *Journal of Biological Chemistry*, 285(8):5479–5487.

[Debeer et al., 2002] Debeer, P., De Ravel, T. J. L., Devriendt, K., Fryns, J. P., Huysmans, C., and Van De Ven, W. J. M. (2002). Human homologues of Osr1 and Osr2 are not involved in a syndrome with distal limb deficiencies, oral abnormalities, and renal defects [7]. *American Journal of Medical Genetics*, 111(4):455–456.

[Dellavalle et al., 2011] Dellavalle, a., Maroli, G., Covarello, D., Azzoni, E., Innocenzi, a., Perani, L., Antonini, S., Sambasivan, R., Brunelli, S., Tajbakhsh, S., and Cossu, G. (2011). Pericytes resident in postnatal skeletal muscle differentiate into muscle fibres and generate satellite cells. *Nature communications*, 2:499.

[Dellavalle et al., 2007] Dellavalle, A., Sampaolesi, M., Tonlorenzi, R., Tagliafico, E., Sacchetti, B., Perani, L., Innocenzi, A., Galvez, B. G., Messina, G., Morosetti, R., Li, S., Belicchi, M., Peretti,

G., Chamberlain, J. S., Wright, W. E., Torrente, Y., Ferrari, S., Bianco, P., and Cossu, G. (2007). Pericytes of human skeletal muscle are myogenic precursors distinct from satellite cells. *Nature cell biology*, 9(3):255–67.

[Deng et al., 2012] Deng, B., Wehling-Henricks, M., Villalta, S. A., Wang, Y., and Tidball, J. G. (2012). IL-10 Triggers Changes in Macrophage Phenotype That Promote Muscle Growth and Regeneration. *The Journal of Immunology*, 189(7):3669–3680.

[Dobek et al., 2013] Dobek, G. L., Fulkerson, N. D., Nicholas, J., and Schneider, B. S. P. (2013). Mouse model of muscle crush injury of the legs. *Comparative Medicine*, 63(3):227–232.

[Domingo et al., 2013] Domingo, A., Mayoral, O., Monterde, S., and Santafé, M. M. (2013). Neuromuscular damage and repair after dry needling in mice. *Evidence-based Complementary and Alternative Medicine*, 2013.

[Economides et al., 2013] Economides, A. N., Frendewey, D., Yang, P., Dominguez, M. G., Dore, A. T., Lobov, I. B., Persaud, T., Rojas, J., McClain, J., Lengyel, P., Droguett, G., Chernomorsky, R., Stevens, S., Auerbach, W., DeChiara, T. M., Pouyemirou, W., Cruz, J. M., Feeley, K., Mellis, I. A., Yasenchack, J., Hatsell, S. J., Xie, L., Latres, E., Huang, L., Zhang, Y., Pefanis, E., Skokos, D., Deckelbaum, R. A., Croll, S. D., Davis, S., Valenzuela, D. M., Gale, N. W., Murphy, A. J., and Yancopoulos, G. D. (2013). Conditionals by inversion provide a universal method for the generation of conditional alleles. *Proceedings of the National Academy of Sciences*, 110(34):E3179–E3188.

[Eisenberg and Eisenberg, 1968] Eisenberg, B. and Eisenberg, R. S. (1968). Transverse tubular system in glycerol-treated skeletal muscle. *Science (New York, N.Y.)*, 160(3833):1243–4.

[Engler et al., 2006] Engler, A. J., Sen, S., Sweeney, H. L., and Discher, D. E. (2006). Matrix Elasticity Directs Stem Cell Lineage Specification. *Cell*, 126(4):677–689.

[Engvall et al., 1990] Engvall, E., Earwicker, D., Haaparanta, T., Ruoslahti, E., and Sanes, J. R. (1990). Distribution and isolation of four laminin variants; tissue restricted distribution of heterotrimers assembled from five different subunits. *Cell regulation*, 1(10):731–40.

[Erovic et al., 2012] Erovic, B. M., Harris, L., Jamali, M., Goldstein, D. P., Irish, J. C., Asa, S. L., and Mete, O. (2012). Biomarkers of parathyroid carcinoma. *Endocrine Pathology*, 23(4):221–231.

[Etchevers et al., 2001] Etchevers, H. C., Vincent, C., Le Douarin, N. M., and Couly, G. F. (2001). The cephalic neural crest provides pericytes and smooth muscle cells to all blood vessels of the face and forebrain. *Development (Cambridge, England)*, 128(7):1059–1068.

[Floss et al., 1997] Floss, T., Arnold, H. H., and Braun, T. (1997). A role for FGF-6 in skeletal muscle regeneration. *Genes and Development*, 11(16):2040–2051.

[Fukada et al., 2007] Fukada, S., Uezumi, A., Ikemoto, M., Masuda, S., Segawa, M., Tanimura, N., Yamamoto, H., Miyagoe-Suzuki, Y., and Takeda, S. (2007). Molecular signature of quiescent satellite cells in adult skeletal muscle. *Stem Cells*, 25(10):2448–2459.

[Fukada et al., 2004] Fukada, S. I., Higuchi, S., Segawa, M., Koda, K. I., Yamamoto, Y., Tsujikawa, K., Kohama, Y., Uezumi, A., Imamura, M., Miyagoe-Suzuki, Y., Takeda, S., and Yamamoto, H. (2004). Purification and cell-surface marker characterization of quiescent satellite cells from murine skeletal muscle by a novel monoclonal antibody. *Experimental Cell Research*, 296(2):245–255.

[Gao et al., 2009] Gao, Y., Lan, Y., Ovitt, C. E., and Jiang, R. (2009). Functional equivalence of the zinc finger transcription factors Osr1 and Osr2 in mouse development. *Developmental biology*, 328(2):200–9.

[Gayraud-Morel et al., 2007] Gayraud-Morel, B., Chrétien, F., Flamant, P., Gomès, D., Zammit, P. S., and Tajbakhsh, S. (2007). A role for the myogenic determination gene Myf5 in adult regenerative myogenesis. *Developmental Biology*, 312(1):13–28.

[Gilbert et al., 2010] Gilbert, P. M., Havenstrite, K. L., Magnusson, K. E. G., Sacco, A., Leonardi, N. A., Kraft, P., Nguyen, N. K., Thrun, S., Lutolf, M. P., and Blau, H. M. (2010). Substrate elasticity regulates skeletal muscle stem cell self-renewal in culture. *Science (New York, N.Y.)*, 329(5995):1078–81.

[Gilbert, 2013] Gilbert, S. F. (2013). Developmental Biology. In *Developmental Biology*, chapter 12. Sinauer Associates Inc., Sunderland (MA), 10th edition.

[Goldstein et al., 2005] Goldstein, R. E., Cook, O., Dinur, T., Pisante, A., Karandikar, U. C., and Virginia, W. (2005). An eh1-Like Motif in Odd-skipped Mediates Recruitment of Groucho and Repression In Vivo. *Molecular and cellular biology*, 25(24):10711–10720.

[Goodpaster et al., 2004] Goodpaster, B. H., Stenger, V. A., Boada, F., McKolanis, T., Davis, D., Ross, R., and Kelley, D. E. (2004). Skeletal muscle lipid concentration quantified by magnetic resonance imaging. *American Journal of Clinical Nutrition*, 79(5):748–754.

[Grounds and McGeachie, 1989] Grounds, M. D. and McGeachie, J. K. (1989). A comparison of muscle precursor replication in crush-injured skeletal muscle of Swiss and BALBc mice. *Cell and tissue research*, 255(2):385–91.

[Guida et al., 2007] Guida, T., Anaganti, S., Provitera, L., Gedrich, R., Sullivan, E., Wilhelm, S. M., Santoro, M., and Carlomagno, F. (2007). Sorafenib inhibits imatinib-resistant KIT and platelet-derived growth factor receptor beta gatekeeper mutants. *Clinical Cancer Research*, 13(11):3363–3369.

[Hardy et al., 2016] Hardy, D., Besnard, A., Latil, M., Jouvion, G., Briand, D., Thépenier, C., Pascal, Q., Guguin, A., Gayraud-Morel, B., Cavaillon, J.-M., Tajbakhsh, S., Rocheteau, P., and Chrétien, F. (2016). Comparative Study of Injury Models for Studying Muscle Regeneration in Mice. *Plos One*, 11(1):e0147198.

[Harris et al., 2003] Harris, J. B., Vater, R., Wilson, M., and Cullen, M. J. (2003). Muscle fibre breakdown in venom-induced muscle degeneration. *Journal of anatomy*, 202(4):363–372.

[Hashimoto et al., 1999] Hashimoto, K., Yokouchi, Y., Yamamoto, M., and Kuroiwa, a. (1999). Distinct signaling molecules control Hoxa-11 and Hoxa-13 expression in the muscle precursor and mesenchyme of the chick limb bud. *Development (Cambridge, England)*, 126(12):2771–2783.

[Hasson et al., 2010] Hasson, P., DeLaurier, A., Bennett, M., Grigorieva, E., Naiche, L. a., Papaioannou, V. E., Mohun, T. J., and Logan, M. P. O. (2010). Tbx4 and tbx5 acting in connective tissue are required for limb muscle and tendon patterning. *Developmental cell*, 18(1):148–56.

[Heredia et al., 2013] Heredia, J. E., Mukundan, L., Chen, F. M., Mueller, A. a., Deo, R. C., Locksley, R. M., Rando, T. a., and Chawla, A. (2013). Type 2 innate signals stimulate fibro/adipogenic progenitors to facilitate muscle regeneration. *Cell*, 153(2):376–88.

[Hill et al., 2003] Hill, M., Wernig, A., and Goldspink, G. (2003). Muscle satellite (stem) cell activation during local tissue injury and repair. *Journal of anatomy*, 203(1):89–99.

[Hughes et al., 1993] Hughes, S. H., Cho, M., Karsch-Mizrachi, I., Travis, M., Silberstein, L., Leinwand, L. A., and Blau, H. M. (1993). Three Slow Myosin Heavy Chains Sequentially Expressed in Developing Mammalian Skeletal Muscle.

[James et al., 2006] James, R. G., Kamei, C. N., Wang, Q., Jiang, R., and Schultheiss, T. M. (2006). Odd-skipped related 1 is required for development of the metanephric kidney and regulates formation and differentiation of kidney precursor cells. *Development (Cambridge, England)*, 133(15):2995–3004.

[Joe et al., 2010] Joe, A. W. B., Yi, L., Natarajan, A., Le Grand, F., So, L., Wang, J., Rudnicki, M. a., and Rossi, F. M. V. (2010). Muscle injury activates resident fibro/adipogenic progenitors that facilitate myogenesis. *Nature cell biology*, 12(2):153–63.

[Julius et al., 1972] Julius, M. H., Masuda, T., and Herzenberg, L. A. (1972). Demonstration that antigen-binding cells are precursors of antibody-producing cells after purification with a fluorescence-activated cell sorter. *Proceedings of the National Academy of Sciences of the United States of America*, 69(7):1934–8.

[Kardon et al., 2003] Kardon, G., Harfe, B. D., and Tabin, C. J. (2003). A Tcf4-positive mesodermal population provides a prepattern for vertebrate limb muscle patterning. *Developmental cell*, 5(6):937–44.

[Karsenty et al., 1996] Karsenty, G., Luo, G., Hofmann, C., and Bradley, A. (1996). BMP 7 is required for nephrogenesis, eye development, and skeletal patterning. *Annals of the New York Academy of Sciences*, 785:98–107.

[Katoh, 2002] Katoh, M. (2002). Molecular cloning and characterization of OSR1 on human chromosome 2p24. *International journal of molecular medicine*, 10(2):221–5.

[Keefe et al., 2015] Keefe, A. C., Lawson, J. A., Flygare, S. D., Fox, Z. D., Colasanto, M. P., Mathew, S. J., Yandell, M., and Kardon, G. (2015). Muscle stem cells contribute to myofibres in sedentary adult mice. *Nature communications*, 6(May):7087.

[Kuang et al., 2007] Kuang, S., Kuroda, K., Le Grand, F., and Rudnicki, M. A. (2007). Asymmetric Self-Renewal and Commitment of Satellite Stem Cells in Muscle. *Cell*, 129(5):999–1010.

[Kuo et al., 1997] Kuo, H.-J., Maslen, C. L., Keene, D. R., and Glanville, R. W. (1997). Type VI Collagen Anchors Endothelial Basement Membranes by Interacting with Type IV Collagen*. 272(42):26522–26529.

[Kyryachenko et al., 2016] Kyryachenko, S., Formicola, L., Ollitrault, D., Correra, R., Denizot, A.-L., Kyrylkova, K., Marazzi, G., and Sassoon, D. (2016). The Adult Stem Cell Niche: Multiple Cellular Players in Tissue Homeostasis and Regeneration. In Bradshaw, R. A. and Stahl, P. D., editors, *Encyclopedia of Cell Biology*, number January, chapter Stem cell, pages 794–806. Elsevier.

[Lan et al., 2001] Lan, Y., Kingsley, P. D., Cho, E. S., and Jiang, R. (2001). Osr2, a new mouse gene related to Drosophila odd-skipped, exhibits dynamic expression patterns during craniofacial, limb, and kidney development. *Mechanisms of development*, 107(1-2):175–179.

[Lepper et al., 2009] Lepper, C., Conway, S. J., and Fan, C.-M. (2009). Adult satellite cells and embryonic muscle progenitors have distinct genetic requirements. *Nature*, 460(7255):627–31.

[Lepper et al., 2011] Lepper, C., Partridge, T. A., and Fan, C. M. (2011). An absolute requirement for Pax7-positive satellite cells in acute injury-induced skeletal muscle regeneration. *Development*, 138(17):3639–3646.

[Lieber, 2010] Lieber, R. L. (2010). *Skeletal Muscle Structure, Function, and Plasticity*. Wolters Kluwer/Lippincott Williams & Wilkins, Baltimore, MD, USA.

[Lionikas et al., 2005] Lionikas, a., Blizard, D. a., Gerhard, G. S., Vandenbergh, D. J., Stout, J. T., Vogler, G. P., McClearn, G. E., and Larsson, L. (2005). Genetic determinants of weight of fast- and slow-twitch skeletal muscle in 500-day-old mice of the C57BL/6J and DBA/2J lineage. *Physiological genomics*, 21(29):184–192.

[Liu et al., 2013] Liu, L., Cheung, T. H., Charville, G. W., Hurgo, B. M. C., Leavitt, T., Shih, J., Brunet, A., and Rando, T. A. (2013). Chromatin Modifications as Determinants of Muscle Stem Cell Quiescence and Chronological Aging. *Cell Reports*, 4(1):189–204.

[Lluís et al., 2001] Lluís, F., Roma, J., Suelves, M., Parra, M., Aniorte, G., Gallardo, E., Illa, I., Rodríguez, L., Hughes, S. M., Carmeliet, P., Roig, M., and Muñoz-Cánoves, P. (2001). Urokinase-dependent plasminogen activation is required for efficient skeletal muscle regeneration in vivo. *Blood*, 97(6):1703–11.

[Mann et al., 2011] Mann, C. J., Perdiguero, E., Kharraz, Y., Aguilar, S., Pessina, P., Serrano, A. L., and Muñoz-Cánoves, P. (2011). Aberrant repair and fibrosis development in skeletal muscle. *Skeletal muscle*, 1(1):21.

[Mathew et al., 2011] Mathew, S. J., Hansen, J. M., Merrell, A. J., Murphy, M. M., Lawson, J. a., Hutcheson, D. a., Hansen, M. S., Angus-Hill, M., and Kardon, G. (2011). Connective tissue fibroblasts and Tcf4 regulate myogenesis. *Development (Cambridge, England)*, 138(2):371–84.

[Mauro, 1961] Mauro, A. (1961). Satellite Cell of Skeletal Muscle Fibers. *Journal of Biophysical and Biochemical Cytology*, 9:493–495.

[Mayer et al., 1997] Mayer, U., Saher, G., Fässler, R., Bornemann, a., Echtermeyer, F., von der Mark, H., Miosge, N., Pöschl, E., and von der Mark, K. (1997). Absence of integrin alpha 7 causes a novel form of muscular dystrophy. *Nature genetics*, 17:318–323.

[McBrier et al., 2009] McBrier, N. M., Neuberger, T., Denegar, C. R., Sharkey, N. A., and Webb, A. G. (2009). Magnetic resonance imaging of acute injury in rats and the effects of buprenorphine on limb volume. *J Am Assoc Lab Anim Sci*, 48(2):147–151.

[McGeachie and Grounds, 1987] McGeachie, J. K. and Grounds, M. D. (1987). Initiation and duration of muscle precursor replication after mild and severe injury to skeletal muscle of mice. An autoradiographic study. *Cell and tissue research*, 248(1):125–130.

[Menetrey et al., 1999] Menetrey, J., Kasemkijwattana, C., Fu, F. H., Moreland, M. S., and Huard, J. (1999). Suturing versus immobilization of a muscle laceration. A morphological and functional study in a mouse model. *The American journal of sports medicine*, 27(2):222–229.

[Mitchell et al., 2010] Mitchell, K. J., Pannérec, A., Cadot, B., Parlakian, A., Besson, V., Gomes, E. R., Marazzi, G., and Sassoon, D. a. (2010). Identification and characterization of a non-satellite cell muscle resident progenitor during postnatal development. *Nature cell biology*, 12(3):257–66.

[Morales et al., 2013] Morales, M. G., Cabrera, D., Céspedes, C., Vio, C. P., Vazquez, Y., Brandan, E., and Cabello-Verrugio, C. (2013). Inhibition of the angiotensin-converting enzyme decreases skeletal muscle fibrosis in dystrophic mice by a diminution in the expression and activity of connective tissue growth factor (CTGF/CCN-2). *Cell and Tissue Research*, 353(1):173–187.

[Morgan and Partridge, 2003] Morgan, J. E. and Partridge, T. A. (2003). Muscle satellite cells. *The international journal of biochemistry & cell biology*, 35(8):1151–1156.

[Moss and Leblond, 1970] Moss, F. P. and Leblond, C. P. (1970). Nature of dividing nuclei in skeletal muscle of growing rats. *Journal of Cell Biology*, 44:459–462.

[Moss and Leblond, 1971] Moss, F. P. and Leblond, C. P. (1971). Satellite cells as the source of nuclei in muscles of growing rats. *The Anatomical record*, 170(4):421–35.

[Mozzetta et al., 2013] Mozzetta, C., Consalvi, S., Saccone, V., Tierney, M., Diamantini, A., Mitchell, K. J., Marazzi, G., Borsellino, G., Battistini, L., Sassoon, D., Sacco, A., and Puri, P. L. (2013). Fibroadipogenic progenitors mediate the ability of HDAC inhibitors to promote regeneration in dystrophic muscles of young, but not old Mdx mice. *EMBO molecular medicine*, 5(4):626–39.

[Mugford et al., 2008] Mugford, J. W., Sipilä, P., McMahon, J. A., and McMahon, A. P. (2008). Osr1 expression demarcates a multi-potent population of intermediate mesoderm that undergoes progressive restriction to an Osr1-dependent nephron progenitor compartment within the mammalian kidney. *Developmental Biology*, 324(1):88–98.

[Murphy et al., 2011] Murphy, M. M., Lawson, J. a., Mathew, S. J., Hutcheson, D. a., and Kardon, G. (2011). Satellite cells, connective tissue fibroblasts and their interactions are crucial for muscle regeneration. *Development (Cambridge, England)*, 138(17):3625–37.

[Muzumdar et al., 2007] Muzumdar, M. D., Tasic, B., Miyamichi, K., Li, L., and Luo, L. (2007). A Global Double-Fluorescent Cre Reporter Mouse. 605(September):593–605.

[Natarajan et al., 2010] Natarajan, A., Lemos, D. R., and Rossi, F. M. V. (2010). Fibro/adipogenic progenitors: A double-edged sword in skeletal muscle regeneration. *Cell Cycle*, 9(11):2045–2046.

[Nehls et al., 1992] Nehls, V., Denzer, K., and Drenckhahn, D. (1992). Pericyte involvement in capillary sprouting during angiogenesis in situ. *Cell and Tissue Research*, 270(3):469–474.

[Noonan et al., 1991] Noonan, D. M., Fulle, A., Valente, P., Cai, S., Horigan, E., Sasaki, M., Yamada, Y., and Hassell, J. R. (1991). The complete sequence of perlecan, a basement membrane heparan sulfate proteoglycan, reveals extensive similarity with laminin A chain, low density lipoprotein-receptor, and the neural cell adhesion molecule. *Journal of Biological Chemistry*, 266(34):22939–22947.

[Nüsslein-Volhard and Wieschaus, 1980] Nüsslein-Volhard, C. and Wieschaus, E. (1980). Mutations affecting segment number and polarity in Drosophila. *Nature*, 287(5785):795–801.

[Ontell et al., 1984] Ontell, M., Feng, K. C., Klueber, K., Dunn, R. F., and Taylor, F. (1984). Myosatellite cells, growth, and regeneration in murine dystrophic muscle: a quantitative study. *Anatomical Record*, 208(2):159–74.

[Orr-Urtreger et al., 1992] Orr-Urtreger, A., Bedford, M. T., Do, M. S., Eisenbach, L., and Lonai, P. (1992). Developmental expression of the alpha receptor for platelet-derived growth factor, which is deleted in the embryonic lethal Patch mutation. *Development (Cambridge, England)*, 115(1):289–303.

[Otani et al., 2014] Otani, K., Dong, Y., Li, X., Lu, J., Zhang, N., Xu, L., Go, M. Y. Y., Ng, E. K. W., Arakawa, T., Chan, F. K. L., Sung, J. J. Y., and Yu, J. (2014). Odd-skipped related 1 is a novel tumour suppressor gene and a potential prognostic biomarker in gastric cancer. *The Journal of pathology*, 234(3):302–15.

[Otis et al., 2014] Otis, J. S., Niccoli, S., Hawdon, N., Sarvas, J. L., Frye, M. A., Chicco, A. J., and Lees, S. J. (2014). Pro-inflammatory mediation of myoblast proliferation. *PLoS ONE*, 9(3):1–10.

[Ozerdem et al., 2001] Ozerdem, U., Grako, K. A., Dahlin-Huppe, K., Monosov, E., and Stallcup, W. B. (2001). NG2 proteoglycan is expressed exclusively by mural cells during vascular morphogenesis. *Developmental Dynamics*, 222(2):218–227.

[Ozerdem and Stallcup, 2003] Ozerdem, U. and Stallcup, W. B. (2003). Early contribution of pericytes to angiogenic sprouting and tube formation. *Angiogenesis*, 6(3):241–249.

[Pannérec et al., 2013] Pannérec, A., Formicola, L., Besson, V., Marazzi, G., and Sassoon, D. a. (2013). Defining skeletal muscle resident progenitors and their cell fate potentials. *Development (Cambridge, England)*, 2891:2879–2891.

[Pisani et al., 2010] Pisani, D. F., Bottema, C. D. K., Butori, C., Dani, C., and Dechesne, C. a. (2010). Mouse model of skeletal muscle adiposity: A glycerol treatment approach. *Biochemical and Biophysical Research Communications*, 396(3):767–773.

[Poole et al., 2008] Poole, D. C., Barstow, T. J., Mcdonough, P., and Jones, A. M. (2008). Control of oxygen uptake during exercise. *Medicine and Science in Sports and Exercise*, 40(3):462–474.

[Raab et al., 2012] Raab, M., Swift, J., Dingal, P. C. D. P., Shah, P., Shin, J. W., and Discher, D. E. (2012). Crawling from soft to stiff matrix polarizes the cytoskeleton and phosphoregulates myosin-II heavy chain. *Journal of Cell Biology*, 199(4):669–683.

[Rehimi et al., 2010] Rehimi, R., Khalida, N., Yusuf, F., Morosan-Puopolo, G., and Brand-Saberi, B. (2010). A novel role of CXCR4 and SDF-1 during migration of cloacal muscle precursors. *Developmental Dynamics*, 239(6):1622–1631.

[Rivers et al., 2008] Rivers, L. E., Young, K. M., Rizzi, M., Jamen, F., Psachoulia, K., Wade, A., Kessaris, N., and Richardson, W. D. (2008). PDGFRA/NG2 glia generate myelinating oligodendrocytes and piriform projection neurons in adult mice. *Nature neuroscience*, 11(12):1392–401.

[Robertson et al., 1993] Robertson, T. A., Maley, M. A., Grounds, M. D., and Papadimitriou, J. M. (1993). The role of macrophages in skeletal muscle regeneration with particular reference to chemotaxis.

[Rogers et al., 2015] Rogers, R. G., Baumann, C. W., and Otis, J. S. (2015). Recovery of skeletal muscle function following injury is not augmented by acute resveratrol supplementation. *International Journal of Clinical and Experimental Physiology*, 2(1):29.

[Rubinstein and Kelly, 2004] Rubinstein, N. A. and Kelly, A. M. (2004). The diversity of muscle fiber types and its origin during development. In Engel, A. G. and Franzini-Armstrong, C., editors, *Myology*, pages 87–103. McGraw-Hill, New York.

[Rudnicki et al., 1993] Rudnicki, M. A., Schnegelsberg, P. N. J., Stead, R. H., Braun, T., Arnold, H. H., and Jaenisch, R. (1993). MyoD or Myf-5 is required for the formation of skeletal muscle. *Cell*, 75(7):1351–1359.

[Ruffell et al., 2009] Ruffell, D., Mourkioti, F., Gambardella, A., Kirstetter, P., Lopez, R. G., Rosenthal, N., and Nerlov, C. (2009). A CREB-C/EBPbeta cascade induces M2 macrophage-specific gene expression and promotes muscle injury repair. *Proceedings of the National Academy of Sciences of the United States of America*, 106(41):17475–17480.

[Sabatelli et al., 2012] Sabatelli, P., Gualandi, F., Gara, S. K., Grumati, P., Zamparelli, A., Martoni, E., Pellegrini, C., Merlini, L., Ferlini, A., Bonaldo, P., Maraldi, N. M., Paulsson, M., Squarzoni, S., and Wagener, R. (2012). Expression of collagen VI α5 and α6 chains in human muscle and in Duchenne muscular dystrophy-related muscle fibrosis. *Matrix Biology*, 31(3):187–196.

[Sacco et al., 2008] Sacco, A., Doyonnas, R., Kraft, P., Vitorovic, S., and Blau, H. M. (2008). Self-renewal and expansion of single transplanted muscle stem cells. *Nature*, 456(7221):502–506.

[Saha et al., 2008] Saha, K., Keung, A. J., Irwin, E. F., Li, Y., Little, L., Schaffer, D. V., and Healy, K. E. (2008). Substrate modulus directs neural stem cell behavior. *Biophysical journal*, 95(9):4426–38.

[Sambasivan et al., 2011] Sambasivan, R., Yao, R., Kissenpfennig, A., Van Wittenberghe, L., Paldi, A., Gayraud-Morel, B., Guenou, H., Malissen, B., Tajbakhsh, S., and Galy, A. (2011). Pax7-expressing satellite cells are indispensable for adult skeletal muscle regeneration. *Development*, 138(17):3647–3656.

[Sanderson et al., 1986] Sanderson, R. D., Fitch, J. M., Linsenmayer, T. R., and Mayne, R. (1986). Fibroblasts promote the formation of a continuous basal lamina during myogenesis in vitro. *Journal of Cell Biology*, 102(3):740–747.

[Sanes, 1994] Sanes, J. R. (1994). The extracellular matrix. In Engel, A. G. and Franzini-Armstrong, C., editors, *Myology: Basic and Clinical*, pages 242–250. McGraw-Hill, Inc., New York.

[Saulier-Le Dréan et al., 1998] Saulier-Le Dréan, B., Nasiadka, a., Dong, J., and Krause, H. M. (1998). Dynamic changes in the functions of Odd-skipped during early Drosophila embryogenesis. *Development (Cambridge, England)*, 125(23):4851–61.

[Schmalbruch and Lewis, 2000] Schmalbruch, H. and Lewis, D. M. (2000). Dynamics of nuclei of muscle fibers and connective tissue cells in normal and denervated rat muscles. *Muscle & nerve*, 23(4):617–26.

[Schultz, 1974] Schultz, E. (1974). A quantitative study of the satellite cell population in postnatal mouse lumbrical muscle. *The Anatomical record*, 180:589–595.

[Schultz, 1996] Schultz, E. (1996). Satellite Cell Proliferative Compartments in Growing Skeletal Muscles. *Developmental Biology*, 175(0097):84–94.

[Schultz et al., 1978] Schultz, E., Gibson, M. C., and Champion, T. (1978). Satellite cells are mitotically quiescent in mature mouse muscle: an EM and radioautographic study. *The Journal of experimental zoology*, 206(3):451–6.

[Schulz et al., 2011] Schulz, T. J., Huang, T. L., Tran, T. T., Zhang, H., Townsend, K. L., Shadrach, J. L., Cerletti, M., McDougall, L. E., Giorgadze, N., Tchkonia, T., Schrier, D., Falb, D., Kirkland, J. L., Wagers, A. J., and Tseng, Y.-H. (2011). Identification of inducible brown adipocyte progenitors residing in skeletal muscle and white fat. *Proceedings of the National Academy of Sciences of the United States of America*, 108(1):143–8.

[Schwanhäusser et al., 2011] Schwanhäusser, B., Busse, D., Li, N., Dittmar, G., Schuchhardt, J., Wolf, J., Chen, W., and Selbach, M. (2011). Global quantification of mammalian gene expression control. *Nature*, 473(7347):337–42.

[Seale et al., 2000] Seale, P., Sabourin, L. A., Girgis-Gabardo, A., Mansouri, A., Gruss, P., and Rudnicki, M. A. (2000). Pax7 is required for the specification of myogenic satellite cells. *Cell*, 102(6):777–786.

[Serrano et al., 2008] Serrano, A. L., Baeza-Raja, B., Perdiguero, E., Jardí, M., and Munoz-Cánoves, P. (2008). Interleukin-6 Is an Essential Regulator of Satellite Cell-Mediated Skeletal Muscle Hypertrophy. *Cell Metabolism*, 7(1):33–44.

[Serrano and Muñoz-Cánoves, 2010] Serrano, A. L. and Muñoz-Cánoves, P. (2010). Regulation and dysregulation of fibrosis in skeletal muscle. *Experimental cell research*, 316(18):3050–8.

[Shafiq et al., 1968] Shafiq, S. A., Gorycki, M. A., and Mauro, A. (1968). Mitosis during postnatal growth in skeletal and cardiac muscle of the rat. *Journal of anatomy*, 103(Pt 1):135–41.

[Shefer et al., 2004] Shefer, G., Wleklinski-Lee, M., and Yablonka-Reuveni, Z. (2004). Skeletal muscle satellite cells can spontaneously enter an alternative mesenchymal pathway. *Journal of cell science*, 117(Pt 22):5393–404.

[Sherwood et al., 2004] Sherwood, R. I., Christensen, J. L., Conboy, I. M., Conboy, M. J., Rando, T. A., Weissman, I. L., and Wagers, A. J. (2004). Isolation of adult mouse myogenic progenitors: Functional heterogeneity of cells within and engrafting skeletal muscle. *Cell*, 119(4):543–554.

[Shi-wen et al., 2007] Shi-wen, X., Kennedy, L., Renzoni, E. A., Bou-Gharios, G., du Bois, R. M., Black, C. M., Denton, C. P., Abraham, D. J., and Leask, A. (2007). Endothelin is a downstream mediator of profibrotic responses to transforming growth factor beta in human lung fibroblasts. *Arthritis and rheumatism*, 56(12):4189–94.

[Shinin et al., 2006] Shinin, V., Gayraud-Morel, B., Gomès, D., and Tajbakhsh, S. (2006). Asymmetric division and cosegregation of template DNA strands in adult muscle satellite cells. *Nature cell biology*, 8(7):677–687.

[So and Danielian, 1999] So, P. L. and Danielian, P. S. (1999). Cloning and expression analysis of a mouse gene related to Drosophila odd-skipped. *Mechanisms of Development*, 84(1-2):157–160.

[Sonnet et al., 2006] Sonnet, C., Lafuste, P., Arnold, L., Brigitte, M., Poron, F., Authier, F. J., Chretien, F., Gherardi, R. K., and Chazaud, B. (2006). Human macrophages rescue myoblasts and myotubes from apoptosis through a set of adhesion molecular systems. *J Cell Sci*, 119(Pt 12):2497–2507.

[Soriano, 1999] Soriano, P. (1999). Generalized lacZ expression with the ROSA26 Cre reporter strain. *Nature genetics*, 21(1):70–71.

[Stricker et al., 2006] Stricker, S., Brieske, N., Haupt, J., and Mundlos, S. (2006). Comparative expression pattern of Odd-skipped related genes Osr1 and Osr2 in chick embryonic development. *Gene expression patterns : GEP*, 6(8):826–34.

[Stricker et al., 2012] Stricker, S., Mathia, S., Haupt, J., Seemann, P., Meier, J., and Mundlos, S. (2012). Odd-skipped related genes regulate differentiation of embryonic limb mesenchyme and bone marrow mesenchymal stromal cells. *Stem cells and development*, 21(4):623–33.

[Suelves et al., 2002] Suelves, M., López-Alemany, R., Lluís, F., Aniorte, G., Serrano, E., Parra, M., Carmeliet, P., and Muñoz-Cánoves, P. (2002). Plasmin activity is required for myogenesis in vitro and skeletal muscle regeneration in vivo. *Blood*, 99(8):2835–44.

[Suelves et al., 2007] Suelves, M., Vidal, B., Serrano, A. L., Tjwa, M., Roma, J., López-Alemany, R., Luttun, A., de Lagrán, M. M., Díaz-Ramos, A., Díaz, M. A., Jardí, M., Roig, M., Dierssen, M., Dewerchin, M., Carmeliet, P., and Muñoz-Cánoves, P. (2007). uPA deficiency exacerbates muscular dystrophy in MDX mice. *The Journal of cell biology*, 178(6):1039–51.

[Ten Broek et al., 2010] Ten Broek, R. W., Grefte, S., and Von Den Hoff, J. W. (2010). Regulatory factors and cell populations involved in skeletal muscle regeneration. *Journal of Cellular Physiology*, 224(1):7–16.

[Tena et al., 2007] Tena, J. J., Neto, A., de la Calle-Mustienes, E., Bras-Pereira, C., Casares, F., and Gómez-Skarmeta, J. L. (2007). Odd-skipped genes encode repressors that control kidney development. *Developmental Biology*, 301(2):518–531.

[Tidball, 1995] Tidball, J. G. (1995). Inflammatory cell response to acute muscle injury. *Medicine and science in sports and exercise*, 27(7):1022–32.

[Tidball and Villalta, 2010] Tidball, J. G. and Villalta, S. A. (2010). Regulatory interactions between muscle and the immune system during muscle regeneration. *American journal of physiology. Regulatory, integrative and comparative physiology*, 298(5):R1173–87.

[Tseng et al., 2008] Tseng, Y., Kokkotou, E., Schulz, T., Huang, T., Winnay, J., Taniguchi, C., Tran, T., Suzuki, R., Espinoza, D., Yamamoto, Y., Ahrens, M., Dudley, A., Norris, A., Kulkarni, R., and Kahn, C. (2008). New role of bone morphogenetic protein 7 in brown adipogenesis and energy expenditure. *Nature*, 454(7207):1000–1004.

[Uezumi et al., 2010] Uezumi, A., Fukada, S.-i., Yamamoto, N., Takeda, S., and Tsuchida, K. (2010). Mesenchymal progenitors distinct from satellite cells contribute to ectopic fat cell formation in skeletal muscle. *Nature cell biology*, 12(2):143–52.

[Uezumi et al., 2011] Uezumi, A., Ito, T., Morikawa, D., Shimizu, N., Yoneda, T., Segawa, M., Yamaguchi, M., Ogawa, R., Matev, M. M., Miyagoe-Suzuki, Y., Takeda, S., Tsujikawa, K., Tsuchida, K., Yamamoto, H., and Fukada, S.-i. (2011). Fibrosis and adipogenesis originate from a common mesenchymal progenitor in skeletal muscle. *Journal of cell science*, 124(Pt 21):3654–64.

[Ugarte et al., 2012] Ugarte, G., Cappellari, O., Perani, L., Pistocchi, A., and Cossu, G. (2012). Noggin recruits mesoderm progenitors from the dorsal aorta to a skeletal myogenic fate. *Developmental Biology*, 365(1):91–100.

[Urciuolo et al., 2013] Urciuolo, A., Quarta, M., Morbidoni, V., Gattazzo, F., Molon, S., Grumati, P., Montemurro, F., Tedesco, F. S., Blaauw, B., Cossu, G., Vozzi, G., Rando, T. a., and Bonaldo, P. (2013). Collagen VI regulates satellite cell self-renewal and muscle regeneration. *Nature communications*, 4:1964.

[Vallecillo García, 2016] Vallecillo García, P. (2016). *Function of the transcription factor Osr1 in the connective tissue-mediated control of muscle formation*. Thesis, Freie Universität Berlin and Université Pierre et Marie Curie (Cotutelle).

[Vasyutina et al., 2005] Vasyutina, E., Stebler, J., Brand-Saberi, B., Schulz, S., Raz, E., and Birchmeier, C. (2005). CXCR4 and Gab1 cooperate to control the development of migrating muscle progenitor cells. *Genes and Development*, 19(18):2187–2198.

[Vincent et al., 2013] Vincent, L. G., Choi, Y. S., Alonso-Latorre, B., Del Álamo, J. C., and Engler, A. J. (2013). Mesenchymal stem cell durotaxis depends on substrate stiffness gradient strength. *Biotechnology Journal*, 8(4):472–484.

[Visser et al., 2005] Visser, M., Goodpaster, B. H., Kritchevsky, S. B., Newman, A. B., Nevitt, M., Rubin, S. M., Simonsick, E. M., and Harris, T. B. (2005). Muscle mass, muscle strength, and muscle fat infiltration as predictors of incident mobility limitations in well-functioning older persons. *The journals of gerontology. Series A, Biological sciences and medical sciences*, 60(3):324–333.

[Wang et al., 2005] Wang, Q., Lan, Y., Cho, E. S., Maltby, K. M., and Jiang, R. (2005). Odd-skipped related 1 (Odd1) is an essential regulator of heart and urogenital development. *Developmental Biology*, 288(2):582–594.

[Warren et al., 2007] Warren, G. L., Summan, M., Gao, X., Chapman, R., Hulderman, T., and Simeonova, P. P. (2007). Mechanisms of skeletal muscle injury and repair revealed by gene expression studies in mouse models. *The Journal of physiology*, 582(Pt 2):825–41.

[Weiss and Leinwand, 1996] Weiss, a. and Leinwand, L. a. (1996). The mammalian myosin heavy chain gene family. *Annual review of cell and developmental biology*, 12:417–439.

[White et al., 2010] White, R. B., Biérinx, A.-S., Gnocchi, V. F., and Zammit, P. S. (2010). Dynamics of muscle fibre growth during postnatal mouse development. *BMC developmental biology*, 10:21.

[Wosczyna et al., 2012] Wosczyna, M. N., Biswas, A. A., Cogswell, C. A., and Goldhamer, D. J. (2012). Multipotent progenitors resident in the skeletal muscle interstitium exhibit robust BMP-dependent osteogenic activity and mediate heterotopic ossification. *Journal of bone and mineral research : the official journal of the American Society for Bone and Mineral Research*, 27(5):1004–17.

[Wren et al., 2008] Wren, T. A. L., Bluml, S., Tseng-Ong, L., and Gilsanz, V. (2008). Three-point technique of fat quantification of muscle tissue as a marker of disease progression in Duchenne muscular dystrophy: preliminary study. *AJR. American journal of roentgenology*, 190(1):8–12.

[Wright et al., 1989] Wright, W. E., Sassoon, D. A., and Lin, V. K. (1989). Myogenin, a factor regulating myogenesis, has a domain homologous to MyoD. *Cell*, 56(4):607–617.

[Wu et al., 2006] Wu, S., Wu, Y., and Capecchi, M. R. (2006). Motoneurons and oligodendrocytes are sequentially generated from neural stem cells but do not appear to share common lineage-restricted progenitors in vivo. *Development (Cambridge, England)*, 133(4):581–590.

[Xu et al., 2014] Xu, J., Liu, H., Park, J.-S., Lan, Y., and Jiang, R. (2014). Osr1 acts downstream of and interacts synergistically with Six2 to maintain nephron progenitor cells during kidney organogenesis. *Development (Cambridge, England)*, 141(7):1442–52.

[Yablonka-Reuveni et al., 1990] Yablonka-Reuveni, Z., Balestreri, T. M., and Bowen-Pope, D. F. (1990). Regulation of proliferation and differentiation of myoblasts derived from adult mouse skeletal muscle by specific isoforms of PDGF. *Journal of Cell Biology*, 111(4):1623–1629.

[Yablonka-Reuveni et al., 2008] Yablonka-Reuveni, Z., Day, K., Vine, A., and Shefer, G. (2008). Defining the transcriptional signature of skeletal muscle stem cells. *Journal of animal science*, 86(14 Suppl).

[Yamamoto and Kuroiwa, 2003] Yamamoto, M. and Kuroiwa, A. (2003). Hoxa-11 and Hoxa-13 are involved in repression of MyoD during limb muscle development. *Development Growth and Differentiation*, 45(5-6):485–498.

[Zou et al., 2008] Zou, Y., Zhang, R.-Z., Sabatelli, P., Chu, M.-L., and Bönnemann, C. G. (2008). Muscle Interstitial Fibroblasts Are the Main Source of Collagen VI Synthesis in Skeletal Muscle. *Journal of Neuropathology and Experimental Neurology*, 67(2):144–154.

A Abstract

Myogenesis in development as well as during muscle regeneration involves a coordinated interplay of various cell and tissue types. Careful orchestration of immune cells, satellite cells, connective tissue and resident cell types is required for effective tissue repair. The muscle interstitium comprises various resident cell types such as interstitial fibroblasts, pericytes or fibro/ adipogenic progenitors (FAPs). While FAPs reside quiescent in the muscle interstitium in homeostatic tissue they are activated upon injury and provide a pro-myogenic environment necessary for regeneration. However, due to the lack of markers to particularly identify activated FAPs the clarification of exact underlying cell specific mechanisms is impeded, and a clear cell discrimination challenging. FAPs are proposed as originating from mesenchymal cells, but confirmation remains elusive.

Odd skipped related-1 (*Osr1*) is expressed in muscle connective tissue derived from the lateral plate mesoderm during embryonic and fetal myogenesis in the limbs. Unpublished data demonstrate its crucial functional role for muscle patterning and contribution to muscle interstitial cells at the time of birth. However, postnatal expression of *Osr1* was not clear, and functional studies in the adult require a conditional *Osr1* allele due to the lethality of a constitutive knock-out of *Osr1* at early fetal stage.

Here, the generation of two novel tools for investigating *Osr1* expression in adult mice was performed. The *Osr1* promotor-driven lacZ-reporter mouse model Osr1-MFA enables identification of Osr1+ cells by histological and immunohistochemical methods as well as by fluorescent-activated cell sorting (FACS) technique. The conditional line Osr1-flox carries a floxed allele of *Osr1* thus allows for a conditional knock-out of *Osr1*.

Previous reports described a transient muscle interstitial cell population present during the first 3 weeks after birth, comprising myogenic non-satellite cell progenitors and juvenile FAPs. Here, expression of *Osr1* in the FAP subpopulation is demonstrated which allows for specific identification of these cells in muscle tissue. Genetic lineage tracing demonstrated that these Osr1+ juvenile FAPs, at least in part, give rise to quiescent FAPs in adult muscle, where *Osr1* expression is downregulated. These data contribute to the clarification of the origin of FAPs in the adult.

Muscle damage triggers *Osr1* expression in FAPs after cell activation, where it remains upregulated during the early phase of muscle regeneration. In a model of muscle injury that promotes fat formation, limited adipocytic contribution of Osr1+ FAPs was observed after lineage tracing. These data are in contrast to previous reports

attributing a strong contribution of FACS isolated and engrafted FAPs to ectopic fatty accumulation. This highlights the importance of the tissue environment and the proneness of FAPs to external cues when removed from the tissue context. Moreover, in regenerated muscle the majority of FAPs had expressed *Osr1* during the early phase of regeneration. These results provide evidence for *Osr1* expression as a specific marker for activated FAPs after muscle injury. A large fraction of TCF4+ fibroblasts in regenerated muscle is derived from TCF4–/ Osr1+ FAPs. This observation elucidates TCF4+ fibroblasts as progenies of FAPs.

A conditional knock-out of *Osr1* after injury results in significantly reduced pro-inflammatory macrophage abundance and abnormal accumulation of aggregates in myofibers during an early stage of regeneration. These results suggest a functional involvement in the plasmin system. It is hypothesized that *Osr1* indirectly regulates the conversion of plasminogen to plasmin, thus mediates extracellular matrix deposition, macrophage recruitment and myofiber degeneration. This hypothesis assigns an essential role to *Osr1* expression in FAPs for an effective muscle regeneration after injury.

B Zusammenfassung

Effektive Myogenese während der pränatalen Entwicklung wie auch während der Muskelregeneration bedarf eines koordinierten Zusammenspiels unterschiedlicher Zell- und Gewebstypen. Regeneration erfordert eine präzise funktionelle Abstimmung der Interaktionen zwischen Immunzellen, Satellitenzellen, Bindegewebe und residenten Zelltypen. Residente Zellarten im Muskelinterstitium umfassen interstitielle Fibroblasten, Perizyten und auch fibro/ adipogene Progenitoren (FAPs). FAPs befinden sich in quieszentem Zustand im Interstitium homöostatischen Muskelgewebes. Durch eine Muskelverletzung werden sie aktiviert, woraufhin sie im Laufe der Regeneration ein pro-myogenes Umfeld schaffen, welches für die Gewebsreparatur notwendig ist. Aus Ermangelung an Markern die spezifisch die Identifikation aktivierter FAPs ermöglicht, konnten deren exakte Funktionsmechanismen bislang nicht tiefgreifend geklärt werden. Der Ursprung von adulten FAPs wird in mesenchymalen Zellen vermutet, was jedoch noch nicht eindeutig bestätigt werden konnte.

Odd skipped related-1 (*Osr1*) wird während der embryonalen und fötalen Muskelentwicklung der Extremitäten im Bindegewebe exprimiert, welches aus dem lateralen Plattenmesoderm entsteht. Unveröffentlichte Daten zeigen eine entscheidende funktionelle Rolle von *Osr1* für die Musterbildung des Muskels. Desweiteren gehen aus embryonal *Osr1* exprimierenden Zellen perinatal interstitielle Zellen hervor. Die Expression von *Osr1* in postnatalen Stadien ist bisher unklar. Eine *Osr1* Defizienz ist letal im frühen fötalen Entwicklungsstadium. Dadurch werden funktionelle Studien zu *Osr1* in erwachsenen Individuen erschwert, was jedoch mithilfe eines konditionellen *Osr1* Allels ermöglicht werden könnte.

Im Rahmen dieser Doktorarbeit wurden zwei neuartige Werkzeuge zur Untersuchungen von *Osr1* in adulten Mäusen generiert. Die Osr1-MFA Mauslinie exprimiert das Reportergen *lacZ* unter dem *Osr1* Promotor, und ermöglicht so die Identifikation von Osr1+ Zellen für histologische und immunhistochemische Anwendungen, sowie für die Durchflusszytometrie (FACS). Das Mausmodell Osr1-flox trägt ein gefloxtes Osr1 Allel, womit ein konditioneller Osr1 Knock-out hervorgerufen werden kann.

In vorhergehenden Veröffentlichungen wurde eine transiente muskelinterstitielle Zellpopulation beschrieben, welche ausschließlich in der juvenilen Phase der Maus, während der ersten 3 Wochen nach Geburt, detektiert werden kann. Diese Population umfasst myogene Progenitoren welche nicht der klassischen myogenen Linie entstammen, und juvenile FAPs, welche sich in ihrer Signatur von adulten FAPs unterscheiden. Im Rahmen dieser Arbeit kann eine spezifische Expression von *Osr1* in dieser juvenilen

FAP Subpopulation berichtet werden. Weiterhin kann durch genetisches Markieren und Verfolgen dieser Osr1+ juvenilen FAPs gezeigt werden, dass aus diesen adulte FAPs gebildet werden. Dadurch wird zum Verständnis über die Herkunft von adulten FAPs beigetragen.

Osr1 wird in intaktem, homöostatischen adulten Muskelgewebe nur in vereinzelten FAPs experimiert. Die Verletzung von Muskelgewebe führt zu einer Aktivierung von FAPs, einhergehend mit einer Aktivierung von *Osr1* Expression in diesen Zellen. Während der frühen Phase der Regeneration bleibt die *Osr1* Expression hochreguliert. In einem Verletzungsmodell welches ektopische Fettbildung fördert wurde dabei nur eingeschränkt adipogenes Potenzial von Osr1+ FAPs *in vivo* beobachtet. Dies widerspricht vorangegangenen Berichten derer zufolge FAPs, welche zunächst aus ihrem Gewebszusammenhang isoliert, dann in ein identisches Verletzungsmodell transplantiert wurden, zu übermäßiger Fettbildung beitragen. Diese Diskrepanz unterstreicht die Bedeutung des Gewebszusammenhangs und verdeutlicht die Anfälligkeit von FAPs für äußere Einflüsse nach Entfernung aus diesem Zusammenhang. Ferner belegt die Expression von *Osr1* in FAPs während der frühen Phase der Regeneration ihre Eigenschaft als spezifischer Marker für aktivierte FAPs nach Muskelverletzung. Damit konnte gezeigt werden, dass ein großer Anteil von TCF4+ Fibroblasten im regenerierten Muskel aus TCF4–/ Osr1+ FAPs hervorgeht. Diese Charakterisierung von aktivierten FAPs als Vorläufer von TCF4+ Fibroblasten trägt zum besseren Verständnis über die Beziehungen interstitieller Zellpopulationen bei.

Mithilfe des Osr1-flox Mausmodells wurde die Muskelregeneration nach konditionellem *Osr1* Knock-out untersucht. *Osr1* Defizienz führt zu signifikant reduzierter Anzahl pro-inflammatorischer Makrophagen und abnormer Anhäufung intrazellulärer Aggregate in Muskelfasern während der frühen Phase der Regeneration. Diese Beobachtungen lassen auf eine funktionelle Beteiligung am Plasmin System schließen. *Osr1* könnte indirekt die Konversion von Plasminogen zu Plasmin Protease regulieren, und dadurch die Ablagerung von extrazelluärer Matrix, die Rekrutierung von Makrophagen und die Faserdegeneration im Zuge der Regeneration vermitteln. Diese Hypothese schreibt der Expression von *Osr1* eine essenzielle Rolle für die Muskelregeneration nach Verletzung zu.

C Publications

C.1 Scientific journals

- Publications in scientific journals did not emerge from the work presented here, yet.

C.2 Talks

- MyoGrad Summer School, Max-Delbrück Center for Molecular Medicine,
  Berlin 2014
  Title: „*Osr1* as a potential signature for a juvenile transient interstitial cell population“

C.3 Posters

- EMBO Conference Molecular Biology of Muscle Development and Regeneration,
  Acaya-Lecce 2014
  Title: „Odd-skipped related 1 – Potential signature discovery of a transient juvenile interstitial cell population“

- MyoGrad DFG Evaluation, Max-Delbrück Center for Molecular Medicine,
  Berlin 2014
  Title: „Role of muscle connective tissue in muscle and muscle stem cell development“

- MyoGrad Summer School, Max-Delbrück Center for Molecular Medicine,
  Berlin 2012
  Title: „Role of muscle connective tissue in muscle development and regeneration“

- Day of Science, Max-Planck-Institute for Molecular Genetics,
  Berlin 2012
  Title: „Role of muscle connective tissue in muscle and muscle stem cell development“

D Acknowledgements

I am grateful to Prof Stefan Mundlos for welcoming me at the Max-Planck-Institute for Molecular Genetics as well as at the Institute of Medical Genetics and Human Genetics at the Charité in Berlin to conduct my PhD thesis.

First, I want to thank Prof Simone Spuler for supervising me and reviewing my thesis.

I am deeply grateful to my lab supervisor Prof Sigmar Stricker to have chosen me as PhD student and for offering this fascinating topic to me. He gave me all the freedom a PhD student could only wish for, so I could give my fancy full scope. At the same time he would not leave me alone but he was always ready to listen, give advice and share his vast knowledge in enthusiastic discussions. And more than once he had to dampen my euphoria and remind me of scientific precision ("Hm, I do really think you need to count these cells!") - thanks a heap for this utterly instructive time!

One might guess the beauty of Paris itself would be enough reason for why I enjoyed my time in France so much. But without my co-supervisors David Sassoon and Giovanna Marazzi this period would only be half as memorable. Their verve was boosting and inspiring. I also need to mention a couple of their people making my stay worthwhile, David Ollitraut, Luigi Formicola, Anne-Lyse Denizot, Rosamaria Correra, Sergiy Kyryachenko, Karo Tanaka and "that dude" Jean-Remy Courbard.

Initially, the focus of my project was not necessarily matching the expertises of all my supervisors equally, but in the at the sparked collaboration was adequately termed "divine intervention". And this collaboration was made possible by MyoGrad, the international research training group for myology. This PhD programme offered top notch conferences in the form of the MyoGrad Summer Schools with renowned scientist speakers, and with it a valuable experience. I am very thankful to the Berlin MyoGrad speaker Prof Simone Spuler, and also to the administrative coordinator Susanne Wissler.

The Max-Planck-Institute for Molecular Genetics was a fantastic place to work at. I want to thank Dr Heiner Schrewe from the Department of Developmental Genetics for all the work he dedicated to generating the transgenic mouse. These mice, and also all other strains I used, were cared for by Katja Zill of the animal facility. She is one example of an animal care taker, always had an overview on plenties of matings and crossings I had asked her to supervize. Moreover, her support in applying injuries was invaluable - thanks so much!

I am also grateful to all the members of the research group "Development and Disease" of Prof Stefan Mundlos. This group was and still is stuffed with freaky and zealous people like Malte Spielmann, Martin Franke, Hendrikje Hein, Daniel Ibrahim,

Sinje Geuer, Alexandra Despang, Bjørt Kragesteen, Lila Allou or Pia Kuss.

Most of all though, a small flourishing myo-research+ subpopulation in this research group contributed to my personal daily wellbeing: Sigmars "Muscle People". Aroo, you brought a lot of warmth to our group making it a cozy place. Sophie, you were a dream of an intern and an excellent master student. And then there are a few people that I also spent time with outside the lab, and that I hold dear.

Krzysztof "Kris-O" Brzezinka, I know you can ferment everything and in the end yield delicious wine, probably even out of my old shoes. Just you try it, you know: "It should work!".

Mickael "El Miguël" Orgeur, your stay in our lab was just not long enough. I will never forget that night at "the beach"!

El Pedro! Vallecillo! Garcííía! If there is anyone knowing how to really take things easy in life, than this is you. With you I just had so much fun, and I already was in a great mood when I saw you in the.. well.. morning. But even during your siesta, when you had your shoes taken off, put on sombrero and poncho, that straw between your lips and your bottle of Tequilla at hand, you always came up with latest reports, a new paper you had read or intruiging ideas! Thanks, loco, for that awesome time!

Was die Unterstützung meiner Familie, meiner Mutter Gabriele Angelika Barbara, ihrem Ehemann Rudi und meinem Bruder Mark, sowie die meines Vaters Klaus, mir über die Jahre hinweg bedeutet haben, ist kaum in ein paar Sätzen zusammenzufassen. Ihr wart jederzeit für mich da, um Erfolge zu feiern, um schlicht gemeinsam die Zeit zu genießen und wenn ich eine Auszeit vom Alltag nehmen wollte. Aber auch wenn ich ein aufbauendes Schulterklopfen benötigt hatte. Ihr habt mir gezeigt, dass jeder Tag am Ende immer etwas Gutes birgt. Zu wissen dass Ihr stolz auf mich seid egal was kommen mag, war ein unbeschreiblicher Rückhalt.

During my time of writing there was that cute little furry thing that periodically, and always most subtly!, reminded me of taking a break. Having her to invite me to play with Kügelchen or Drahti helped me to relax, and those staring contest challenges gave me time to take a breath. Puma, miau miuu!

The best I have saved for last, and that is you, Saniye. I can't recall everything of my first day at the institute, but I clearly remember that moment I saw you in the microscopy room. Immediately I knew that you are extraordinary and someone very special. Throughout all the years, you showed your enthusiasm about my work and your constant trust in me. In times of frustration you have always been eager to strengthen my back and give me confidence. You would never believe how much your support meant to me. Thank you with all my heart.

E List of Figures

F List of Tables

G List of Abbreviations

αsma	alpha-smooth muscle actin
Cd31	Cluster of differentiation 31
Cd34	Cluster of differentiation 34
Cd45	Cluster of differentiation 45
Mac-1	Macrophage-1 antigen
Myf5	Myogenic factor 5
MyoD	Myogenic differentiation 1
Ng2	Neural/ glial antigen 2
Odd	Odd-skipped
Osr1	Odd-skipped related 1
Osr2	Odd-skipped related 2
Pax3	Paired box 3
Pax7	Paired box 7
Pdgfrα	Platelet derived growth factor receptor alpha
Pdgfrβ	Platelet derived growth factor receptor beta
Sca-1	Stem cells antigen-1
Tcf4	Transcription factor 4
µg	Microgram
µl	Microliter
µM	Micromolar
µm	Micrometer(s)
ATG	Start codon
$BaCl_2$	Barium chloride
bp	Basepair(s)
BSA	Bovine serum albumin
$CaCl_2$	Calcium chloride
cDNA	Complementary deoxyribonucleic acid
CNV	Copy number variation
CTX	Cardiotoxin
Cxcl12	C-X-C motif chemokine 12
Cxcr4	C-X-C chemokine receptor type 4
dd	Double distilled
DEPC	Diethylpyrocarbonate
DMD	Duchenne muscular dystrophy
DMSO	Dimethyl sulfoxide
DNA	Deoxyribonucleic acid
dNTP	Nucleoside triphosphate
e.g.	Exempli gratia
ECM	Extracellular matrix
EDL	*Extensor digitorum longus*
EDTA	Ethylenediaminetetraacetic acid
embMyHC	Embryonic myosin heavy chain
ERT2	Estrogen receptor type 2
ESC	Embryonic stem cell
FACS	Fluorescence-activated cell sorting
FAP	Fibro/ adipogenic progenitor
g	Gram
GAPDH	Glyceraldehyde 3-phosphate dehydrogenase
GC	*Gastrocnemius*
GCE	GFP-Cre-ERT2
GFP	Green fluorescent protein
h	Hour(s)
H&E	Hematoxylin and eosin
HBSS	Hank's buffered salt solution
IL	Interleukin
IRES	Internal ribosome entry site
kb	Kilobase(s)
kDa	Kilodalton

LOA	Loss-Of-Allele
MFA	Multi-functional-allele
mG	Membranous GFP
$MgCl_2$	Magnesium chloride
min	Minute(s)
ml	Milliliter
mM	Millimolar
mm	Millimeter
mRNA	Messenger-RNA
mT	Membranous Tomato
MyHC	Myosin heavy chain
ng	Nanogram(s)
NTX	Notexin
P/S	Penicillin/ streptomycin
PBS	Phosphate buffered saline
PCR	Polymerase chain reaction
PFA	Paraformaldehyde
PIC	PW1-expressing interstitial cell
qPCR	Quantitative polymerase chain reaction
RNA	Ribonucleic acid
RT	Room temperature
s	Second(s)
SSC	Saline sodium citrate
TA	*Tibialis anterior*
TAE	Tris base/ acetic acid/ EDTA
T_m	Meltingtemperature
U	Enzyme unit
V	Volt
v/v	Volume per volume
WT	Wildtype
°C	Celsius degree